ON THE PROJECTIVE GEOMETRY OF ENTANGLEMENT AND CONTEXTUALITY

FRÉDÉRIC HOLWECK

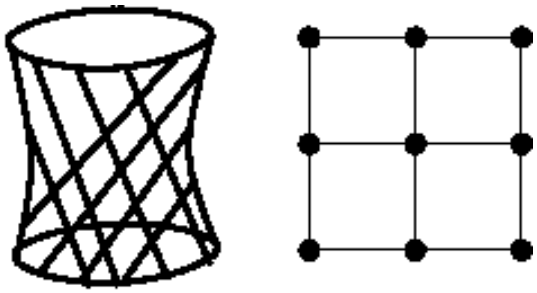

A dissertation submitted for the Habilitation (HDR) in Applied Mathematics of University Bourgogne Franche-Comté

Defended on September 11, 2019 at UTBM Belfort
In presence of the following commitee

Ingemar Bengtsson	-	Professor, Stockholm University	(Reviewer)
Alessandra Bernardi	-	Associate Professor, Trento University	(Examinator)
Matthias Christandl	-	Professor, Copenhagen University	(Reviewer)
Uwe Franz	-	Professor, University Bourgogne Franche-Comté	(Examinator)
José-Luis Jaramillo	-	Professor, University Bourgogne Franche-Comté	(Examinator)
Hans-Rudolf Jauslin	-	Professor, University Bourgogne Franche-Comté	(Examinator)
Jean-Gabriel Luque	-	Professor, University of Rouen	(Examinator)
Bernard Mourrain	-	Senior Researcher (DR), INRIA Sophia Antipolis	(Reviewer)
Metod Saniga	-	Senior Researcher, Slovak Academy of Sciences	(Examinator)

Laboratoire Interdisciplinaire Carnot de Bourgogne UMR 6363, ICB/UTBM, University Bourgogne Franche-Comté

Frédéric Holweck: *On the projective geometry of entanglement and contextuality,* A dissertation submitted for the Habilitation (HDR) in Applied Mathematics of University Bourgogne Franche-Comté, © September 11, 2019

PUBLICATIONS

The work presented in this habilitation thesis is based on the following publications listed in chronological order. These references are also included in the bibliography of the thesis following the authors' alphabetic order.

1. Holweck, F., Luque, J. G., & Thibon, J. Y. (2012). Geometric descriptions of entangled states by auxiliary varieties. Journal of Mathematical Physics, 53(10), 102203.

2. Planat, M., Saniga, M., & Holweck, F. (2013). Distinguished three-qubit «magicity» via automorphisms of the split Cayley hexagon. Quantum Information Processing, 12(7), 2535-2549.

3. Holweck, F., Luque, J. G., & Thibon, J. Y. (2014). Entanglement of four qubit systems: A geometric atlas with polynomial compass I (the finite world). Journal of Mathematical Physics, 55(1), 012202.

4. Holweck, F., Luque, J. G., & Planat, M. (2014). Singularity of type D_4 arising from four-qubit systems. Journal of Physics A: Mathematical and Theoretical, 47(13), 135301.

5. Holweck, F., Saniga, M., & Lévay, P. (2014). A Notable Relation between N-Qubit and 2^{N-1}-Qubit Pauli Groups via Binary $LGr(N, 2N)$. SIGMA. Symmetry, Integrability and Geometry: Methods and Applications, 10, 041.

6. Lévay, P., & Holweck, F. (2015). Embedding qubits into fermionic Fock space: Peculiarities of the four-qubit case. Physical Review D, 91(12), 125029.

7. Saniga, M., Havlicek, H., Holweck, F., Planat, M., & Pracna, P. (2015). Veldkamp-space aspects of a sequence of nested binary Segre varieties. Annales de l'Institut Henri Poincaré D, 2(3), 309-333.

8. Holweck, F., & Jaffali, H. (2016). Three-qutrit entanglement and simple singularities. Journal of Physics A: Mathematical and Theoretical, 49(46), 465301.

9. Holweck, F., Jaffali, H., & Nounouh, I. (2016). Grover's algorithm and the secant varieties. Quantum Information Processing, 15(11), 4391-4413.

10. Holweck, F., & Lévay, P. (2016). Classification of multipartite systems featuring only $|W\rangle$ and $|GHZ\rangle$ genuine entangled states. Journal of Physics A: Mathematical and Theoretical, 49(8), 085201.

11. Saniga, M., Holweck, F., & Pracna, P. (2017). Veldkamp spaces: From (Dynkin) diagrams to (Pauli) groups. International Journal of Geometric Methods in Modern Physics, 14(05), 1750080.

12. Holweck, F., Luque, J. G., & Thibon, J. Y. (2017). Entanglement of four-qubit systems: A geometric atlas with polynomial compass II (the tame world). Journal of Mathematical Physics, 58(2), 022201.

13. Holweck, F., & Saniga, M. (2017). Contextuality with a small number of observables. International Journal of Quantum Information, 15(04), 1750026.

14. Lévay, P., Holweck, F., & Saniga, M. (2017). Magic three-qubit Veldkamp line: A finite geometric underpinning for form theories of gravity and black hole entropy. Physical Review D 96, 026018

15. Lévay, P., & Holweck, F. (2018). A fermionic code related to the exceptional group E 8. Journal of Physics A: Mathematical and Theoretical.

16. Holweck, F., & Oeding, L. (2018). Hyperdeterminants from the E_8 Discriminant. arXiv preprint arXiv:1810.05857.

17. Saniga, M., Boulmier, J., Pinard, M., & Holweck, F. (2019). Veldkamp Spaces of Low-Dimensional Ternary Segre Varieties. Results Math 74: 54

18. Holweck, F. (2019) Geometric constructions over $\mathbb{C}$ and $\mathbb{F}_2$ for Quantum Information. To appear in the special volume Quantum Physics and Geometry, Lecture Notes of the Unione Matematica Italiana, Springer.

19. Jaffali, H., & Holweck, F. (2019). Quantum entanglement involved in Grover's and Shor's algorithms: the four-qubit case. Quantum Information Processing, 18(5), 133.

20. Lévay, P., & Holweck, F. (2019). A finite geometric toy model of space time as an error correction code. Phys. Rev. D 99, 086015.

PROJECTS

Several projects have supported my research and collaborations on quantum information over the past six years. The list is given in chronological order.

2013 CoGIT (Combinatoire et Géométrie pour l' InTrication): Project PEPS CNRS on quantum information. PI: Ion Nechita (Toulouse Univ. CNRS). 10kE

2014 UTBM (University of Technology of Belfort-Montbéliard) one month guest professor position to invite Metod Saniga from the Slovak Academy of Sciences. 5kE

2015 UTBM one month guest professor position to invite Péter Lévay from Budapest University of Technology and Economics. 5kE

2016 Exploration of the geometry of generalized Pauli group. Regional grant for international mobility of senior researchers. Obtained 4 months to invite Metod Saniga. 24kE

2016 UTBM research quality grant. Obtained to organize 3 meetings on quantum information for UBFC researchers. 2.5 kE

2017 Entanglement in quantum algorithms and protocols. Regional grant for international mobility of senior researchers. Obtained 4 months to invite Péter Lévay. 24kE

2017-2020 I-QUINS (Integrated QUantum Information at the NanoScale). Research grant obtained from ISITE-Bourgogne Franche-Comté (contract ANR-15-IDEX-03). The goal of this project is to conduct and develop different researches on the site of University Bourgogne Franche Comté on quantum information addressing questions from the mathematics of quantum computation to the realization of integrated quantum devices. The project gather 20 researchers of UBFC from 5 different research units. PI: F. Holweck. 150kE

2017-2020 PHYFA (Photonic Platform for HYperentanglement in Frequencies and its Applications). Research grant from the Région Bourgogne Franche-Comté. The goal of this project is to conduct simultaneously theoretical studies on the entanglement involved in quantum algorithms and experimental development on a photonic platform. This grant support the salary of my PhD student Hamza Jaffali. PI: F. Holweck and J.-M. Merolla. 248 kE+PhD contract

2018 UTBM two months guest professor position to invite Luke Oeding from Auburn University. 10kE

2018-2019 Finite Geometries Shaping quantum information. French-Slovak program financed by Campus France (PHC Hubert Curien) to develop mobility and cooperation with my co-author Metod Saniga from the Slovak Academy of Sciences. 10kE

SUPERVISIONS

I currently co-supervise two PhD and had supervised various Master projects on topics related to quantum information.

- PhD

2017-2020 I co-supervise with Jean-Marc Merolla, within the project PHYFA the PhD thesis of Hamza Jaffali. Hamza is studying entanglement in quantum algorithms as well as different ways of measuring entanglement of pure quantum systems.

2018-2021 I co-supervise with Alain Giorgetti and Pierre-Alain Masson the PhD of Henry de Boutray on specification and correction of quantum algorithms.

- Master projects

Spring 2018 M1 project of Yeva Poghosyan for the International Master Physics Photonics and Nanotechnology, University Bourgogne Franche-Comté. Yeva worked on the use of Finite Elements Methods for solving Schrödinger equation.

Spring 2018 M1 projet of Jérôme Boulmier and Maxime Pinard for the engineering Master degree in computer science of the University of Technology Belfort-Montbéliard (UTBM). This work was co-supervised with Metod Saniga. The paper *Veldkamp Spaces of Low-Dimensional Ternary Segree* in Results in Mathematics has been written at the end of the projet and is based on Jérôme and Maxime's programs.

Fall 2016 M2 project of Hamza Jaffali and Ismaël Nounouh for the engineering Master degree in computer science of UTBM. Hamza and Ismaël wrote a report on quantum games and potential applications to Smart grids.

Spring 2016 M1 project of Hamza Jaffali (UTBM). Hamza computed the singular types of hyperplane sections of the variety of separable states in the three-qutrit case. His work was used to write the paper *Three-qutrit entanglement and simple singularities* published in Journal of Physics A.

ACKNOWLEDGEMENTS

Here we are,
15 years ago (September 10, 2004) I defended my PhD in algebraic geometry at Toulouse University (Paul Sabatier). Then I started my professional life as a high school teacher. A few years later I was a teacher/lecturer at UTBM with a large teaching load and some administrative responsibilities but without any research activities. In 2011, I sent an email to Jean-Gabriel Luque, who I did not know at that time, to ask him a simple question about the concept of hyperpfaffian. His response and the long-term email exchanges that followed was the beginning of my work in quantum information theory. Over the past 8 years, I have been fortunate to meet great people like Jean-Gabriel who made it possible for me to start a new research activity and I would like to take the advantage of this acknowledgement section to warmly thank them.

It is pleasure to start this section by thanking my defense committee.

I would like to express all my gratitude to Ingemar Bengtsson, Matthias Christandl and Bernard Mourrain for accepting to review my habilitation and for writing positive and encouraging words on my present and future work. I am honored that this thesis has been evaluated by worldwide experts that have demonstrated in their career the efficiency and the beauty of geometry in physics, quantum information, mathematics and computer science.

Alessandra Bernardi comes from Trento University to participate in this committee. I would like to thank you Alessandra for inviting me in 2017 to the international workshop on *Quantum Physics and Geometry* that you organized. I started to work on my habilitation thesis after this meeting and the review paper that followed.

Uwe Franz, Hans Jauslin and José-Luis Jaramillo are colleagues from University Bourgogne Franche-Comté. In the last couple of years we have been involved in common projects on quantum information and it has been a real pleasure to work, discuss and collaborate with you. In 2013 Hans and Stéphane Guérin came to the mathematics seminar in Dijon as next door physicists and I remember that you were the only two people in the audience really interested in the talk I was giving that day!

It was important for me to invite some of my co-authors in the committee. The change of direction in my professional career owes a lot

to Jean-Gabriel Luque. I learned about Miyake's papers on hyperdeterminant and entanglement from you and our first joint paper was the starting point of my work on quantum information.
I was admitted to the beautiful world of finite geometry thanks to the guidance of Metod Saniga. Our annual meetings with Péter Lévay in the Tatras have always been a source of inspiration and I value our collaboration a lot both scientifically and personally.

My work on the geometry of quantum information has generated a lot of collaborations and I would like to thank all my co-authors. This dissertation is also an extended review of our joint contributions. In chronological order of appearance: Jean-Gabriel Luque, Jean-Yves Thibon, Michel Planat, Metod Saniga, Péter Lévay, Hans Havlicek, Petr Pracna, Alain Giorgetti, Hamza Jaffali, Ismaël Nounouh, Jérome Boulmier, Maxime Pinard and Luke Oeding.
Michel deserves special thanks for being the first to show me a Mermin square and for introducing me to Metod. Péter also deserves very special thanks for our productive collaboration both on the geometry of entanglement and contextuality but also for the very nice discussions about physics, mathematics and music we have had these past years.

I would also like to thank all the colleagues involved in the I-QUINS and PHYFA projects. In particular Stéphane Guérin and Jean-Marc Merolla who have been helping me a lot with writing the proposals and managing the projects.

Between 2011 and 2017 I also collaborated with colleagues at UTBM on the application of the theory of invariants to behaviour laws in continuum mechanics. These years in the M3M team (now the ICB-COMM dept) helped a lot to launch my career as an associate professor. I would like to thank François Peyraut, the former director of M3M, for welcoming me in his team and for the help and encouragements he has provided since then.

Finally I would like to write a few words to my family. When he was 6 my son Anatole thought that I was trying to build a quantum computer by myself. My daughters, Clarisse and Zoé and my wife Laure were more interested in the quantum teleportation protocol and they were hoping that at some point my research could be useful to go across the country faster when we go down south on vacation. I am very sorry to disappoint them all, but the research presented here is harmless in this respect... As a geometer I would say that this work takes place in Plato's space of forms and it is mostly about trying to understand some beautiful geometrical aspects of quantum information.

CONTENTS

LIST OF FIGURES

LIST OF TABLES

1 INTRODUCTION

This *habilitation thesis* is an extended version of the review paper I published in the Lecture Notes of the Unione de Matematica Italiana (Springer 2019) [50] in their special issue on Quantum Physics and Geometry. This special issue was following an international workshop on quantum physics hosted by the University of Trento in Italy in July 2017.

The aim of the review [50] was to provide an elementary introduction to a series of papers I published on the geometry of the classification of entanglement for pure multipartite quantum systems on the one hand [54, 55, 56, 53, 77, 57, 51] and on the geometry of observable-based proofs of the Kochen-Specker Theorem on the other hand [59, 101, 60, 80]. The review also emphasized the connection in both problems with (classical) representation theory of simple Lie algebras. I kept for this habilitation this splitting in essentially two parts, Part I *The Geometry of Entanglement*, Part II *The Geometry of Contextuality*. I also added more details: In Part I, I give an introduction to covariants and our analysis with Jean-Gabriel Luque and Jean-Yves Thibon of the 4-qubits classification from this perspective [55] and in Part II, I added explanations about potential experimental tests of the operators-based proofs of contextuality and also the description of the Lagrangian mapping. The Appendices A, B, C, D provide also complementary details that could not fit in [50]. In the text I also propose more connections with other geometrical works I have done [16, 104, 105]. Finally the third part, Part III *Perspectives*, completes this text to introduce recent developments [78, 79, 58] and also emphasizes the potential of applications of this geometric way of looking at quantum information [52, 64].

At a first sight the problem of the classification of entanglement of multipartite systems and the problem of finding operator-based proofs of contextuality have no direct connection and the geometrical constructions to describe them are of distinguished nature. I will use projective complex geometry to describe entanglement classes and I will work with finite geometry over the two elements field $\mathbb{F}_2$ to describe operator-based proofs of the Kochen-Specker Theorem. However, when we look at both geometries from a representation theory point of view, one observes that the same semi-simple Lie groups are acting behind the scene. This observation may invite us to look for a more direct (physical) connection between these two questions.

In fact, historically, both problems are linked to the question of the existence of *hidden variables*.

In the development of quantum science, the paradoxes raised by questioning the foundations of quantum physics turn out to be considered as quantum resources once they have been tested experimentally. A famous example of such a change of status for a scientific question is of course the EPR paradox which started by a criticism of the foundation of quantum physics by Einstein Podolsky and Rosen [40].

The EPR paradox deals with what we nowadays call a pure 2-qubit quantum system. This is a physical system made of two parts A and B such that each part or each particle is a two-level quantum system. Mathematically a pure 2-qubit state is a vector of $\mathcal{H}_{AB} = \mathbb{C}^2_A \otimes \mathbb{C}^2_B$. Denote by $(|0\rangle, |1\rangle)$ the standard basis of the vector spaces $\mathbb{C}^2_A$ and $\mathbb{C}^2_B$ and let $(|00\rangle, |01\rangle, |10\rangle, |11\rangle)$ be the associated basis of $\mathcal{H}_{AB}$. The laws of quantum mechanics tell us that $|\psi\rangle \in \mathcal{H}_{AB}$ can be described as

$$|\psi\rangle = a_{00}|00\rangle + a_{10}|10\rangle + a_{01}|01\rangle + a_{11}|11\rangle, \tag{1}$$

with $a_{ij} \in \mathbb{C}$ and $|a_{00}|^2 + |a_{10}|^2 + |a_{01}|^2 + |a_{11}|^2 = 1$. In this language, the argument of Einstein, Podolsky and Rosen would be based on the following admissible state

$$|\mathrm{EPR}\rangle = \frac{1}{\sqrt{2}}(|00\rangle + |11\rangle) \tag{2}$$

to argue that quantum mechanics is incomplete. The EPR reasoning consists of saying that, according to quantum mechanics, a measurement of particle A will project the system $|\mathrm{EPR}\rangle$ to either $|00\rangle$ or $|11\rangle$ fixing instantaneously the possible outcomes of the measurement of particle B no matter how far the distance between particles A and B is. In a letter to Born, Einstein characterized it as *spooky action at a distance*. According to Einstein Podolsky and Rosen [40] this was showing that *hidden variables* were necessary to make the theory complete. Note that not all 2-qubit quantum states can produce spooky action at a distance. If $|\psi\rangle = (\alpha_A|0\rangle + \beta_A|1\rangle) \otimes (\alpha_B|0\rangle + \beta_B|1\rangle)$, then the measurement of particle A has no effect on the state of particle B. From Eq (1) one sees that the possibility to factorize a state $|\psi\rangle$ translates to

$$a_{00}a_{11} - a_{01}a_{10} = 0. \tag{3}$$

This homogeneous equation defines a quadratic hypersurface in $\mathbb{P}^3 = \mathbb{P}(\mathbb{C}^2 \otimes \mathbb{C}^2)$ corresponding to the projectivization of the states that can be factorized; those states are called *non-entangled states*. The complement of the quadric is the set of non-factorizable states, i.e. *entangled states*.

The philosophical questioning of Einstein and his co-authors about the existence of hidden-variables to make quantum physics complete, becomes a scientific question after the work of John Bell [10], thirty

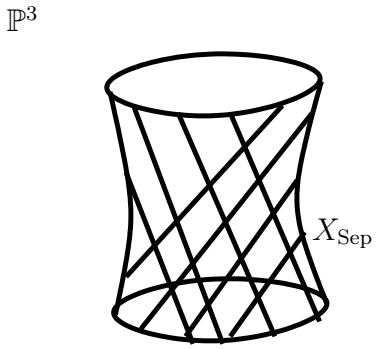

Figure 1: Non-entangled states, denoted by X_{Sep}, and entangled states, $\mathbb{P}^3 \backslash X_{\text{Sep}}$, in $\mathbb{P}(\mathbb{C}^2 \otimes \mathbb{C}^2)$.

years later, whose inequalities have opened up the path to experimental tests. Those experimental tests have been performed many times starting with the pioneering works of Alain Aspect [6] and *entanglement* in multipartite systems is nowadays recognized as an essential resource in quantum information.

Another paradox of quantum physics, maybe less famous than EPR, is *contextuality*. Interestingly, the notion of contextuality in quantum physics is also related to the question of the existence of hidden-variables. In 1967 Kochen and Specker[1] [67] introduced this notion by proving there is no non-contextual hidden-variable theory which can reproduce the outcomes predicted by quantum physics. Here *contextual* means that the outcome of a measurement on a quantum system depends on the context, i.e. a set of compatible measurements (set of mutually commuting observables[2]) that are performed in the same experiment. The original proof of Kochen and Specker is based on the impossibility to assign colouring (i.e. predefinite values for the outcomes) to some vector basis associated to some set of projection operators. Let us present here a simple and elegant observable-based proof of the Kochen-Specker Theorem due to Mermin [88] and Peres [98]. Let us denote by X, Y and Z, the usual Pauli matrices,

$$X = \begin{pmatrix} 0 & 1 \\ 1 & 0 \end{pmatrix}, Y = \begin{pmatrix} 0 & -i \\ i & 0 \end{pmatrix}, Z = \begin{pmatrix} 1 & 0 \\ 0 & -1 \end{pmatrix}. \tag{4}$$

1 This concept of contextuality also appears in Bell's paper [10, 88].

2 In quantum physics, the outcomes of a measurement are encoded in a hermitian operator, called an observable. The eigenvalues of the observable correspond to the possible outcomes of the measurement and the eigenvectors correspond to the possible projections of the state after the measurement.

These three hermitian operators encode the possible measurement outcomes of a spin $\frac{1}{2}$ particle in a Stern-Gerlach apparatus oriented in three different space directions. Taking tensor products of two such Pauli matrices we can define Pauli operators acting on two qubits. In [98, 88] Mermin and Peres considered a set of 2-qubit Pauli operators similar to the one reproduced in Figure 2.

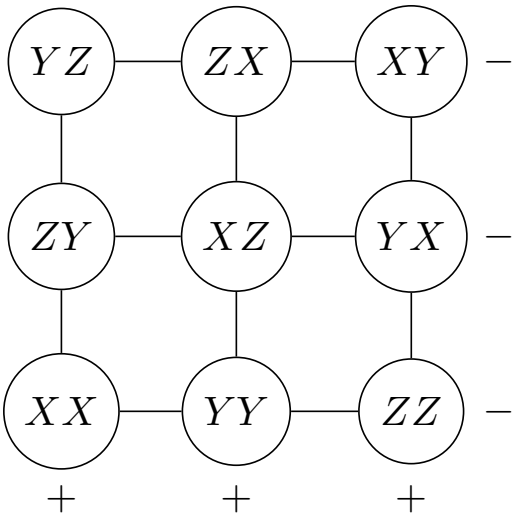

Figure 2: The Mermin-Peres «Magic» square: Each node represents a two-qubit (non-trivial) Pauli observable and the rows and columns are sets of mutually commuting observables (contexts). The signs indicate for each row and column when the product of the contexts gives $+\mathrm{I}_4$ or $-\mathrm{I}_4$.

This diagram, called the «Magic» Mermin-Peres square, furnishes a proof of the impossibility to predict the outcomes of quantum physics with a non-contextual hidden-variables theory as I now explain. Each node of the square represents a 2-qubit observable which squares to identity, i.e. the possible eigenvalues of each node (the possible measurement outcomes) are ± 1. The operators which belong to a line or a column are mutually commuting, i.e. they represent a context or a set of compatible observables. The products of each line or column give either I_4 or $-\mathrm{I}_4$ as indicated by the signs on the diagram. The odd number of negative lines makes it impossible to pre-assign to each node outcomes (± 1) which are simultaneously compatible with the constraints on the lines (the products of the eigenvalues should be negative) and columns (the product of the eigenvalues are positive). Therefore any hidden-variable theory, capable of reproducing the outcomes of the measurement that can be achieved with the Mermin-Peres square, should be contextual, i.e. the deterministic values that we wish to assign should be context dependent. This other paradox has been studied intensively in the last decade and experiments [1, 25, 9, 66] are now conducted to produce contextuality in

the laboratory, leading to consider contextuality as another quantum resource for quantum computation or quantum processing [1, 62].

Both entanglement of multipartite pure quantum systems and contextual configurations of multi-Pauli observables can be nicely described by geometric constructions. In Part I, I will explain my work on the projective geometry of complex algebraic varieties involved in the description of multipatite entanglement. The quadric in Figure 1 is one of the simplest examples of such variety. In Part II, I will present the projective geometry over the finite field $\mathbb{F}_2$ used to describe configuration of operators. The grid, Figure 2, is also defined as the zero locus of a quadric but now in the symplectic polar space $\mathcal{W}(3,2)$.

Part I

THE GEOMETRY OF ENTANGLEMENT

In this first part of the thesis, Chapters 2-5, I present the work I have done with my co-authors Jean-Gabriel Luque, Jean-Yves Thibon [54, 55, 56], Péter Lévay [53, 77] and Hamza Jaffali [51]. As explained in detail, the idea is to use a combination of techniques from algebraic geometry, invariant theory, singularity theory and representation theory to describe the (projectivized) Hilbert space of a pure multipartite system by different entanglement classes. Chapter 2 introduces the idea of auxiliary varieties: These are algebraic varieties that are built from the "core" variety, which in our case is the variety of separable states. Because the set of separable states is a SLOCC closed orbit, the auxiliary varieties are SLOCC invariant. Chapter 3 provides more illustrative examples and shows how classical invariant theory can be used to provide defining equations of the entanglement stratas corresponding to auxiliary varieties. In Chapter 4 I focus on dual varieties which are a special type of auxiliary varieties and I make the connection with the study of singular hypersurfaces defined by a quantum state. This idea allows one to attach a singular type to an entanglement class and open the path to an intriguing correspondence between simple singularities, entanglement classes and group action. The last Chapter of Part I, Chapter 5, considers the general case of spinorial representation. It allows us to embedd in the fermionic Fock space various multipartite systems (bosonic, qubit, fermionic). With the language of representation theory one recovers in one picture the three-partite classification for all those different systems.

In Part III I present more recent works where those ideas have been used to investigate the field of quantum algorithms and quantum error correcting codes.

2

AUXILIARY VARIETIES AND ENTANGLEMENT

In this chapter I introduce the main idea that I have been dealing with in my study of entanglement of pure multipartite systems: The entanglement classes can be described by means of geometrical objects, *auxiliary varieties*, built from the set of separable states. This idea is already in our initial paper with Jean-Gabriel Luque and Jean-Yves Thibon [54] on entanglement of pure multipartite systems. The chapter starts by introducing the necessary definitions and vocabulary from algebraic geometry (Section 2.1). Then I illustrate this idea with the famous three-qubit classification (Section 2.2) and conclude with a few more examples of quantum systems' description by auxiliary varieties (Section 2.3).

2.1 ENTANGLEMENT UNDER SLOCC AND ALGEBRAIC GEOMETRY

The Hilbert space of an n-partite system will be the tensor product of n-vector spaces where each vector space is the Hilbert space of each individual part. Thus the Hilbert space of an n-qudit system is $\mathcal{H} = \mathbb{C}^{d_1} \otimes \cdots \otimes \mathbb{C}^{d_n}$. A quantum state being defined up to a phase we will work in the projective Hilbert space and denote by $[\psi] \in \mathbb{P}(\mathcal{H})$ the class of quantum states $|\psi\rangle \in \mathcal{H}$. The group of local invertible operations, $G = \mathrm{SL}_{d_1}(\mathbb{C}) \times \cdots \times \mathrm{SL}_{d_n}(\mathbb{C})$ acts on $\mathbb{P}(\mathcal{H})$ by its natural action. This group is known in physics as the group of Stochastic Local Operations with Classical Communications [12, 36] and will be denoted by SLOCC.

According to the axioms of quantum physics, it would be more natural to look at entanglement classes of multipartite quantum systems under the group of Local Unitary transformations, $\mathrm{LU} = \mathrm{SU}(d_1) \times \cdots \times \mathrm{SU}(d_n)$. In quantum information theory one also considers a larger set of transformations, called LOCC transformations (Local Operations with Classical Communication), which includes local unitaries and measurement operations (coordinated by classical communication). Under LOCC two quantum states are equivalent if they can be exactly interconverted by LU operations[1]. However, the SLOCC equivalence also has a physical meaning as explained in [12, 36]. It corresponds to an equivalence between states that can be interconverted into each other but not with certainty. Another feature of SLOCC is that if we consider measure of entanglement, the amount

1 Physically one may imagine that each part of the system is in a different location and experimentalists only apply local quantum transformations, i.e. some unitaries defined by local Hamiltonians.

of entanglement may increase or decrease under SLOCC while it is invariant under LU and non-increasing under LOCC. However, entanglement cannot be created or destroyed by SLOCC and a communication protocol based on a quantum state $|\psi_1\rangle$ can also be achieved with a SLOCC equivalent state $|\psi_2\rangle$ (eventually with different probability of success). In this sense SLOCC equivalence is more a qualitative way of separating non equivalent quantum states.

The set of separable, or non-entangled, states is the set of quantum states $|\psi\rangle$ which can be factorized, i.e.

$$|\psi\rangle = |\psi_1\rangle \otimes \cdots \otimes |\psi_n\rangle \text{ with } |\psi_k\rangle \in \mathbb{C}^{d_k}. \tag{5}$$

In algebraic geometry the projectivization of this set is a well-known algebraic variety[2] of $\mathbb{P}(\mathcal{H})$, known as the Segre embedding of the product of projective spaces $\mathbb{P}^{d_1-1} \times \cdots \times \mathbb{P}^{d_n-1}$.

More precisely, let us consider the following map,

$$\begin{array}{rccc} Seg: & \mathbb{P}^{d_1-1} \times \cdots \times \mathbb{P}^{d_n-1} & \to & \mathbb{P}^{d_1 \times \cdots \times d_n - 1} = \mathbb{P}(\mathcal{H}) \\ & ([\psi_1], \ldots, [\psi_n]) & \mapsto & [\psi_1 \otimes \cdots \otimes \psi_n]. \end{array} \tag{6}$$

The image of this map is the Segre embedding of the product of projective spaces and clearly coincides with X_{Sep}, the projectivization of the set of separable states. We will thus write

$$X_{Sep} = \mathbb{P}^{d_1-1} \times \cdots \times \mathbb{P}^{d_n-1} \subset \mathbb{P}(\mathcal{H}). \tag{7}$$

The Segre variety has the property to be the only closed orbit of $\mathbb{P}(\mathcal{H})$ for the SLOCC action. Up to local invertible transformations every separable state $|\psi\rangle = |\psi_1\rangle \otimes \cdots \otimes |\psi_n\rangle$ can be transformed to $|0\rangle \otimes \cdots \otimes |0\rangle = |0 \ldots 0\rangle$ if we assume that each vector space $\mathbb{C}^{d_i}$ is equipped with a basis denoted by $|0\rangle, \ldots, |d_i - 1\rangle$,

$$X_{Sep} = \mathbb{P}^{d_1-1} \times \cdots \times \mathbb{P}^{d_n-1} = \mathbb{P}(\text{SLOCC}.\,|0 \ldots 0\rangle) \subset \mathbb{P}(\mathcal{H}). \tag{8}$$

A quantum state $|\psi\rangle \in \mathcal{H}$ is entangled iff it is not separable, i.e.

$$|\psi\rangle \text{ entangled } \Leftrightarrow [\psi] \in \mathbb{P}(\mathcal{H} \setminus X_{Sep}). \tag{9}$$

In algebraic geometry, it is usual to study properties of X by introducing auxiliary varieties, i.e. varieties built from the knowledge of X, whose attributes (dimension, degree) will tell us something about the geometry of X.

Let us first introduce two auxiliary varieties of importance for quantum information and entanglement: the secant and tangential varieties.

2 In this thesis an algebraic variety will always be the zero locus of a collection of homogeneous polynomials [47].

Definition 2.1.1. *Let $X \subset \mathbb{P}(V)$ be a projective algebraic variety, the secant variety of X is the Zariski closure of the union of secant lines, i.e.*

$$\sigma_2(X) = \overline{\cup_{x,y \in X} \mathbb{P}^1_{xy}}, \tag{10}$$

where $\mathbb{P}^1_{xy}$ is the projective line corresponding to the projectivization of the linear span $Span(\hat{x}, \hat{y}) \subset V$ (a 2-dimensional linear subspace of V).

Remark 2.1.1. This definition can be extended to higher dimensional secant varieties. More generally, one may define the kth-secant variety of X,

$$\sigma_k(X) = \overline{\cup_{x_1,\ldots,x_k \in X} \mathbb{P}^{k-1}_{x_1,\ldots,x_k}}, \tag{11}$$

where now $\mathbb{P}^{k-1}_{x_1,\ldots,x_k}$ is a projective subspace of dimension $k-1$ obtained as the projectivization of the linear span $\mathrm{Span}(\hat{x}_1, \ldots, \hat{x}_k) \subset V$. If X is not contained in a linear subspace of $\mathbb{P}(V)$, there is a natural sequence of inclusions given by $X \subset \sigma_2(X) \subset \sigma_3(X) \subset \cdots \subset \sigma_q(X) = \mathbb{P}(V)$, where q is the smallest integer such that the qth secant variety fills the ambient space.

Remark 2.1.2. The notion of secant varieties is deeply connected to the notion of rank of tensors. One says that a tensor $T \in \mathbb{C}^{d_1} \otimes \cdots \otimes \mathbb{C}^{d_n}$ has rank r iff r is the smallest integer such that $T = T_1 + \cdots + T_r$ and each tensor T_i can be factorized, i.e. $T_i = a^i_1 \otimes \cdots \otimes a^i_n$. From the definition one sees that the Segre variety $\mathbb{P}^{d_1-1} \times \cdots \times \mathbb{P}^{d_n-1}$ corresponds to the projectivization of rank-one tensors of $\mathcal{H}$ and the secant variety of the Segre is the Zariski closure of the (projectivization of) rank -two tensors because a generic point of $\sigma_2(\mathbb{P}^{d_1-1} \times \cdots \times \mathbb{P}^{d_n-1})$ is the sum of two rank-one tensors. Similarly the definition implies that $\sigma_k(\mathbb{P}^{d_1-1} \times \cdots \times \mathbb{P}^{d_n-1})$ is the algebraic closure of the set of rank at most k tensors. Tensors (states) which belong to $\sigma_k(\mathbb{P}^{d_1-1} \times \cdots \times \mathbb{P}^{d_n-1}) \backslash \sigma_{k-1}(\mathbb{P}^{d_1-1} \times \cdots \times \mathbb{P}^{d_n-1})$ will be called tensors (states) of border rank k, i.e. they can be expressed as (limits) of rank-k tensors.

Another auxiliary variety of importance is the tangential variety, i.e. the union of tangent spaces. When $x \in X$ is a smooth point of the variety, I denote by $T_x X$ the projective tangent space and $\hat{T}_x X$ its cone in $\mathcal{H}$ (see [63, Chapter 3]).

Definition 2.1.2. *Let $X \subset \mathbb{P}(V)$ be a smooth projective algebraic variety, the tangential variety of X is defined by*

$$\tau(X) = \cup_{x \in X} T_x X, \tag{12}$$

(here the smoothness of X implies that the union is closed).

The auxiliary varieties built from X_{Sep} are of importance to understand the entanglement stratification of Hilbert spaces of pure quantum systems under SLOCC for mainly two reasons. First, the auxiliary varieties are SLOCC invariant by construction because X_{Sep} is

a SLOCC-orbit. Thus the construction of auxiliary varieties from the core set of separable states X_{Sep} produces a stratification of the ambient space by SLOCC-invariant algebraic varieties. The possibility to stratify the ambient space by secant varieties was known to geometers more than a century ago [115], but it was noticed to be useful for studying entanglement classes only recently by Heydari [61]. It is equivalent to a stratification of the ambient space by the (border) rank of the states which, as pointed out by Brylinski, can be considered as an algebraic measure of entanglement [23].

The second interesting aspect of those auxiliary varieties, in particular the secant and tangent ones, is that they may have a nice quantum information interpretation. To be more precise, let us recall the definition of the $|GHZ_n\rangle$ and $|W_n\rangle$ states,

$$|GHZ_n\rangle = \frac{1}{\sqrt{2}}(|0\dots0\rangle + |1\dots1\rangle), \tag{13}$$

$$|W_n\rangle = \frac{1}{\sqrt{n}}(|100\dots0\rangle + |010\dots0\rangle + \dots + |00\dots1\rangle). \tag{14}$$

These states are well-known in quantum information theory [46]. Then we have the following geometric interpretations of the closure of their corresponding SLOCC classes,

$$\overline{SLOCC.[GHZ_n]} = \sigma_2(X_{Sep}) \text{ and } \overline{SLOCC.[W_n]} = \tau(X_{Sep}). \tag{15}$$

It is not difficult to see why the Zariski closure of the SLOCC orbit of the $|GHZ_n\rangle$ state is the secant variety of the set of separable states. Recall that a generic point of $\sigma_2(X_{Sep})$ is a rank 2 tensor. Thus, if $[z]$ is a generic point of $\sigma_2(X_{Sep})$, one has

$$[z] = [\lambda x_1 \otimes x_2 \otimes \dots \otimes x_n + \mu y_1 \otimes y_2 \otimes \dots \otimes y_n], \tag{16}$$

with $x_i, y_i \in \mathbb{C}^{d_i}$. Because $[z]$ is generic we may assume that (x_i, y_i) are linearly independent. Therefore, there exists $g_i \in SL_{d_i}(\mathbb{C})$ such that $g_i.x_i \propto |0\rangle$ and $g_i.y_i \propto |1\rangle$ for all $i \in \{1,\dots,n\}$. Thus we can always find $g \in SLOCC$ such that $[g.z] = [GHZ_n]$.

To see why the tangential variety of the variety of separable states always corresponds to the (projective) orbit closure of the $|W_n\rangle$ state, we need to show that a generic tangent vector of X_{Sep} is always SLOCC equivalent to $|W_n\rangle$. A tangent vector can be obtained by differentiating a curve of X_{Sep}. Let $[x(t)] = [x_1(t) \otimes x_2(t) \otimes \dots \otimes x_n(t)] \subset X_{Sep}$ with $[x(0)] = [x_1 \otimes x_2 \otimes \dots \otimes x_n]$. Because we are considering a generic tangent vector, we assume that for all i, $x_i'(0) = u_i$ and u_i is not colinear to x_i. Then Leibniz's rule insures that

$$[x'(0)] = [u_1 \otimes x_2 \otimes \dots \otimes x_n + x_1 \otimes u_2 \otimes \dots \otimes x_n + \dots + x_1 \otimes x_2 \otimes \dots \otimes u_n]. \tag{17}$$

Let us consider $g_i \in SL_{d_i}(\mathbb{C})$ such that $g_i.x_i \propto |0\rangle$ and $g_i.u_i \propto |1\rangle$, then we obtain $[g.x'(0)] = [W_n]$ for $g = (g_1, \ldots, g_n)$.

An important result regarding the relationship between tangent and secant varieties is due to Fulton and Hansen [41, 124].

Theorem 1 ([41]). *Let $X \subset \mathbb{P}(V)$ be a projective algebraic variety of dimension d. Then one of the following two properties holds,*

1. $\dim(\sigma_2(X)) = 2d + 1$ *and* $\dim(\tau(X)) = 2d$,
2. $\dim(\sigma_2(X)) \leqslant 2d$ *and* $\tau(X) = \sigma_2(X)$.

To get information from Fulton and Hansen's Theorem one needs to compute the dimension of the secant variety of X. This can be done by an old geometrical result from the beginning of the XXth century known as Terracini's Lemma.

Lemma 1 (Terracini's Lemma). *Let $[z] \in \sigma_2(X)$ with $[z] = [x + y]$ and $([x], [y]) \in X \times X$ be a general pair of points. Then*

$$\hat{T}_{[z]}\sigma_2(X) = \hat{T}_{[x]}X + \hat{T}_{[y]}X. \tag{18}$$

Terracini's Lemma tells us that if X is of dimension d, the expected dimension of $\sigma_2(X)$ is $2(d+1) - 1 = 2d + 1$. Thus by Theorem 1, one knows that if $\sigma_2(X)$ has the expected dimension then the tangential variety is a proper subvariety of $\sigma_2(X)$ and otherwise both varieties are the same.

Example 2.1.1. *Let us look at the case where $X_{Sep} = \mathbb{P}^1 \times \mathbb{P}^1 \times \mathbb{P}^1 \subset \mathbb{P}^7$. The dimension of $\sigma_2(X_{Sep})$ can be obtained as a simple application of Terracini's Lemma. Let $[x] = [\phi_1 \otimes \phi_2 \otimes \phi_3] \in X_{Sep}$ then $\hat{T}_{[x]}X_{Sep} = \mathbb{C}^2 \otimes \phi_2 \otimes \phi_3 + \phi_1 \otimes \mathbb{C}^2 \otimes \phi_3 + \phi_1 \otimes \phi_2 \otimes \mathbb{C}^2$. Thus one gets for $[GHZ] = [|000\rangle + |111\rangle] \in \sigma_2(X_{Sep})$,*

$$\begin{aligned} \hat{T}_{[GHZ]}\sigma_2(X_{Sep}) &= \hat{T}_{[|000\rangle]}X_{Sep} + \hat{T}_{[|111\rangle]}X_{Sep} \\ &= \mathbb{C}^2 \otimes |0\rangle \otimes |0\rangle + |0\rangle \otimes \mathbb{C}^2 \otimes |0\rangle + |0\rangle \otimes |0\rangle \otimes \mathbb{C}^2 \\ &\quad + \mathbb{C}^2 \otimes |1\rangle \otimes |1\rangle + |1\rangle \otimes \mathbb{C}^2 \otimes |1\rangle + |1\rangle \otimes |1\rangle \otimes \mathbb{C}^2. \end{aligned} \tag{19}$$

Therefore $\dim(\hat{T}_{[GHZ]}\sigma_2(X_{Sep})) = 8$, *i.e.* $\dim(\sigma_2(X_{Sep})) = 7$.

2.2 THE THREE-QUBIT CLASSIFICATION

The problem of the classification of multipartite quantum systems got a lot of attention after Dür, Vidal and Cirac's paper [36] on the classification of three-qubit states where it was first shown that two quantum states can be entangled in two genuine non-equivalent ways. The authors showed that for three-qubit systems there are exactly 6 SLOCC orbits whose representatives can be chosen to be: $|Sep\rangle = |000\rangle$, $|B_1\rangle =$

$\frac{1}{\sqrt{2}}(|000\rangle + |011\rangle)$, $|B_2\rangle = \frac{1}{\sqrt{2}}(|000\rangle + |101\rangle)$, $|B_3\rangle = \frac{1}{\sqrt{2}}(|000\rangle + |110\rangle)$, $|W_3\rangle = \frac{1}{\sqrt{3}}(|100\rangle + |010\rangle + |001\rangle)$ and $|GHZ_3\rangle = \frac{1}{\sqrt{2}}(|000\rangle + |111\rangle)$.

The state $|Sep\rangle$ is a representative of the orbit of separable states and the states $|B_i\rangle$ are bi-separable. The only genuinely entangled states are $|W_3\rangle$ and $|GHZ_3\rangle$. It turns out that this orbit classification of the Hilbert space of three qubits was known long before the famous paper of Dür, Vidal and Cirac from different mathematical perspectives (see for example [96, 44]). Probably the oldest mathematical proof of this result goes back to the work of Le Paige (1881) who classified the trilinear binary forms under (local) linear transformations in [74]. With this new context coming from [36], these classification problems regained a lot of interest in the quantum information literature.

From a geometrical point of view the existence of two distinguished orbits corresponding to $|W_3\rangle$ and $|GHZ_3\rangle$ can be obtained as a consequence of Theorem 1. Indeed, in Example 2.1.1 one shows that the secant variety of the variety of separable three-qubit states has the expected dimension and fills the ambient space. According to Fulten and Hansen's Theorem this implies that the tangential variety $\tau(X_{Sep})$ is a codimension-one subvariety of $\sigma_2(X_{Sep}) = \mathbb{P}^7$ and therefore both orbits are distinguished. In other words, from a geometrical perspective there exists two non-equivalent genuinely entangled states for the three-qubit system because the secant variety of the set of separable states has the expected dimension and fills the ambient space (see Chapter 5 for a generalization of this argument).

In this language of auxiliary varieties let us mention that the orbit closures defined by the bi-separable states $|B_i\rangle$ have also a geometric interpretation. For instance, $|B_1\rangle = |0\rangle \otimes \frac{1}{\sqrt{2}}(|00\rangle + |11\rangle) = |0\rangle \otimes |EPR\rangle$. The projective orbit closure is

$$\mathbb{P}(\overline{\mathrm{SLOCC}.|B_1\rangle}) = \mathbb{P}^1 \times \mathbb{P}^3 \subset \mathbb{P}^7, \tag{20}$$

where $\mathbb{P}^3 = \sigma_2(\mathbb{P}^1 \times \mathbb{P}^1)$. The geometric stratification by SLOCC invariant algebraic varieties in the 3-qubit case can be represented as in Figure 3.

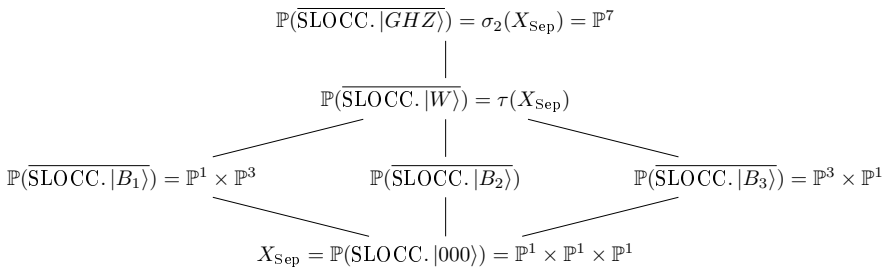

Figure 3: Stratification of the (projectivized) Hilbert space of three qubits by SLOCC-invariant algebraic varieties (the secant and tangent).

Remark 2.2.1. An alternative geometric interpretation of the three-qubit classification can be obtained by introducing another type of auxiliary variety: the dual variety of the variety of separable states. For a given algebraic variety $X \subset \mathbb{P}(V)$, the dual variety is the closure of the set of tangent hyperplanes. More precisely,

$$X^* = \overline{\{H \in \mathbb{P}(V^*), \exists x \in X_{\text{smooth}}, T_x X \subset H\}}. \tag{21}$$

If one considers $X = X_{\text{Sep}}$, then by construction X^* will be SLOCC invariant. In fact, in the case of three qubits, X^* is a hypersurface defined by the so-called Cayley hyperdeterminant [44]. The singular locus of this hypersurface is also SLOCC invariant and we can provide a SLOCC stratification of the (dual) Hilbert space using this idea. This was, in fact, explored by Miyake in a series of papers [89, 90, 91] and lately reconsidered in [54, 57, 51]. I will get back to dual varieties in Chapter 4.

Remark 2.2.2. This idea of introducing auxiliary varieties to describe SLOCC classes of entanglement also appears in [109, 111].

2.3 MORE AUXILIARY VARIETIES AND MULTIPARTITE QUANTUM SYSTEMS

The secant and tangential varieties are examples of auxiliary varieties, i.e. varieties built from the knowledge of a variety X. I define now more of such varieties to be able to describe more entanglement stratas from the knowledge of $X_{\text{Sep}} = \mathbb{P}^{n_1-1} \times \dots \mathbb{P}^{n_k-1} \subset \mathbb{P}^{n_1 \dots n_k - 1}$. The following two definitions generalize the notions of secant and tangent of Section 2.1.

Definition 2.3.1. *Let X and Y be two projective algebraic varieties such that $Y \subset X$; the join of X and Y is*

$$J(X, Y) = \overline{\bigcup_{x \in X, y \in Y, x \neq y} \mathbb{P}^1_{xy}}. \tag{22}$$

The join generalizes the notion of secant variety as we have $J(X, X) = \sigma(X)$. If we define by induction $J(Y_1, \dots, Y_k) = J(Y_1, J(Y_2, \dots, Y_k))$ one also recovers the notion of k-th secant variety of X by considering the join of k copies of X.

$$\sigma_k(X) = J(X, \dots, X) \tag{23}$$

We can also generalize the notion of tangential varieties. Suppose $Y \subset X$ and let $T^\star_{X,Y,y_0}$ denote the union of $\mathbb{P}^1_*$'s where $\mathbb{P}^1_*$ is the limit of $\mathbb{P}^1_{xy}$ with $x \in X$, $y \in Y$ and $x, y \to y_0 \in Y$. If $Y = X$ and y_0 is a smooth point, then $T^\star_{X,X,y_0}$ is nothing but the projection of the affine

tangent space of $\hat{X}$ at $\hat{y}_0$. The union of the $T^{\star}_{X,Y,y_0}$ is defined as the variety of relative tangent stars [124] of X with respect to Y:

$$T(Y,X) = \bigcup_{y \in Y} T^{\star}_{X,Y,y}. \tag{24}$$

For $Y = X$ one recovers the notion of tangential variety. The following Theorem is the analogue of Theorem 1 and is due to Fyodor Zak [124, Chapter I Theorem 1.4].

Theorem 2. *An arbitrary irreducible subvariety $Y^n \subset X^m, n \geqslant 0$, satisfies one of the following two conditions:*

1. *$dim(J(X,Y)) = n + m + 1$ and $dim(T(X,Y)) = n + m$;*
2. *$J(X,Y) = T(X,Y)$.*

There is a version of Terracini's Lemma for join varieties and varieties of relative tangent stars (see Ivey and Landsberg [63, Chapter III]).

Lemma 2. *[Terracini's Lemma] If $z \in J(X,Y)_{smooth}$ with $z = [\hat{x} + \hat{y}]$ such that $x \in X_{smooth}$, $y \in Y_{smooth}$, then*

$$\widehat{T}_z J(X,Y) = \widehat{T}_x X + \widehat{T}_y Y. \tag{25}$$

The following definition makes the idea of "partial" secant for multipartite systems more precise.

Definition 2.3.2. *Let $Y_i \subset \mathbb{P}^{n_i}$, $1 \leqslant i \leqslant m$ be m nondegenerate varieties and let us consider $X = Y_1 \times Y_2 \times \cdots \times Y_m \subset \mathbb{P}^{(n_1+1)(n_2+1)\ldots(n_m+1)-1}$ the corresponding Segre product. For $J = \{j_1, \ldots, j_k\} \subset \{1, \ldots, m\}$, a J-pair of points of X will be a pair $(x,y) \in X \times X$ such that $x = [v_1 \otimes v_2 \otimes \cdots \otimes v_{j_1} \otimes v_{j_1+1} \otimes \cdots \otimes v_{j_2} \otimes \cdots \otimes v_{j_k} \otimes \cdots \otimes v_m]$ and $y = [w_1 \otimes w_2 \otimes \cdots \otimes v_{j_1} \otimes w_{j_1+1} \otimes \cdots \otimes v_{j_2} \otimes \cdots \otimes v_{j_k} \otimes \cdots \otimes w_m]$, i.e. the tensors $\hat{x}$ and $\hat{y}$ have colinear components for the indices in J.*

The J-subsecant variety of $\sigma_2(X)$, denoted by $\sigma_2(Y_1 \times \cdots \times \underline{Y}_{j_1} \times \cdots \times \underline{Y}_{j_k} \times \cdots \times Y_m) \times Y_{j_1} \times Y_{j_2} \times \cdots \times Y_{j_k}$, is the closure of the union of line $\mathbb{P}^1_{xy}$ with (x,y) a J-pair of points:

$$\sigma_2(Y_1 \times \cdots \times \underline{Y}_{j_1} \times \cdots \times \underline{Y}_{j_k} \times \cdots \times Y_m) \times Y_{j_1} \times Y_{j_2} \times \cdots \times Y_{j_k} = \overline{\bigcup_{(x,y) \in X \times X, (x,y)\, J-pair\ of\ points} \mathbb{P}^1_{xy}}. \tag{26}$$

Remark 2.3.1. In the notation of the J-subsecant varieties, the underlined varieties correspond to the common components for the points which define a J-pair. Roughly speaking, those components are the "common factor" of x and y in the decomposition of $z = x + y \in$

$\sigma_2(Y_1 \times \cdots \times \underline{Y}_{j_1} \times \cdots \times \underline{Y}_{j_k} \times \cdots \times Y_m) \times Y_{j_1} \times Y_{j_2} \times \cdots \times Y_{j_k}$. For instance, when we consider the $\{1\}$-subsecant (respectively the $\{m\}$-subsecant) variety we can indeed factorize the first (respectively the last) component and we have the equality $\sigma_2(\underline{Y}_1 \times Y_2 \times \cdots \times Y_m) \times Y_1 = Y_1 \times \sigma_2(Y_2 \times \cdots \times Y_m)$.

Using the classification tensors of $\mathbb{C}^2 \otimes \mathbb{C}^2 \otimes \mathbb{C}^{n+1}$ of Parfenov [96] one can provide a geometric description of the entanglement classes for $2 \times 2 \times (n+1)$ quantum systems via auxiliary varieties. For an alternative description of those systems using the stratification by duals, see [90].

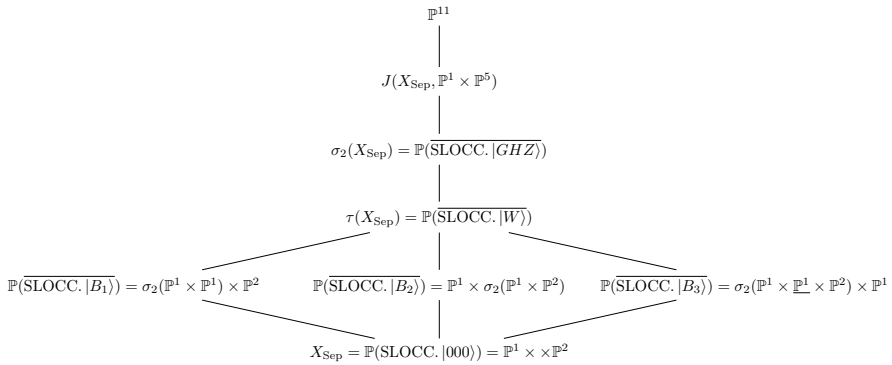

Figure 4: Stratification of the ambient space for the $2 \times 2 \times 3$ quantum system by auxiliary varieties.

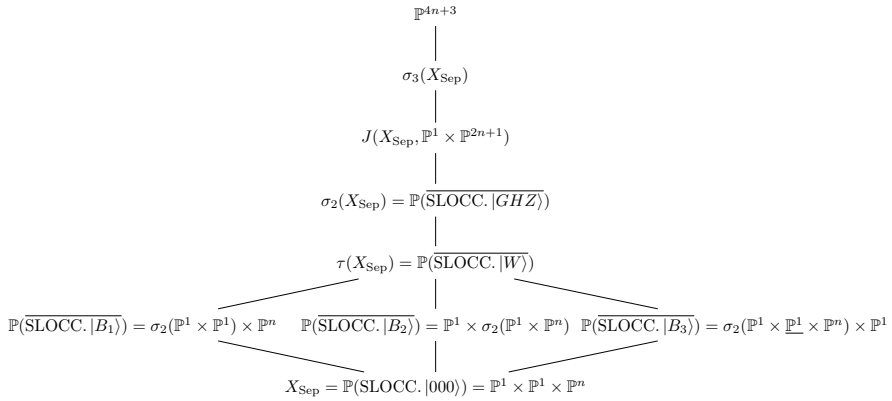

Figure 5: Stratification of the ambient space for the $2 \times 2 \times (n+1)$, $n \geqslant 3$, quantum system by auxiliary varieties.

3

ENTANGLEMENT ATLAS (SOME EXAMPLES)

This idea of introducing auxiliary varieties to describe SLOCC classes of entanglement allows one to connect the study of entanglement in quantum information to a large literature in mathematics, geometry and their applications. For instance, the question of finding defining equations of auxiliary varieties is central to many areas of applications of mathematics to computer science, signal processing or phylogenetics (see the introduction of [70] and the references therein). Those equations can be obtained by mixing techniques from representation theory and geometry [72, 73, 94]. In the context of quantum information finding defining equations of auxiliary varieties provides tests to decide if two states could be SLOCC equivalent. Classical invariant theory also provides tools to generate invariant and covariant polynomials [20, 21, 86, 87]. With my co-authors Jean-Gabriel Luque and Jean-Yves Thibon we used these techniques in [54, 55, 56] to identify entanglement classes with auxiliary varieties as I now explain.

3.1 THE THREE-QUBIT CASE FROM CLASSICAL INVARIANT THEORY PERSPECTIVE

In order to provide algorithms to separate the orbits given by Figure 3, one needs to consider more than only invariant polynomials. Indeed, in the three-qubit case, the algebra of invariant polynomials for the SLOCC $(SL_2\mathbb{C} \times SL_2\mathbb{C} \times SL_2\mathbb{C})$ action is generated by only one polynomial, i.e. $\mathbb{C}[\mathcal{H}]^{\text{SLOCC}} = \mathbb{C}[\Delta]$ where Δ is the equation of the tangential variety $\tau(\mathbb{P}^1 \times \mathbb{P}^1 \times \mathbb{P}^1)$, also known as the Cayley hyperdeterminant (see Chapter 4 and [43, 44]). By introducing auxiliary binary variables x_i, y_i, z_i, with $i \in \{0, 1\}$, spanning the vector spaces $V_x^* = (\mathbb{C}^2)^*$, $V_y = (\mathbb{C}^2)^*$ and $V_z = (\mathbb{C}^2)^*$, one may consider the algebra of covariant polynomials $\text{Cov} = \mathbb{C}[\mathcal{H} \otimes V_x^* \otimes V_y^* \otimes V_z^*]^{\text{SLOCC}}$. A covariant is, therefore, a polynomial $P(|\psi\rangle, \mathbf{x}, \mathbf{y}, \mathbf{z})$ depending on the tensor $|\psi\rangle \in \mathcal{H}$ and auxiliary variables which is left invariant by the following action

$$\forall g = (g_1, g_2, g_3) \in \text{SLOCC}, g(|\psi\rangle, \mathbf{x}, \mathbf{y}, \mathbf{z}) = (g.|\psi\rangle, g_1^{-1}.\mathbf{x}, g_2^{-1}.\mathbf{y}, g_3^{-1}.\mathbf{z}). \tag{27}$$

The simplest covariant associated to a three-qubit state is the ground form:

$$f(|\psi\rangle, \mathbf{x}, \mathbf{y}, \mathbf{z}) = \sum_{i,j,k\in\{0,1\}} a_{ijk} x_i y_j z_k \text{ where } |\psi\rangle = \sum_{i,j,k\in\{0,1\}} a_{ijk} |ijk\rangle . \tag{28}$$

In 1881, Le Paige [74] found a complete system of covariants for the space of binary trilinear forms. It includes the ground form f and three quadratic forms

$$B_x(x) = \det\left(\frac{\partial^2 f}{\partial y_i \partial z_j}\right)_{0\leqslant i,j\leqslant 1}, \tag{29}$$

$$B_y(y) = \det\left(\frac{\partial^2 f}{\partial x_i \partial z_j}\right)_{0\leqslant i,j\leqslant 1}, \tag{30}$$

and

$$B_z(z) = \det\left(\frac{\partial^2 f}{\partial x_i \partial y_j}\right)_{0\leqslant i,j\leqslant 1}. \tag{31}$$

A trilinear form is obtained by computing any of the three Jacobians of f with one of the quadratic forms, which turns out to be the same

$$C(x,y,z) = \begin{vmatrix} \frac{\partial f}{\partial x_0} & \frac{\partial f}{\partial x_1} \\ \frac{\partial B_x}{\partial x_0} & \frac{\partial B_x}{\partial x_1} \end{vmatrix}. \tag{32}$$

The three quadratic forms B_x, B_y and B_z have the same discriminant, which is nothing but Δ, the unique invariant of the algebra $\mathbb{C}[\mathcal{H}]^{\mathrm{SLOCC}}$. The generators of the covariant algebra satisfy a syzygy relation

$$C^2 + \frac{1}{2}B_x B_y B_z + \Delta f^2 = 0. \tag{33}$$

To any three-qubit state $|\psi\rangle$ we now associate the vector

$$v_\psi := \langle [B_x], [B_y], [B_z], [C], [\Delta]\rangle, \tag{34}$$

where $[P] = 0$ if $P(|\psi\rangle, \mathbf{x}, \mathbf{y}, \mathbf{z}) = 0$ and $[P] = 1$ if $P(|\psi\rangle, \mathbf{x}, \mathbf{y}, \mathbf{z}) \neq 0$. The evaluation of v_ψ is now enough to distinguish between the different orbits (see Table 1).

Variety (orbit closure)	Representatives $\lvert\_\rangle$	v_ψ
$\sigma(X_{\mathrm{Sep}}) = \mathbb{P}^7$	$\lvert 000\rangle + \lvert 111\rangle$	$\langle 1,1,1,1,1\rangle$
$\tau(X_{\mathrm{Sep}})$	$\lvert 001\rangle + \lvert 010\rangle + \lvert 100\rangle$	$\langle 1,1,1,1,0\rangle$
$\mathbb{P}^3 \times \mathbb{P}^1$	$\lvert 111\rangle + \lvert 001\rangle$	$\langle 0,0,1,0,0\rangle$
$\mathbb{P}^1 \times \mathbb{P}^3$	$\lvert 111\rangle + \lvert 100\rangle$	$\langle 1,0,0,0,0\rangle$
$\sigma(\mathbb{P}^1 \times \mathbb{P}^1 \times \mathbb{P}^1) \times \mathbb{P}^1$	$\lvert 111\rangle + \lvert 010\rangle$	$\langle 0,1,0,0,0\rangle$
$X_{\mathrm{Sep}} = \mathbb{P}^1 \times \mathbb{P}^1 \times \mathbb{P}^1$	$\lvert 111\rangle$	$\langle 0,0,0,0,0\rangle$

(35)

Table 1: The covariant algorithm to identify SLOCC classes in the three-qubit case.

Remark 3.1.1. Figure 3 and Table 1 furnish the geometric atlas and the corresponding algorithm in the famous three-qubit case. In the next sections we develop the same approach to study more interesting examples.

3.2 CAYLEY OMEGA PROCESS FOR QUANTUM INFORMATION

The description of the invariant/covariant algebras is an old subject of classical invariant theory, but got a regain of interest at the beginning of the XXI st century when these concepts appeared to be useful to separate SLOCC classes of entanglement as illustrated with Table 1 of the previous section. New examples of invariants for quantum information classification were found by Jean-Gabriel Luque and Jean-Yves Thibon [86, 87]. Together with Emmanuel Briand they found a complete system of covariants for the four-qubit case [20] and for the three-qutrit case with Frank Verstraete [21]. The principle and methodology of their work is explained in detail in the *Habilitation thesis* of Jean-Gabriel Luque [85]. I do not reproduce here the full methodology, but just recall the main steps followed to find the generators of the concomitant algebra $\mathbb{C}[\mathcal{H} \otimes V_1^* \otimes \cdots \otimes V_k^*]^{\mathrm{SLOCC}}$:

1. Compute (when possible) the Hilbert series of the algebra to have some *a priori* information on the degree and number of generators,
2. Apply the Cayley-Omega process starting from the ground form $f = \sum_{i_1,\ldots i_k} a_{i_1\cdots k} x^1_{i_1} \ldots x^k_{i_k}$ to generate new concomitants.
3. Simplify the set of concomitants by considering relations.

I only recall here the principle of the Cayley-Omega process that has been used to compute the covariants and concomitants. The Cayley-Omega process consists of applying iteratively the transvection operator. The transvection of two multi-binary forms on the binary variables $x^{(1)} = (x_0^{(1)}, x_1^{(1)}), \ldots, x^{(p)} = (x_0^{(p)}, x_1^{(p)})$ is defined by

$$(f, g)_{i_1,\ldots,i_p} = \mathrm{tr}\Omega^{i_1}_{x^{(1)}} \ldots \Omega^{i_p}_{x^{(p)}} f(x'^{(1)}, \ldots, x'^{(p)}) g(x''^{(1)}, \ldots, x''^{(p)}), \tag{36}$$

where Ω is the Cayley operator

$$\Omega_x = \begin{vmatrix} \frac{\partial}{\partial x'_0} & \frac{\partial}{\partial x''_0} \\ \frac{\partial}{\partial x'_1} & \frac{\partial}{\partial x''_1} \end{vmatrix} \tag{37}$$

and tr sends each variable x', x'' to x (erases $'$ and $''$).

Gordan's algorithm shows that for binary multilinear forms a complete set of invariants can be obtained by applying a finite number of transvections starting from the ground form.

Such an algorithm could be stated as follow. Let us denote by $\mathcal{S}$ the set of covariants.

1. $\mathcal{S} \leftarrow f$, the ground form is the only covariant of degree one.
2. Generate all possible covariants of degree d, $(f, C)^{i_1,\ldots,i_k}$, where C is a covariant of degree $d-1$ already calculated.

3. Simplify all new covariants of degree d which are not an algebraic combination of covariants of degree less than $d-1$ and add those new invariants to $\mathcal{S}$.

4. If there are no new invariants of degree d other than algebraic combinations of covariants of degree less than $d-1$, then stop the algorithm.

Remark 3.2.1. As already mentioned, a complete set of covariants can be obtained for multiqubit systems by Gordan's algorithm[1]. But for multiqudit systems one may need more concomitants. For example, if one particle of the system is a qutrit, one has to consider a ternary contravariant variable $\zeta = (\zeta_0, \zeta_1, \zeta_2)$ and one uses an adapted version of the transvection:

$$(f, g, h)^{\ell}_{i,j,k} = \mathrm{tr}\Omega^i_x \Omega^j_y \Omega^k_z \Omega^{\ell}_{\zeta} f(x', y', z', \xi') g(x'', y'', z'', \zeta'') h(x''', y''', z''', \zeta''')$$

where

$$\Omega_p = \begin{vmatrix} \frac{\partial}{\partial p'_0} & \frac{\partial}{\partial p''_0} \\ \frac{\partial}{\partial p'_1} & \frac{\partial}{\partial p''_1} \end{vmatrix}$$

for $p = x$, or $p = y$,

$$\Omega_p = \begin{vmatrix} \frac{\partial}{\partial p'_0} & \frac{\partial}{\partial p''_0} & \frac{\partial}{\partial p'''_0} \\ \frac{\partial}{\partial p'_1} & \frac{\partial}{\partial p''_1} & \frac{\partial}{\partial p'''_1} \\ \frac{\partial}{\partial p'_2} & \frac{\partial}{\partial p''_2} & \frac{\partial}{\partial p'''_2} \end{vmatrix}$$

if $p = z$ or $p = \zeta$ and tr is the mapping which erases the symbols $'$, $''$ and $'''$, as previously. One used this adaptation of the transvection operation in [54] to generate concomitants of the $2 \times 2 \times 3$ and $2 \times 3 \times 3$ quantum systems.

For example, in the $2 \times 2 \times 3$ case, the entanglement classes of Figure 4 can be distinguished by concomitants. Starting from the ground form which is of degree one,

$$f = \sum_{i=0}^{1} \sum_{j,k=0}^{2} a_{ijk} x_i y_j z_k, \tag{38}$$

one applies the Cayley-Omega process to obtain covariants of a higher degree:

1 However, in terms of computational complexity the complete set of covariants is out of reach if one considers more than 4 qubits [87]. The computation of the Hilbert series in the 5-qubit case was achieved by Jean-Gabriel Luque and Jean-Yves Thibon. It says that every 5-qubit invariant polynomial can be expressed as a linear combination of the secondary invariants - there are 3014400 of such - with polynomial coefficients in the primary invariants - there are 17 of such-...

- A covariant of degree 2

$$B = (f, f)_{110} = \det\left(\frac{\partial^2 f}{\partial x_i \partial y_i}\right)_{0\leqslant i,j\leqslant 1}. \tag{39}$$

- A covariant of degree 3

$$C = (f, B)_{001} = \begin{vmatrix} a_{000} & a_{100} & a_{010} & a_{110} \\ a_{001} & a_{101} & a_{011} & a_{111} \\ a_{002} & a_{102} & a_{012} & a_{112} \\ x_1 y_1 & -x_0 y_1 & -x_1 y_0 & x_0 y_0 \end{vmatrix}. \tag{40}$$

- An invariant of degree 4 and two covariants of degree 4

$$\Delta = (C, C)_{110} = \det\left(\frac{\partial^2 C}{\partial x_i \partial y_j}\right), \tag{41}$$

$$D_x = (f, C)_{010} \text{ and } D_y = (f, C)_{100}. \tag{42}$$

Extra concomitants are necessary using the generalization of the transvection operation (Remark 3.2.1),

$$B_{x\zeta} := (f, f, P_\zeta)^0_{1,0,1},\ B_{y\zeta} := (f, f, P_\zeta)^0_{0,1,1} \text{ and } D_\zeta := (B, B, P_\zeta)^0_{2,0,0}, \tag{43}$$

where

$$P_\zeta := \sum_{i=0}^{2} z_i \zeta_i. \tag{44}$$

Let $w_\varphi = \langle [B], [B_{x\zeta}], [B_{y\zeta}], [C], [\Delta], [D_\zeta]\rangle$, we resume the evaluation of w_φ on the various orbits in Table 2.

Normal form (representative)	Variety	w_A
$\|000\rangle + \|011\rangle + \|101\rangle + \|112\rangle$	$\mathbb{P}^{11}$	$\langle 1,1,1,1,1,1\rangle$
$\|000\rangle + \|011\rangle + \|102\rangle$	$J(X_{Sep}, \mathbb{P}^1 \times \mathbb{P}^5)$	$\langle 1,1,1,1,0,1\rangle$
$\|000\rangle + \|111\rangle$	$\sigma_2(X_{Sep})$	$\langle 1,1,1,0,0,1\rangle$
$\|000\rangle + \|011\rangle + \|101\rangle$	$\tau(X_{Sep})$	$\langle 1,1,1,0,0,0\rangle$
$\|000\rangle + \|011\rangle$	$\mathbb{P}^1 \times \sigma_2(\mathbb{P}^1 \times \mathbb{P}^2) \simeq \mathbb{P}^1 \times \mathbb{P}^5$	$\langle 0,1,0,0,0,0\rangle$
$\|000\rangle + \|101\rangle$	$\sigma_2(\mathbb{P}^1 \times \underline{\mathbb{P}^1} \times \mathbb{P}^2) \times \mathbb{P}^1$	$\langle 0,0,1,0,0,0\rangle$
$\|000\rangle + \|110\rangle$	$\sigma_2(\mathbb{P}^1 \times \mathbb{P}^1) \times \mathbb{P}^2 \simeq \mathbb{P}^3 \times \mathbb{P}^2$	$\langle 1,0,0,0,0,0\rangle$
$\|000\rangle$	$X_{Sep} = \mathbb{P}^1 \times \mathbb{P}^1 \times \mathbb{P}^2$	$\langle 0,0,0,0,0,0\rangle$

Table 2: The covariant algorithm to identify SLOCC classes in the $2 \times 2 \times 3$ quantum system.

Table 2 furnishes an algorithm to distinguish the orbit for the $2 \times 2 \times 3$ quantum systems.

Remark 3.2.2. The invariant Δ is the defining equation of $J(X, \overline{\mathcal{O}}_{IV})$. It is also the equation of the dual variety of X_{Sep} also known as the hyperdeterminant of format $2 \times 2 \times 3$ [44]. Dual varieties and entanglement will be discussed in Chapter 4.

3.3 THE FOUR-QUBIT ATLAS (PART I)

The $2 \times 2 \times 2 \times 2$ quantum system, aka the four-qubit case, is more interesting in many respects. First, the corresponding Hilbert space $\mathcal{H} = \mathbb{C}^2 \otimes \mathbb{C}^2 \otimes \mathbb{C}^2 \otimes \mathbb{C}^2$ has infinitely many orbits under the action of $\text{SLOCC} = \text{SL}_2(\mathbb{C})^{\times 4}$. These orbits have been classified by Verstraete and his co-authors [117] into 9 families (6 families are described with parameters) but the classification contains an error which was corrected later by Chen and Djokovic [30]. The four-qubit case has also been investigated within the context of the black-hole/qubit correspondence, a mathematical construction allowing to establish correspondence between entanglement formulas and black-hole entropy formulas [13, 15, 76]. Finally this case is also interesting as it provides an intriguing correspondence between simple singularities of hypersurfaces and entanglement classes, as we discuss in Chapter 4.

The four-qubit algebra of invariant polynomials has been calculated in [86],

$$\mathbb{C}[\mathbb{C}^2 \otimes \mathbb{C}^2 \otimes \mathbb{C}^2 \otimes \mathbb{C}^2]^{\text{SLOCC}} = \mathbb{C}[H, L, M, D_{xy}]. \tag{45}$$

The four generators H, L, M, D are defined as follows, with the ground form being $f = \sum_{i,j,k,l \in \{0,1\}} a_{ijkl} x_i y_j z_k t_l$.

1. One invariant of degree 2:

$$H = a_{0000}a_{1111} - a_{1000}a_{0111} - a_{0100}a_{1011} + a_{1100}a_{0011}$$
$$-a_{0010}a_{1101} + a_{1010}a_{0101} + a_{0110}a_{1001} - a_{1110}a_{0001}.$$

2. Two invariants of degree 4:

$$L := \begin{vmatrix} a_{0000} & a_{0010} & a_{0001} & a_{0011} \\ a_{1000} & a_{1010} & a_{1001} & a_{1011} \\ a_{0100} & a_{0110} & a_{0101} & a_{0111} \\ a_{1100} & a_{1110} & a_{1101} & a_{1111} \end{vmatrix},$$

$$M := \begin{vmatrix} a_{0000} & a_{0001} & a_{0100} & a_{0101} \\ a_{1000} & a_{1001} & a_{1100} & a_{1101} \\ a_{0010} & a_{0011} & a_{0110} & a_{0111} \\ a_{1010} & a_{1011} & a_{1110} & a_{1111} \end{vmatrix}.$$

3. One invariant of degree 6: Set $b_{xy} := \det\left(\frac{\partial^2 f}{\partial z_i \partial t_j}\right)$. This quadratic form is interpreted as a bilinear form on the three dimensional space $\mathrm{Sym}^2(\mathbb{C}^2)$, so we can find a 3×3 matrix B_{xy} satisfying

$$b_{xy} = [x_0^2, x_0x_1, x_1^2]B_{xy}\begin{bmatrix} y_0^2 \\ y_0y_1 \\ y_1^2 \end{bmatrix}.$$

The generator of degree 6 is $D_{xy} := \det(B_{xy})$.

Note that we can alternatively replace L or M by

$$N := -L - M = \begin{vmatrix} a_{0000} & a_{1000} & a_{0001} & a_{1001} \\ a_{0100} & a_{1100} & a_{0101} & a_{1101} \\ a_{0010} & a_{1010} & a_{0011} & a_{1011} \\ a_{0110} & a_{1110} & a_{0111} & a_{1111} \end{vmatrix}$$

and D_{xy} by $D_{xz}, \ldots, D_{zt}$ defined in a similar way with respect to the variables $xz, \ldots, zt$ (see [86]).

In [55] we first considered the geometric orbits of the null-cone, i.e. the algebraic variety $\mathbb{P}(\mathfrak{N}) \subset \mathbb{P}(\mathcal{H})$ defined by the vanishing of all invariants,

$$\mathfrak{N} = \{|\varphi\rangle \in \mathcal{H}, H(\varphi) = L(\varphi) = M(\varphi) = D_{xy}(\varphi) = 0\}. \tag{46}$$

It is known that the number of orbits in $\mathfrak{N}$ is finite and the techniques of [54] can be applied. Moreover, by restricting the amplitudes of the quantum states $|\varphi\rangle$ to $\{0, 1\}$ we were able to recover, by a computer calculation, all the orbits of the null cone. More precisely, like in the previous section, given a state $|\varphi\rangle$ and a covariant P, one sets $P_\varphi = 1$ if the corresponding covariant is nonzero and zero otherwise. Thus, two nilpotent states will belong to two distinguished SLOCC orbits if their evaluations on all the generators of the algebra of covariants differ. Let us define the number of a state $|\varphi\rangle = \sum_{i,j,k,l\in\{0,1\}} a_{ijkl}|ijkl\rangle$ by

$$n_\varphi = \sum_{i,j,k,l\in\{0,1\}} a_{ijkl} 2^{i+2j+4k+8}. \tag{47}$$

Then by evaluating all possible 11662 nilpotent states with amplitudes in $\{0, 1\}$ on the generators of the algebra of covariants reproduced in Appendix A, one obtains 31 distinguished classes whose representatives are given by the corresponding state's number,

$$\{0, 65535, 65520, 65484, 65450, 64764, 64250, 61166, 64160, 61064, 64704, 59624, 59520, 65530, 65518, 65532, 65278, 64700, 65041, 65075, 61158, 65109, 64218, 65508, 64762, 65506, 65482, 65511, 65218, 65271, 65247\}. \tag{48}$$

The adherence graph of those orbits can be obtained by looking at the evaluation on the generators of the covariant algebra. Given two orbit closures of two states $|\varphi_1\rangle$ and $|\varphi_2\rangle$, denoted by $\overline{\mathcal{O}}_{\varphi_1}$ and $\overline{\mathcal{O}}_{\varphi_2}$, one has the inclusion $\overline{\mathcal{O}}_{\varphi_1} \subset \overline{\mathcal{O}}_{\varphi_2}$ if and only if $P_{\varphi_2} = 0$ implies $P_{\varphi_1} = 0$ for all covariants P.

The graph of Figure 6 is directly obtained from the computer calculations.

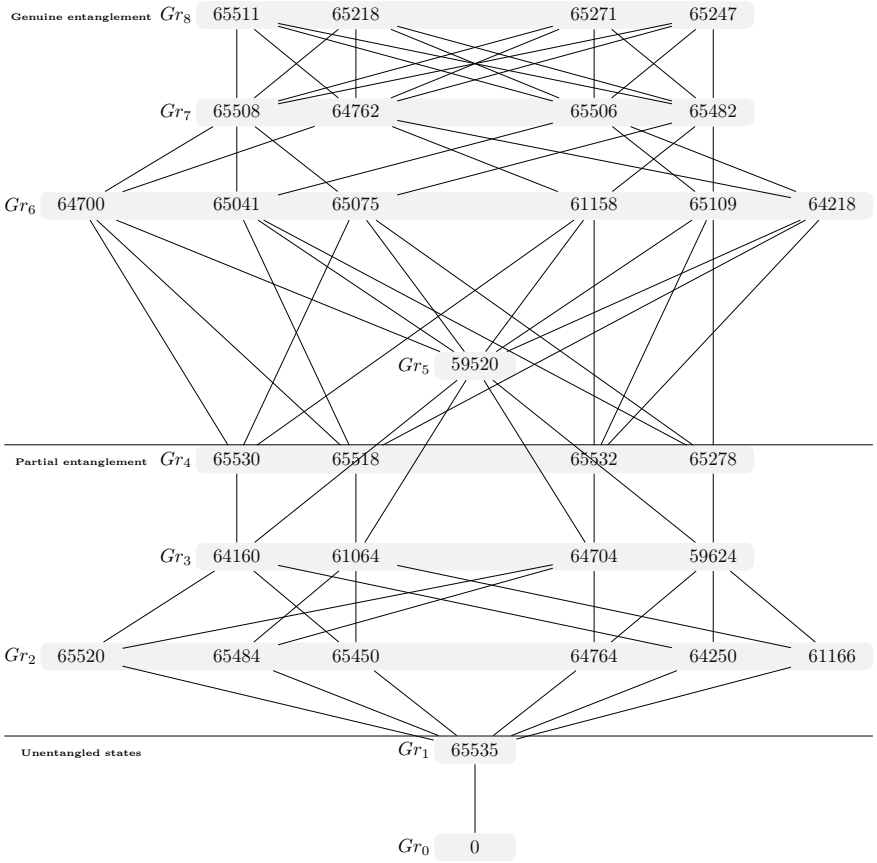

Figure 6: Varieties of the null-cone .

All orbits can be distinguished by using the following set of covariants (see Appendix A),

$$T := \begin{array}{|c|}\hline A \\ \hline B_{2200}, B_{2020}, B_{2002}, B_{0220}, B_{0202}, B_{0022} \\ \hline C_{3111}, C_{1311}, C_{1131}, C_{1113} \\ \hline D_{4000}, D_{0400}, D_{0040}, D_{0004} \\ \hline D_{2200}, D_{2020}, D_{2002}, D_{0220}, D_{0202}, D_{0022} \\ \hline F^1_{2220}, F^1_{2202}, F^1_{2022}, F^1_{0222} \\ \hline L_{6000}, L_{0600}, L_{0060}, L_{0006} \\ \hline \end{array} . \tag{49}$$

Once we have the normal forms given by the previous calculation one can identify the algebraic varieties. This leads to the following theorem proved in [55].

Theorem 3. *The null-cone $\mathcal{N}^{11} \subset \mathbb{P}^{15}$ is the union of 4 irreducible algebraic varieties of dimension 11 and contains 30 non-equivalent classes of (entangled) states*[2] *. The Zariski closure of those classes are algebraic varieties which can be built up by geometric constructions from the set of separable states $X = \mathbb{P}^1 \times \mathbb{P}^1 \times \mathbb{P}^1 \times \mathbb{P}^1 \subset \mathbb{P}^{15}$. The identifications of those algebraic varieties are given in Table 3 (genuine entangled states) and Table 4 (partially entangled states). The stratification of the null-cone by those G-varieties is the adherence graph of Figure 6 (without the trivial orbit).*

Remark 3.3.1. The varieties $\mathrm{Osc}(X_{\mathrm{Sep}})$, $\mathrm{Osc}_J(X_{\mathrm{Sep}})$ and $Z_i(X_{\mathrm{Sep}})$ are auxiliary varieties, introduced in the work of Buczynski and Landsberg [24]. Those auxiliary varieties are built from first- and second-order information.

$$\mathrm{Osc}(X) = \overline{\{x'(0) + x''(0),\ \text{where } x(t) \subset X \text{ is a sufficiently smooth curve}\}}, \tag{50}$$

$$Z(X) = \{x'(0) + y'(0), x(t), y(t) \subset X \text{ two curves such that } \mathbb{P}^1_{x(0)y(0)} \subset X\}. \tag{51}$$

Considering the fact that the first (tangent) and second osculating space of $X_{\mathrm{Sep}} = \mathbb{P}^1 \times \mathbb{P}^1 \times \mathbb{P}^1 \times \mathbb{P}^1$ are given respectively by

$$\hat{T}_{|0000\rangle} X = \underbrace{\mathbb{C}^2 \otimes |000\rangle}_{V_1} + \underbrace{|0\rangle \otimes \mathbb{C}^2 \otimes |00\rangle}_{V_2} + \underbrace{|00\rangle \otimes \mathbb{C}^2 \otimes |0\rangle}_{V_3} + \underbrace{|000\rangle \otimes \mathbb{C}^2}_{V_4}, \tag{52}$$

$$\hat{T}^{(2)}_{|0000\rangle} X = \underbrace{\mathbb{C}^2 \otimes \mathbb{C}^2 \otimes |00\rangle}_{W_1} + \underbrace{\mathbb{C}^2 \otimes |0\rangle \otimes \mathbb{C}^2 \otimes |0\rangle}_{W_2} + \underbrace{\mathbb{C}^2 \otimes |00\rangle \otimes \mathbb{C}^2}_{W_3} \tag{53}$$

$$+ \underbrace{|0\rangle \otimes \mathbb{C}^2 \otimes \mathbb{C}^2 \otimes |0\rangle}_{W_4} + \underbrace{|0\rangle \otimes \mathbb{C}^2 \otimes |0\rangle \otimes \mathbb{C}^2}_{W_5} + \underbrace{|00\rangle \otimes \mathbb{C}^2 \otimes \mathbb{C}^2}_{W_6}, \tag{54}$$

one get subvarieties of $Z(X_{\mathrm{Sep}})$ and $\mathrm{Osc}(X_{\mathrm{Sep}})$ by restricting the possibilities of $x'(0)$ and $x''(0)$. Thus $Z_i(X_{\mathrm{Sep}})$ corresponds to a subset of $Z(X_{\mathrm{Sep}})$ where the curves $x(t)$ and $y(t)$ are such that for $t = 0$ only their ith components of their tensor product are distinct. The varieties $\mathrm{Osc}_J(X_{\mathrm{Sep}})$ correspond to subsets of $\mathrm{Osc}(X_{\mathrm{Sep}})$ such that $x''(0) \in \sum_{i \in J} W_i$. For more explanations and details, see [55].

2 The set of separable states as well as the sets of partially entangled states are part of the orbits.

Name	Variety (orbit closure)	Normal form	dim
65247	$\mathrm{Osc}_{135}(X)$	$\|0001\rangle+\|0010\rangle+\|0100\rangle+\|1000\rangle+\|1100\rangle+\|1001\rangle+\|0101\rangle$	11
65271	$\mathrm{Osc}_{236}(X)$	$\|0001\rangle+\|0010\rangle+\|0100\rangle+\|1000\rangle+\|1010\rangle+\|1001\rangle+\|0011\rangle$	11
65218	$\mathrm{Osc}_{456}(X)$	$\|0001\rangle+\|0010\rangle+\|0100\rangle+\|1000\rangle+\|0110\rangle+\|0101\rangle+\|0011\rangle$	11
65511	$\mathrm{Osc}_{124}(X)$	$\|0001\rangle+\|0010\rangle+\|0100\rangle+\|1000\rangle+\|1100\rangle+\|1010\rangle+\|0110\rangle$	11
65482	$Z_3(X)$	$\|1000\rangle+\|0100\rangle+\|0110\rangle+\|0011\rangle$	10
65506	$Z_2(X)$	$\|1000\rangle+\|0010\rangle+\|1100\rangle+\|0101\rangle$	10
64762	$Z_4(X)$	$\|1000\rangle+\|0100\rangle+\|0101\rangle+\|0011\rangle$	10
65508	$Z_1(X)$	$\|0100\rangle+\|0001\rangle+\|1100\rangle+\|1010\rangle$	10
64218	$\mathrm{Osc}_5(X)$	$\|0000\rangle+\|1000\rangle+\|0100\rangle+\|0010\rangle+\|0001\rangle+\|0101\rangle$	9
65109	$\mathrm{Osc}_4(X)$	$\|0000\rangle+\|1000\rangle+\|0100\rangle+\|0010\rangle+\|0001\rangle+\|0110\rangle$	9
61158	$\mathrm{Osc}_6(X)$	$\|0000\rangle+\|1000\rangle+\|0100\rangle+\|0010\rangle+\|0001\rangle+\|0011\rangle$	9
65075	$\mathrm{Osc}_2(X)$	$\|0000\rangle+\|1000\rangle+\|0100\rangle+\|0010\rangle+\|0001\rangle+\|1010\rangle$	9
65041	$\mathrm{Osc}_1(X)$	$\|0000\rangle+\|1000\rangle+\|0100\rangle+\|0010\rangle+\|0001\rangle+\|1100\rangle$	9
64700	$\mathrm{Osc}_3(X)$	$\|0000\rangle+\|1000\rangle+\|0100\rangle+\|0010\rangle+\|0001\rangle+\|1001\rangle$	9
59520	$\tau(\mathbb{P}^1\times\mathbb{P}^1\times\mathbb{P}^1\times\mathbb{P}^1)$	$\|0001\rangle+\|0010\rangle+\|0100\rangle+\|1000\rangle$	8

Table 3: Genuine entangled states (G-orbits) of the null-cone, their geometric identifications (varieties), their representatives and the dimensions of the varieties.

Name	Variety (orbit closure)	Normal form	dim
65278	$\mathbb{P}^7\times\mathbb{P}^1$	$\|0000\rangle+\|1110\rangle$	8
65532	$\mathbb{P}^1\times\mathbb{P}^7$	$\|0000\rangle+\|0111\rangle$	8
65518	$\sigma(\mathbb{P}^1\times\mathbb{P}^1\times\underline{\mathbb{P}^1}\times\mathbb{P}^1)\times\mathbb{P}^1$	$\|0000\rangle+\|1101\rangle$	8
65530	$\sigma(\mathbb{P}^1\times\underline{\mathbb{P}^1}\times\mathbb{P}^1\times\mathbb{P}^1)\times\mathbb{P}^1$	$\|0000\rangle+\|1011\rangle$	8
59624	$\tau(\mathbb{P}^1\times\mathbb{P}^1\times\times\mathbb{P}^1)\times\mathbb{P}^1$	$\|0110\rangle+\|1010\rangle+\|1100\rangle$	7
64704	$\mathbb{P}^1\times\tau(\mathbb{P}^1\times\mathbb{P}^1\times\times\mathbb{P}^1)$	$\|0011\rangle+\|0101\rangle+\|0110\rangle$	7
61064	$\tau(\mathbb{P}^1\times\mathbb{P}^1\times\underline{\mathbb{P}^1}\times\mathbb{P}^1)\times\mathbb{P}^1$	$\|0101\rangle+\|1001\rangle+\|1100\rangle$	7
64160	$\tau(\mathbb{P}^1\times\underline{\mathbb{P}^1}\times\mathbb{P}^1\times\mathbb{P}^1)\times\mathbb{P}^1$	$\|0011\rangle+\|1001\rangle+\|1010\rangle$	7
61166	$\sigma(\mathbb{P}^1\times\mathbb{P}^1)\times\mathbb{P}^1\times\mathbb{P}^1$	$\|0000\rangle+\|1100\rangle$	5
64250	$\sigma(\mathbb{P}^1\times\underline{\mathbb{P}^1}\times\mathbb{P}^1\times\underline{\mathbb{P}^1})\times\mathbb{P}^1\times\mathbb{P}^1$	$\|0000\rangle+\|1010\rangle$	5
64764	$\mathbb{P}^1\times\sigma(\mathbb{P}^1\times\mathbb{P}^1)\times\mathbb{P}^1$	$\|0000\rangle+\|0110\rangle$	5
65450	$\sigma(\mathbb{P}^1\times\underline{\mathbb{P}^1}\times\underline{\mathbb{P}^1}\times\mathbb{P}^1)\times\mathbb{P}^1\times\mathbb{P}^1$	$\|0000\rangle+\|1001\rangle$	5
65484	$\mathbb{P}^1\times\sigma(\mathbb{P}^1\times\underline{\mathbb{P}^1}\times\mathbb{P}^1)\times\mathbb{P}^1$	$\|0000\rangle+\|0101\rangle$	5
65520	$\mathbb{P}^1\times\mathbb{P}^1\times\sigma(\mathbb{P}^1\times\mathbb{P}^1)$	$\|0000\rangle+\|0011\rangle$	5
65635	$\mathbb{P}^1\times\mathbb{P}^1\times\mathbb{P}^1\times\mathbb{P}^1$	$\|0000\rangle$	4

Table 4: Partially entangled states (G-orbits) of the null-cone, their geometric identifications (varieties), their representatives and the dimensions of the varieties.

4

THE GEOMETRY OF HYPERPLANES I: THE DUAL VARIETY

The search for a SLOCC classification via invariant and covariant approaches is hopeless once the number of parts of the system increases. For instance, for $n = 5$ the description of the algebra of covariants is already out of reach [87]. Thus one needs to focus on a restricted set of invariants/covariants. One way of limiting the number of invariants/covariants is to focus on the ones which have a geometrical and/or quantum information meaning and to study their properties. An example of such geometrical/quantum information meaningful invariant is the hyperdeterminant. Geometrically, it is defined as the equation of the dual variety, i.e. the variety of singular hyperplane sections of the variety of separable states. From a quantum information perspective this invariant can be used as a measure of entanglement [45, 29]. The hypersurface defined by this invariant polynomial is an auxiliary variety in the sense of Chapter 2 and the singular components of this hypersurface are SLOCC subvarieties (Section 4.1). Miyake [89, 90, 91] first introduces this idea of using the dual variety and its singular locus to distinguish entanglement classes in the projectivized Hilbert space of a multipartite system. One can go further by looking at the specific singular type of hyperplane sections parametrized by the dual variety (Section 4.2, Theorem 4, 5). Combining the onion-like structure defined by Figure 9 and some four-qubit covariants, one finds a covariant type algorithm to identify a four-qubit state with its corresponding normal form in the Verstraete *et al*. classification.

4.1 THE DUAL VARIETY

Another auxiliary variety of interest in the studying of entanglement classes is the dual variety of X_{Sep}. Let us start with the general definition of the dual variety.

Definition 4.1.1. *Let $X \subset \mathbb{P}(V)$ be a projective nondegenerate variety (i.e. not contained in a hyperplane). Then the dual variety of X is defined as,*

$$X = \overline{\{H \in \mathbb{P}(V^*), \exists x \in X_{smooth}, T_x X \subset H\}}. \tag{55}$$

The variety X parametrizes the set of hyperplanes defining singular (non-smooth) hyperplane sections of X.

When we restrict to $V = \mathcal{H}$ and $X = X_{Sep}$, we can use the hermitian inner product on $\mathcal{H}$ and identify the dual variety of X_{Sep} with the

set of states which define singular hyperplane sections of X_{Sep}. More precisely, given a state $|\psi\rangle \in \mathcal{H}$ we have

$$[\psi] \in X^*_{\text{Sep}} \text{ iff } X_{\text{Sep}} \cap H_\psi = \{[\varphi] \in X_{\text{Sep}}, \langle \psi, \varphi \rangle = 0\} \text{ is singular.} \quad (56)$$

For $X_{\text{Sep}} = \mathbb{P}^{d_1-1} \times \mathbb{P}^{d_2-1} \times \cdots \times \mathbb{P}^{d_n-1}$ (with $d_j \leqslant \sum_{i \neq j} d_i$), the variety X^*_{Sep} is always a hypersurface. The defining equation of X^*_{Sep} is called the hyperdeterminant of format $d_1 \times d_2 \times \cdots \times d_n$ [44]. By construction the hyperdeterminant is SLOCC-invariant and so is its singular locus. Therefore the hyperdeterminant and its singular locus can be used to stratify the (projectivized) Hilbert space under SLOCC.

This idea goes back to Miyake [89, 90, 91] who interpreted previous results of Weyman and Zelevinksy on singularities of hyperdeterminant [122] to partially describe the entanglement structure for the 3- and 4-qubit systems, as well as, for the $2 \times 2 \times n$ systems. Following Miyake, the stratification induced by the hyperdeterminant of format $2 \times 2 \times 2$, also known as the Cayley hyperdeterminant, provides a dual picture of the three-qubit classification (Figure 7).

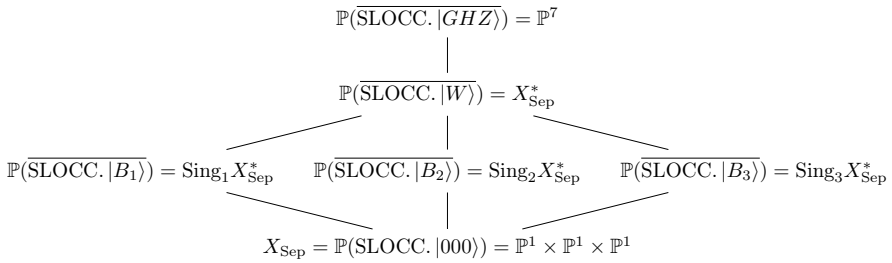

Figure 7: Stratification of the (projectivized) Hilbert space of three-qubit by SLOCC-invariant algebraic varieties (the dual and its singular locus): $\text{Sing}_i X^*_{\text{Sep}}$ represent different components of the singular locus [89, 122] (to be compared with Figure 3).

Figure 8 provides another example of stratification of the ambient space by X^*_{Sep} and its singular locus. Note that in this example some singular components are dual varieties of well known orbits, like the tangential and secant varieties. The node component of the singular locus corresponds to hyperplanes having at least two singular points. There are different types of node components depending on whether the singular points have vectors in common in their decomposition. More precisely, one can show using Terracini's Lemma and the definitions of Chapter 2, that:

$$(X^*_{\text{Sep}})_{\text{node}}(\emptyset) = \sigma_2(X_{\text{Sep}})^* \text{ and } (\sigma_2(X_{\text{Sep}})\{J\})^* = (X^*_{\text{Sep}})_{\text{node}}\{J\}. \quad (57)$$

4.2 ENTANGLEMENT CLASSES AND SIMPLE SINGULARITIES

Because X_{Sep} is a SLOCC orbit, the singular type of $X_{\text{Sep}} \cap H_\psi$ is also SLOCC invariant. Therefore, one can ask about the different types of

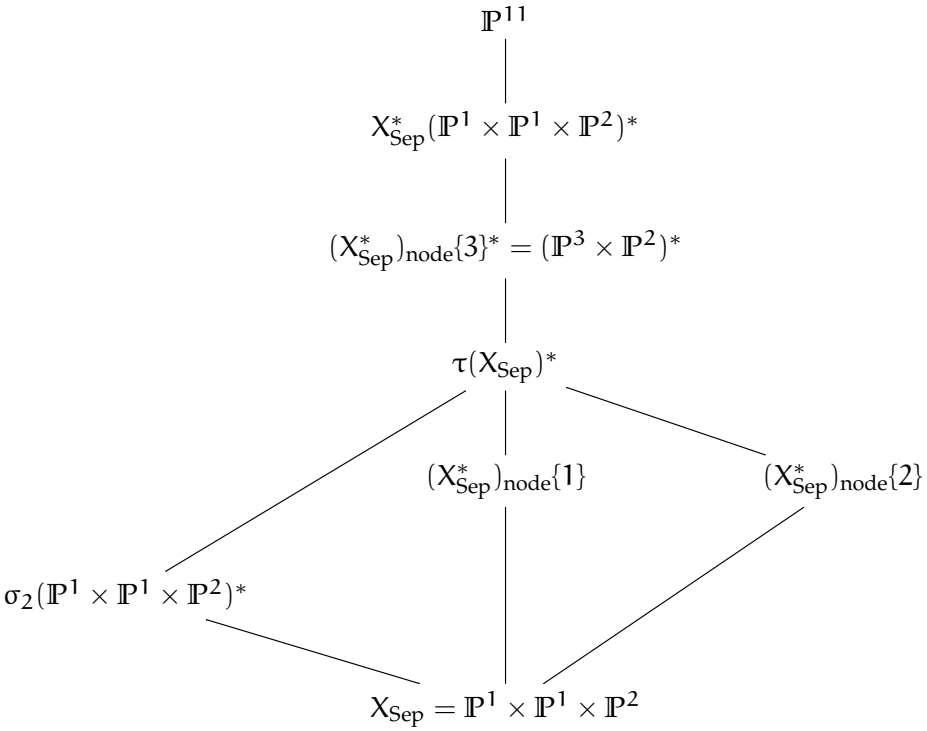

Figure 8: Stratification of the ambient space for the $2 \times 2 \times 3$ quantum system by dual varieties. The varieties $(X^*_{\mathrm{Sep}})_{\mathrm{node}}\{J\}$ are duals of the J-subsecant varieties. This corresponds to the set of hyperplanes having at least two singular points such that the two singular points $x = x_1 \otimes x_2 \otimes x_3$ and $y = y_1 \otimes y_2 \otimes y_3$ have the directions x_j and y_j in common for $j \in J$.

singular section and use this characterization by a singular type as invariant of a class of entanglement.

To do so we use the rational map defining the Segre embedding to obtain the equations of the hyperplane sections:

$$\begin{array}{rccl} Seg: & \mathbb{P}^{d_1-1} \times \cdots \times \mathbb{P}^{d_n-1} & \to & \mathbb{P}(\mathcal{H}) \\ & ([x_1^1 : \cdots : x_{d_1}^1], \ldots, [x_1^n : \cdots : x_{d_n}^n]) & \mapsto & [x_1^1 x_1^2 \ldots x_1^n : \cdots : \mathbf{x}_J : \cdots : x_{d_1}^1 x_{d_2}^2 \ldots x_{d_n}^n], \end{array} \tag{58}$$

where $\mathbf{x}_J$, for $J = (i_1, \ldots, i_n)$ with $1 \leqslant i_j \leqslant d_j$, denotes the monomial $\mathbf{x}_J = x_{i_1}^1 x_{i_2}^2 \ldots x_{i_n}^n$. In (58) the monomials $\mathbf{x}_J$ are ordered by the lexicographic order of the multi-indices J. Therefore, to a state $|\psi\rangle = \sum a_{i_1 \ldots i_n} |i_1 \ldots i_n\rangle$ one associates the hypersurface of X_{Sep} defined by

$$f_{|\psi\rangle} = \sum_{i_1, \ldots, i_n} a_{i_1 \ldots i_n} x_{i_1}^1 \ldots x_{i_n}^n = 0. \tag{59}$$

If $|\psi\rangle \in X^*_{\mathrm{Sep}}$ then $f_{|\psi\rangle}$ is a singular homogeneous polynomial, i.e. there exists $\overline{x} \in X_{\mathrm{Sep}}$ such that

$$f_{|\psi\rangle}(\overline{x}) = 0 \text{ and } \partial_{i_k} f_{|\psi\rangle}(\overline{x}) = 0. \tag{60}$$

In the 70s Arnol'd defined and classified *simple singularities* of complex functions [4, 5].

Definition 4.2.1. *One says that* $(f_{|\psi\rangle}, \overline{x})$ *is simple iff under a small perturbation it can only degenerate to a finite number of non-equivalent singular hypersurfaces* $(f_{|\psi\rangle} + \varepsilon g, \overline{x}')$ *(up to a biholomorphic change of coordinates).*

Simple singularities are always isolated, i.e. their Milnor number, which is a topological invariant of the singularity defined by

$$\mu = \dim_{\mathbb{C}} \mathbb{C}[x_1, \ldots, x_n]/(\nabla f_{\overline{x}}), \tag{61}$$

is finite. Simple singularities have be classified into 5 families (Table 5).

Type	A_k	D_k	E_6	E_7	E_8
Normal form	x^{k+1}	$x^{k-1} + xy^2$	$x^3 + y^4$	$x^3 + xy^3$	$x^3 + y^5$
Milnor number	k	k	6	7	8

Table 5: Simple singularities and their normal forms. If f is a complex function in n variables with x_0 being a simple singular point of type A_k, then there exists a biholomorphic change of coordinates such that $f \sim x_1^{k+1} + x_2^2 + \cdots + x_n^2$.

The singular type can be determined by computing the Milnor number, the corank of the Hessian and the cubic term in the degenerate directions.

Example 4.2.1. *Let us consider the 4-qubit state* $|\psi\rangle = |0000\rangle + |1011\rangle + |1101\rangle + |1110\rangle$. *The parametrization of the variety of separable states is given by* $\mathrm{Seg}([x_0 : x_1], [y_0 : y_1], [z_0 : z_1], [t_0 : t_1]) = [x_0y_0z_0t_0 : \cdots : x_1y_1z_1t_1]$. *The homogeneous polynomial associated to* $|\psi\rangle$ *is*

$$f_{|\psi\rangle} = x_0y_0z_0t_0 + x_1y_0z_1t_1 + x_1y_1z_0t_1 + x_1y_1z_1t_0. \tag{62}$$

In the chart $x_0 = y_1 = z_1 = t_1 = 1$ *one obtains locally the hypersurface defined by*

$$f(x, y, z, t) = yzt + xy + xz + xt. \tag{63}$$

The point $(0, 0, 0, 0)$ *is the only singular point of* $f_{|\psi\rangle}$ *(the hyperplane section is tangent to* $[|0111\rangle]$*). The Hessian matrix of this singularity has co-rank* 2 *and* $\mu = 4$. *Therefore the hyperplane section defined by* $|\psi\rangle$ *has a unique singular point of type* D_4 *and this is true for all states SLOCC equivalent to* $|\psi\rangle$.

The four-qubit and three-qutrit pure quantum systems are examples of systems with an infinite number of SLOCC-orbits. However, in both cases the orbit structure can still be described in terms of family of normal forms by introducing parameters. The 4-qubit classification was originally obtained by Verstraete et al. [117] with a small

correction provided by [30]. Regarding the 3-qutrit classification it has not yet been published in the quantum physics literature, but it can be directly translated from the orbit classification of the $3 \times 3 \times 3$ complex hypermatrices under $GL_3(\mathbb{C}) \times GL_3(\mathbb{C}) \times GL_3(\mathbb{C})$ obtained by Nurmiev [92]. In [57, 51] I calculated with my co-authors the types of isolated singularities associated to these forms. First of all, all isolated singularities are simple but the worst, in terms of degeneracy, isolated singularity that arises is, in both cases, of type D_4. This allows us to get a more precise onion-like description [89] of the classification, see Figure 9. It also gives information about how a state can be perturbed to another one. For instance, for a sufficiently small perturbation a state corresponding to a singular hyperplane section with only isolated singularities can only be changed to a state with isolated singularities of lower degeneracy.

Theorem 4 ([57]). *Let H_ψ be a hyperplane of $\mathbb{P}(\mathcal{H})$ tangent to $X_{Sep} = \mathbb{P}^1 \times \mathbb{P}^1 \times \mathbb{P}^1 \times \mathbb{P}^1 \subset \mathbb{P}^{15}$ and such that $X_{Sep} \cap H_\psi$ has only isolated singular points. Then the singularities are either of types A_1, A_2, A_3, or of type D_4, and there exist hyperplanes realizing each type of singularity. Moreover, if we denote by $\widehat{X}^*_{Sep} \subset \mathcal{H}$ the cone over the dual variety of X_{Sep},* i.e. *the zero locus of the Cayley hyperdeterminant of format $2 \times 2 \times 2 \times 2$, then the quotient map[1] $\Phi : \mathcal{H} \to \mathbb{C}^4$ is such that $\Phi(\widehat{X}^*_{Sep}) = \Sigma_{D_4}$, where Σ_{D_4} is the discriminant of the miniversal deformation[2] of the D_4-singularity.*

Theorem 5 ([51]). *Let $H_\psi \cap X$ be a singular hyperplane section of the algebraic variety of separable states for three-qutrit systems, i.e. $X_{Sep} = \mathbb{P}^2 \times \mathbb{P}^2 \times \mathbb{P}^2 \subset \mathbb{P}^{26}$ defined by a quantum pure state $|\psi\rangle \in \mathbb{P}^{26}$. Then $H_\psi \cap X_{Sep}$ only admits simple or nonisolated singularities. Moreover, if x is an isolated singular point of $H_\psi \cap X_{Sep}$, then its singular type is either A_1, A_2, A_3 or D_4.*

Remark 4.2.1. The singular types associated to the normal forms of the four-qubit and three-qutrit classifications are reproduced in Appendix B.

4.3 THE FOUR-QUBIT ATLAS (PART II)

In the four-qubit case one can identify to which part of the onion-like structure of Figure 9 a given state $|\psi\rangle$ belongs based on the evaluation of specific covariants. More precisely, in [56] we provide a covariant based algorithm to identify the Verstraete family of a given state.

1 As explained in Chapter 3, in the four-qubit case, the ring of SLOCC invariant polynomials is generated by four polynomials denoted by H, L, M and D in [86]. One way of defining the quotient map is to consider $\Phi : \mathcal{H} \to \mathbb{C}^4$ defined by $\Phi(\hat{x}) = (H(\hat{x}), L(\hat{x}), N(\hat{x}), D(\hat{x}))$, see [57].

2 The discriminant of the miniversal deformation of a singularity parametrizes all singular deformations of the singularity [4].

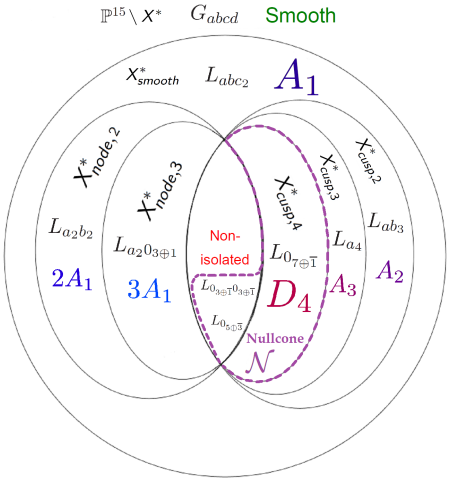

Figure 9: Four-qubit entanglement stratification by singular types of the hyperplane sections. These cusp components correspond to states with singularities which are not of type A_1 and the node components correspond to states with at least two singular points [122]. The names of the normal forms are the ones of [117].

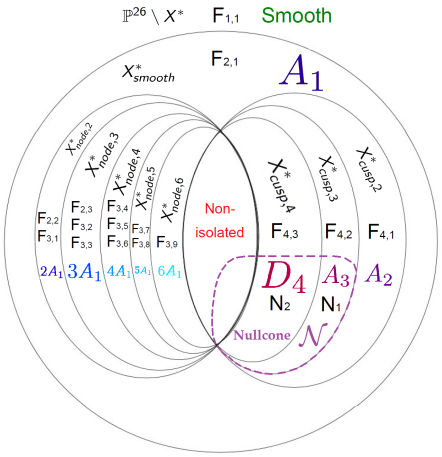

Figure 10: Three-qutrit entanglement stratification by singular types of the hyperplane sections. The names of the normal forms are the ones of [92].

I now describe this algorithm. First note that if the form is nilpotent it is easy to find a Verstraete equivalent form from the results of Chapter 3 (This is explicitly done in [55]). Now suppose that the form $|\psi\rangle$ is not nilpotent. We consider the following three quartics:

$$Q_1(|\psi\rangle) := x^4 - 2Bx^3y + (B^2 + 2L + 4M)x^2y^2 + (4D_{xy} - 4B(M + \frac{1}{2}L))xy^3 + L^2y^4, \tag{64}$$

$$Q_2(|\psi\rangle) := x^4 - 2Bx^3y + (B^2 - 4L - 2M)x^2y^2 + (-2MB + 4D_{xy})xy^3 + M^2y^4, \tag{65}$$

$$Q_3(|\psi\rangle) := x^4 - 2Bx^3y + (B^2 + 2L - 2M)x^2y^2 - (2LB + 2MB - 4D_{xy})xy^3 + N^2y^4. \tag{66}$$

Evaluated on $|G_{abcd}\rangle$, the roots of Q_1 are a^2, b^2, c^2 and d^2 and the roots of Q_2 (resp. Q_3) are the squares of the four polynomial factors of $M(|G_{abcd}\rangle)$ (resp. $N(|G_{abcd}\rangle)$ which are obtained by applying an invertible linear transformation to (a, b, c, d). Hence, those three quartics have the same invariants.

The invariant polynomials of a quartic of the form

$$f := \alpha x^4 - 4\beta x^3 y + 6\gamma x^2 y^2 - 4\delta x y^3 + \omega y^4 \tag{67}$$

are algebraic combinations of $I_2 = \alpha\omega - 4\beta\delta + 3\gamma^2$, an invariant of degree 2, which is the apolar of the form with itself (that is the polynomial $f\left(\frac{d}{dy}, -\frac{d}{dx}\right) f(x, y)$), and $I_3 = \det \begin{pmatrix} \alpha & \beta & \gamma \\ \beta & \gamma & \delta \\ \gamma & \delta & \omega \end{pmatrix} = \alpha\gamma\omega - \alpha\delta^2 - \beta^2\omega - \gamma^3 + 2\beta\gamma\omega$, an invariant of degree 3 called the catalecticant, see [95, p29]. In particular, the discriminant of the quartic is $\Delta = I_2^3 - 27I_3^2$. We can easily check that $\Delta(Q_i(|\psi\rangle))$ is also the hyperdeterminant of format $2 \times 2 \times 2 \times 2$ evaluated at $|\psi\rangle$.

We also use the 170 covariants computed in [55] (Appendix A) in order to discriminate between the Verstraete forms. In particular, we define:

$$\mathcal{L} = L_{6000} + L_{0600} + L_{0060} + L_{0006},$$

$$\mathcal{K}_5 = K_{5111} + K_{1511} + K_{1151} + K_{1115},$$

$$\mathcal{K}_3 = K_{3311} + K_{3131} + K_{3113} + K_{1331} + K_{1313} + K_{1133},$$

$$\overline{\mathcal{G}} = G^1_{3111}G^1_{1311}G^1_{1131}G^1_{1113},\ \mathcal{G} = G^2_{3111} + G^2_{1311} + G^2_{1131} + G^2_{1113},$$

$$\mathcal{D} = D_{4000} + D_{0400} + D_{0040} + D_{0004},$$

$$\mathcal{H} = H_{2220} + H_{2202} + H_{2022} + H_{0222}$$

and $\mathcal{C} = C^2_{1111}$.

We proceed as follows: First we classify the forms with respect to the roots of the three quartics Q_1, Q_2 and Q_3. To describe the roots of the quartics, we will use two other covariant polynomials: the Hessian

$$\mathrm{Hess}(f) := \begin{vmatrix} \frac{\partial^2}{\partial x^2} f & \frac{\partial^2}{\partial x \partial y} f \\ \frac{\partial^2}{\partial y \partial x} f & \frac{\partial^2}{\partial y^2} f \end{vmatrix} \tag{68}$$

and the Jacobian of the Hessian

$$T(f) = \begin{vmatrix} \frac{\partial}{\partial x} f & \frac{\partial}{\partial y} f \\ \frac{\partial}{\partial x}\mathrm{Hess}(f) & \frac{\partial}{\partial y}\mathrm{Hess}(f) \end{vmatrix}. \tag{69}$$

From the values of the covariants one can compute the multiplicity of the roots of a quartic f, according to Table 6. For each case we deter-

Covariants	Interpretation
$\Delta \neq 0$	Four distinct roots
$\Delta = 0$ and $T \neq 0$	Exactly one double root
$T = 0$ and $I_2 \neq 0$	Two distinct double roots
$I_2 = I_3 = 0$ and $\mathrm{Hess} \neq 0$	A triple root
$\mathrm{Hess} = 0$	A quadruple root

Table 6: Roots of a quartic.

mine which Verstraete forms can occur and, when there are several possibilities, we use one of the covariants previously defined to discriminate between them. Let V be a vector, we denote by $ev(V)$ the vector such that $ev(V)[i] = 0$ if $V[i] = 0$ and $ev(V)[i] = 1$ if $V[i] \neq 0$.

Algorithm 4.3.1. *Let $|\psi\rangle$ be a four-qubit state and let us consider the three quadrics $Q_i(\psi)$. Then,*

1. *If the quartics have only nonzero roots:*
   a) *If all the roots are simple then this is the generic case and the Verstraete type is $[G_{abcd}; \emptyset]$.*
   b) *If each quartic has a double root and two simple roots (equivalently $T_1 = T_2 = T_3 = 0$ and $I_2, I_3 \neq 0$ then two cases can occur. Either the Verstraete type is $[G_{abcd}; c = d]$ or it is $[L_{abcc}; \emptyset]$. We determine the forms noticing that $\mathcal{L}(L_{abc_2}) \neq 0$ and $\mathcal{L}(G_{abcc}) = 0$.*
   c) *If each quartic has a single simple root and a triple root (equivalently $I_2 = I_3 = 0$) then three cases can occur: $[G_{abcd}; b = c = d]$, $[L_{abc_2}; b = c]$ and $[L_{ab_3}; \emptyset]$. In order to determine the type, we evaluate the vector $V = [\mathcal{K}_5, \mathcal{L}]$ on each form. We can decide the type of the form according to the values*

$$ev(V(G_{abbb})) = [0,0],\ ev(V(L_{abb_2})) = [1,0],$$

$$\text{and } ev(V(L_{ab_3})) = [1,1].$$

2. *If only one of the quartics Q_i has a zero root, then:*
   a) *If Q_i has only simple roots then the only possibility is $[G_{abcd}; d = 0]$.*
   b) *If Q_i has a double zero root and two simple roots then we have three possibilities $[G_{abcd}; c = d = 0]$, $[L_{abc_2}; c = 0]$ or $[L_{a_2b_2}; \emptyset]$. We evaluate the form on the vector $V = [\mathcal{K}_3, \mathcal{L}]$ and compare with*

$$ev\,(V(G_{ab00})) = [0,0],\ ev\,(V(L_{ab0_2})) = [1,0],$$

$$\text{and } ev\,(V(L_{a_2b_2})) = [1,1].$$

c) *If* Q_i *has triple zero root and a simple root then we have the five possibilities* $[G_{abcd}; c = b = d = 0]$, $[L_{abc_2}; b = c = 0]$, $[L_{ab_3}; a = 0]$, $[L_{a_2b_2}; a = b]$ *and* $[L_{a_4}; \emptyset]$. *We evaluate the form on the vector* $V = [\mathcal{C}, \mathcal{D}, \mathcal{K}_5, \mathcal{L}]$ *and compare to the identities*

$$ev(V(G_{a000})) = [0,0,0,0],\ ev(V(L_{a00_2})) = [1,0,0,0],$$

$$ev(V(L_{0b_3})) = [1,1,1,0],\ ev(V(L_{a_2a_2})) = [1,1,0,0]$$

and $ev(V(L_{a_4})) = [1,1,1,1]$.

d) *If* Q_i *has a double nonzero root and two simple roots then there are two possibilities* $[G_{abcd}; b = c, d = 0]$ *and* $[L_{abc_2}; b = 0]$ *which can be identified by noticing that* $\mathcal{L}(G_{abb0}) = 0$ *and* $\mathcal{L}(L_{a0c_2}) \neq 0$.

e) *If* Q_i *has a triple nonzero root then one has to examine 3 possibilities:* $[G_{abcd}; a = b = c, d = 0]$, $[L_{abcc}; b = c, a = 0]$ *and* $L_{abbb}; b = 0]$. *It suffices to consider the vector* $V = [\mathcal{D}, \mathcal{L}]$ *and notice that*

$$ev(V(G_{aaa0})) = [0,0],\ ev(V(L_{0cc_2})) = [1,0],$$

$$\textit{and } ev(V(L_{a0_3})) = [1,1].$$

3. *If each quartic has at least one zero root, then*

a) *If all the roots are simple then the type is* $[G_{abcd}; d = 0]$.

b) *If all the zero roots are simple and there is a nonzero double root, then we have 2 possibilities* $[G_{abcd}; b = a, c = -2a, d = 0]$, $[L_{ab_2}; a = 0, c = \frac{b}{2}]$. *We can discriminate between these two cases by noticing that* $\mathcal{L}(G_{aa(-2a)0}) = 0$ *and* $\mathcal{L}(L_{0(2b)b_2}) \neq 0$.

c) *If all the zero roots are double, then we have to consider 5 cases:* $[G_{abcd}; a = b = 0, c = d]$, $[L_{abc_2}; a = b, c = 0]$, $[L_{abc_2}; a = b = 0]$, $[L_{a_2b_2}; a = 0]$, *and* $[L_{a_20_{3\oplus\overline{1}}}; \emptyset]$. *We consider the vector* $V = [\overline{\mathcal{G}}, \mathcal{G}, \mathcal{H}, \mathcal{L}]$. *The evaluation of this vector on the different cases gives*

$$ev(V(G_{00aa})) = [0,0,0,0],\ ev(V(L_{aa0_2})) = [0,1,1,0],$$

$$ev(V(L_{00c_2})) = [0,0,1,0], ev(L_{0_2a_2}) = [1,1,1,0],$$

$$\textit{and } ev(L_{a_20_{3\oplus\overline{1}}}) = [1,1,1,1].$$

Remark 4.3.1. Our algorithm is based on a discussion on the roots of the quartics $\mathcal{Q}_1, \mathcal{Q}_2$ and $\mathcal{Q}_3$. Geometrically, we can translate it to the following:

1. If $|\psi\rangle$ does not vanish the hyperdeterminant Δ, then we are in cases 1.(a), 2.(a) and 3.(a).

2. If $|\psi\rangle$ is a smooth point of Δ, then we are in cases 1.(b), 2.(d) and 3.(b).

3. If $|\psi\rangle$ is a smooth point of the cusp component $(\tau(X)^*)$, then we are in cases 1.(c) and 2.(e).

4. If $|\psi\rangle$ is a smooth point of the cusp component of multiplicity 3 $(X_{cusp,3})$, then we are in case 2.(c).

5. If $|\psi\rangle$ is a smooth point of the node components, then we are in cases 2.(b).

6. If $|\psi\rangle$ is a smooth point of the node component of multiplicity 3 $(X_{node,3})$, then we are in the case 3.(c).

7. Otherwise $|\psi\rangle$ belongs to the null-cone.

5

WHAT REPRESENTATION THEORY TELLS US ABOUT QUANTUM INFORMATION

In this last chapter of the first part, dedicated to the geometry of entanglement, one considers the entanglement classification from the point of view of representation theory. From this new perspective we show that the SLOCC group action, as described in the previous chapters, can be generalized as a Spin group action on a fermionic Fock space (Section 5.1), as it was initially proposed in [110]. This allows us to provide a unified picture to a series of results on tripartite entanglement based on classical results of representation theory regarding sequence of Lie algebras (Section 5.2). This chapter is based on papers [53, 77].

5.1 REPRESENTATION THEORY AND QUANTUM SYSTEMS

Let us now consider G, a complex semi-simple Lie group, and V, an irreducible representation of G, i.e. one considers a map $\rho : G \to GL(V)$ defining an action of G on V such that there is no proper subspace of V stabilized by G. The projectivization of an irreducible representation $\mathbb{P}(V)$ always contains a unique closed orbit $X_G \subset \mathbb{P}(V)$, called the highest weight orbit [42]. The Hilbert space $\mathcal{H} = \mathbb{C}^{d_1} \otimes \cdots \otimes \mathbb{C}^{d_n}$ is an irreducible representation of $\text{SLOCC} = \text{SL}_{d_1}(\mathbb{C}) \times \cdots \times \text{SL}_{d_n}(\mathbb{C})$ and in this particular case the highest weight orbit is nothing but the Segre variety $X_{\text{Sep}} = \mathbb{P}^{d_1-1} \times \cdots \times \mathbb{P}^{d_n-1}$.

It is natural to ask if other semi-simple Lie groups and representations have physical interpretations in terms of quantum systems. Let us first introduce the case of symmetric and skew-symmetric states.

- Consider the simple complex Lie group $\text{SLOCC} = \text{SL}_n(\mathbb{C})$ and its irreducible representation $\mathcal{H}_{bosons} = \text{Sym}^k(\mathbb{C}^n)$, where we denote by $\text{Sym}^k(\mathbb{C}^n)$ is the kth symmetric tensor product of $\mathbb{C}^n$. Then $\mathcal{H}_{bosons}$ is the Hilbert space of k indistinguishable symmetric particles, each particle being a n-single particle state. Physically, it corresponds to k bosonic n-qudit states. Geometrically, the highest weight orbit is the so-called Veronese embedding of $\mathbb{P}^{n-1}$ [47]:

$$\begin{array}{rccc} \nu_k : & \mathbb{P}^{n-1} & \to & \mathbb{P}(\text{Sym}^k(\mathbb{C}^n)) \\ & [\psi] & \mapsto & [\underbrace{\psi \circ \psi \circ \cdots \circ \psi}_{k \text{ times}}]. \end{array} \tag{70}$$

  The variety $\nu_k(\mathbb{P}^{n-1}) \subset \mathbb{P}(\text{Sym}^k(\mathbb{C}^n))$ is geometrically the analogue of the variety of separable states for multiqudit systems

given by the Segre embedding. It is not completely clear what entanglement physically means for bosonic systems. The ambiguity comes from the fact that symmetric states like $|W_3\rangle = \frac{1}{3}(|100\rangle + |010\rangle + |001\rangle)$ can be factorized under the symmetric tensor product $|W_3\rangle = |1\rangle \circ |0\rangle \circ |0\rangle$. However, we can define entanglement in such symmetric systems by considering the space of symmetric states as a subset of the space of k n-dits states $\mathbb{C}^n \otimes \cdots \otimes \mathbb{C}^n$. In this case the kth-Veronese embedding of $\mathbb{P}^{n-1}$ corresponds to the intersection of the variety of separable states $\mathbb{P}^{n-1} \times \cdots \times \mathbb{P}^{n-1}$ with $\mathbb{P}(\mathrm{Sym}^k(\mathbb{C}^n))$ [22]. In the special case of $n = 2$, the variety $\nu_k(\mathbb{P}^1) \subset \mathbb{P}^k$ can also be identified with the variety of spin s-coherent states ($2s = k$), when a spin s-state is given as a collection of $2s$ spin $\frac{1}{2}$-particles [31, 8]. For a comprehensive study about entanglement of symmetric states see [7].

- Consider the simple complex Lie group SLOCC $= \mathrm{SL}_n(\mathbb{C})$ and its irreducible representation $\mathcal{H}_{fermions} = \bigwedge^k \mathbb{C}^n$, which is the space of k-skew symmetric tensors over $\mathbb{C}^n$. This Hilbert space represents the space of k-skew symmetric particles with n-modes, i.e. k fermions with n-single particle states. In this case the highest weight orbit is also a well-known algebraic variety, called the Grassmannian variety $G(k, n)$. The Grassmannian variety $G(k, n)$ is the set of k planes in $\mathbb{C}^n$ and it is defined as a subvariety of $\mathbb{P}(\bigwedge^k \mathbb{C}^n)$ by the Plücker embedding [47]:

$$\begin{array}{lcl} G(k,n) & \hookrightarrow & \mathbb{P}(\bigwedge^k \mathbb{C}^n) \\ \mathrm{Span}\{v_1, v_2, \ldots, v_k\} & \mapsto & [v_1 \wedge v_2 \wedge \cdots \wedge v_k]. \end{array} \tag{71}$$

  From the point of view of quantum physics the Grassmannian variety represents the set of fermions with Slater rank one and is naturally considered as the set of non-entangled states.

Another type of a quantum system which can be described by means of representation theory is the case of particles in a fermionic Fock space with finite N-modes [110]. A fermionic Fock space with finite N-modes physically describes fermionic systems with N-single particles states, where the number of particles is not necessarily conserved by the admissible transformations. Let us recall the basic ingredient to describe such Hilbert space. Let V be an $N = 2n$-dimensional complex vector space corresponding to one particle states. The associated fermionic Fock space is given by:

$$\mathcal{F} = \wedge^\bullet V = \mathbb{C} \oplus V \oplus \wedge^2 V \oplus \cdots \oplus \wedge^N V = \underbrace{\wedge^{even} V}_{\mathcal{F}_+} \oplus \underbrace{\wedge^{odd} V}_{\mathcal{F}_-}. \tag{72}$$

Similarly to the bosonic Fock space description of the Harmonic oscillator, one may describe this vector space as generated from the

vacuum $|0\rangle$ (a generator of $\wedge^0 V$) by applying creation operators $\mathbf{p}_i$, $1 \leqslant i \leqslant N$. Thus a state $|\psi\rangle \in \mathcal{F}$ is given by

$$|\psi\rangle = \sum_{i_1,\dots,i_k} \psi_{i_1,\dots,i_k} \mathbf{p}_{i_1} \dots \mathbf{p}_{i_k} |0\rangle \text{ with } \psi_{i_1,\dots,i_k} \text{ skew symmetric tensors.} \tag{73}$$

The annihilation operators $\mathbf{n}_j$, $1 \leqslant j \leqslant N$ are defined such that $\mathbf{n}_j |0\rangle = 0$ and satisfy the Canonical Anticommutation Relations (CAR)

$$\{\mathbf{p}_i, \mathbf{n}_j\} = \mathbf{p}_i \mathbf{n}_j + \mathbf{n}_j \mathbf{p}_i = \delta_{ij}, \{\mathbf{p}_i, \mathbf{p}_j\} = 0, \{\mathbf{n}_i, \mathbf{n}_j\} = 0. \tag{74}$$

To see the connection with Lie group representations, let us consider $W = V \oplus V'$, where V and V' are isotropic subspaces with basis $(e_j)_{1 \leqslant j \leqslant 2N}$, for the quadratic form $Q = \begin{pmatrix} 0 & I_N \\ I_N & 0 \end{pmatrix}$ and let us denote by $Cl(W, Q)$ the corresponding Clifford algebra [42]. Thus $\mathcal{F}$ is a $Cl(W, Q)$ module

$$w = x_i e_i + y_j e_{N+j} \mapsto \sqrt{2}(x_i \mathbf{p}_i + y_j \mathbf{n}_j) \in End(\mathcal{F}). \tag{75}$$

It follows that $\mathcal{F}_+$ and $\mathcal{F}_-$ are irreducible representations of the simple Lie group $Spin(2N)$, i.e. the spin group[1]. Those irreducible representations are known as spinor representations.

Example 5.1.1 (The box picture). *Let $V = \mathbb{C}^{2n} = \mathbb{C}^2 \otimes \mathbb{C}^n$, i.e. a single particle can be in two different modes ($\uparrow$ or $\downarrow$) and n different locations. We denote by $\mathbf{p}_1, \dots, \mathbf{p}_n, \mathbf{p}_{\overline{1}}, \dots, \mathbf{p}_{\overline{n}}$ the corresponding creation operators, where $\mathbf{p}_i$ creates a $\uparrow$ particle in the i-th location and $\mathbf{p}_{\overline{i}}$ creates a $\downarrow$ particle in the i-th location. One can give a box picture representation of the embedding of n qubits in the Hilbert space $\mathcal{F} = \mathcal{F}_+ \oplus \mathcal{F}_-$. With the chirality decomposition $\mathcal{F} = \mathcal{F}_+ \oplus \mathcal{F}_-$ one gets two different ways of embedding n qubits, Figure 11 and Figure 12.*

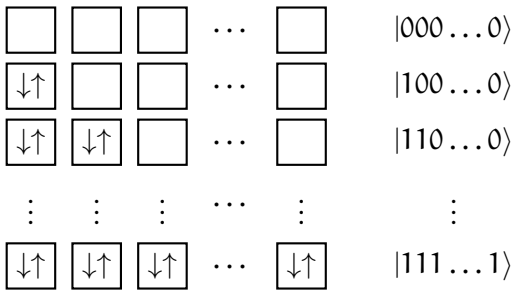

Figure 11: Double occupancy embedding of the n-qubit Hilbert space (2^n basis vectors) inside $\mathcal{F}_+$ (n boxes and $N = 2n$ single particle states).

1 The spin group $Spin(2N)$ corresponds to the simply connected double cover of $SO(2N)$ [42].

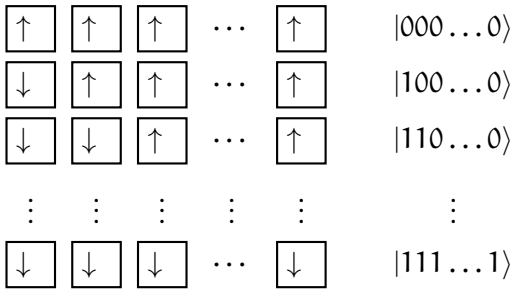

Figure 12: Single occupancy embedding of the n-qubit Hilbert space (2^n basis vectors) inside $\mathcal{F}_+$ (for $n = 2k$ boxes and $N = 2n$ single particle states) or $\mathcal{F}_-$ (for $n = 2k+1$ boxes and $N = 2n$ single particle states).

If we consider quantum information processing involving n bosonic qubits, n qubits or n fermions with $2n$ modes, all systems can be naturally embedded in the fermionic Fock space with $N = 2n$ modes and the restriction of the action of the $\mathrm{Spin}(2N) = \mathrm{Spin}(4n)$ group to those sub-Hilbert-spaces boils down to their natural SLOCC group, as shown in Table 7. In this sense the Spin group can be regarded as a natural generalization of the SLOCC group.

Lie algebra	$\mathfrak{sl}_2$	$\subset$	$\mathfrak{sl}_2 + \cdots + \mathfrak{sl}_2$	$\subset$	$\mathfrak{sl}_{2n}$	$\subset$	$\mathfrak{so}_{4n}$
Lie group	$\mathrm{SL}_2(\mathbb{C})$	$\subset$	$\mathrm{SL}_2(\mathbb{C}) \times \cdots \times \mathrm{SL}_2(\mathbb{C})$	$\subset$	$\mathrm{SL}_{2n}(\mathbb{C})$	$\subset$	$\mathrm{Spin}(4n)$
Representation	$\mathbb{P}(\mathrm{Sym}^n(\mathbb{C}^2))$	$\hookrightarrow$	$\mathbb{P}(\mathbb{C}^2 \otimes \cdots \otimes \mathbb{C}^2)$	$\hookrightarrow$	$\mathbb{P}(\bigwedge^n \mathbb{C}^{2n})$	$\hookrightarrow$	$\mathbb{P}(\Delta_{4n})$
Highest weight orbit	$v_n(\mathbb{P}^1)$	$\subset$	$\mathbb{P}^1 \times \cdots \times \mathbb{P}^1$	$\subset$	$G(n, 2n)$	$\subset$	S_{2n}

Table 7: Embedding of n bosonic qubit, n qubits, n fermions with $2n$ single particle states into fermionic Fock space with $2N = 4n$ modes.

Let us denote by Δ_{4n} the irreducible representations $\mathcal{F}_\pm$, the algebraic variety $S_{2n} \subset \mathbb{P}(\Delta_{4n})$ corresponding to the highest weight orbit of $\mathrm{Spin}(4n)$ is called the spinor variety and generalizes the set of separable states. Table 7 indicates that the classification of spinors could be considered as the general framework to study entanglement classification of pure quantum systems. The embedding of qubits into fermionic systems (with a fixed number of particles) was used in [28] to answer the question of SLOCC equivalence in the four-qubit case. In [77], with Péter Lévay, we used the embedding within the fermionic Fock space to recover the polynomial invariants of the four-qubit case from the invariants of the spinor representation.

5.2 SEQUENCE OF SIMPLE LIE ALGEBRAS AND TRIPARTITE ENTANGLEMENT

Let us go back to the three-qubit classification of Chapter 2 and the $|W_3\rangle$ and $|GHZ_3\rangle$ states. After the seminal paper of Dür, Vidal and

Cirac [36], other papers were published in the quantum information literature providing other quantum systems featuring only two types of genuine entangled states similar to the $|W_3\rangle$ and $|GHZ_3\rangle$ states.

In [53] we showed how all those similar classifications correspond to a sequence of varieties studied from representation theory and algebraic geometry in connection with the Freudenthal magic square [71]. Consider a Lie group G acting by its adjoint action on its Lie algebra $\mathfrak{g}$. The adjoint variety $X_G \subset \mathbb{P}(\mathfrak{g})$ is the highest weight orbit for the adjoint action. Take any point $x \in X_G$ and let us consider the set of all lines of X_G passing through x (these lines are tangent to X_G). This set of lines is a smooth homogeneous variety $Y \subset \mathbb{P}(T_x X_G)$, called the subadjoint variety of X_G . Consider the sequence of Lie algebras

$$\mathfrak{g}_2 \subset \mathfrak{so}_8 \subset \mathfrak{f}_4 \subset \mathfrak{e}_6 \subset \mathfrak{e}_7. \tag{76}$$

This sequence gives rise to a series of subadjoint varieties called, the *subexceptional series*. In [71] this sequence is obtained as the third row of the geometric version of Freudenthal's magic square.

To see how the subexceptional series is connected to the different classifications of [22, 84, 110, 14, 35, 75] let us ask the following question: What are the Hilbert spaces $\mathcal{H}$ and the corresponding SLOCC groups G such that the only genuine entanglement types are $|W\rangle$ and $|GHZ\rangle$ like ?

If we assume that G is a Lie group and $\mathcal{H}$ an irreducible representation such that the only two types of genuine entangled states are $|W\rangle$ and $|GHZ\rangle$ then one knows from Chapter 2 that the secant variety of the variety of separable states should fill the ambient space and be of the expected dimension. Because the secant variety is an orbit, this orbit is dense by our assumption and, therefore, the ring of SLOCC invariant polynomials should be generated by at most one element. But one also knows, under our assumption and by Zak's theorem, that in this case the tangential variety, i.e. the $|W\rangle$-orbit, is a codimension-one orbit in the ambient space. Thus the ring of G-invariant polynomials for the representation $\mathcal{H}$ should be generated by a unique polynomial. The classification of such representations was given in the 70's by Kac, Popov and Vinberg [65]. From this classification one just needs to keep the representation where the dimension of the secant variety of the highest weight orbit is of the expected dimension. This leads naturally to the sequence of subexceptional varieties as given in Table 8.

Remark 5.2.1. The relation between the Freudenthal magic square and the tripartite entanglement was already pointed out in [14, 118]. Other subadjoint varieties for the Lie algebra $\mathfrak{so}_{2n}$, $n \neq 4$, not included in the subexceptional series, also share the same orbit structure. The physical interpretation of those systems is clear for $n = 3, 5, 6$ [53, 118], but more obscure in the general case $n \geqslant 7$.

$\mathcal{H}$	SLOCC	QIT interpretation	$X_{\text{Sep}} \subset \mathbb{P}(\mathcal{H})$	$\mathfrak{g}$
$\mathrm{Sym}^3(\mathbb{C}^2)$	$\mathrm{SL}_2(\mathbb{C})$	Three bosonic qubit [22, 118] (2007)	$\nu_3(\mathbb{P}^1) \subset \mathbb{P}^3$	$\mathfrak{g}_2$
$\mathbb{C}^2 \otimes \mathbb{C}^2 \otimes \mathbb{C}^2$	$\mathrm{SL}_2(\mathbb{C}) \times \mathrm{SL}_2(\mathbb{C}) \times \mathrm{SL}_2(\mathbb{C})$	Three qubit [36] (2001)	$\mathbb{P}^1 \times \mathbb{P}^1 \times \mathbb{P}^1 \subset \mathbb{P}^7$	$\mathfrak{so}_8$
$\bigwedge^{(3)} \mathbb{C}^6$	$\mathrm{Sp}_6(\mathbb{C})$	Three fermions with with 6 single particles state with a symplectic condition	$\mathrm{LG}(3,6) \subset \mathbb{P}^{13}$	$\mathfrak{f}_4$
$\bigwedge^3 \mathbb{C}^6$	$\mathrm{SL}_6(\mathbb{C})$	Three fermions with with 6 single particles state [84] (2008)	$\mathrm{G}(3,6) \subset \mathbb{P}^{19}$	$\mathfrak{e}_6$
Δ_{12}	$\mathrm{Spin}(12)$	Particles in fermionic Fock space [110] (2014)	$\mathrm{S}_6 \subset \mathbb{P}^{31}$	$\mathfrak{e}_7$
V_{56}	E_7	Three partite entanglement of seven qubit [35, 75] (2007)	$\mathrm{E}_7/\mathrm{P}_1 \subset \mathbb{P}^{55}$	$\mathfrak{e}_8$
			Freudenthal subexceptionnal series	

Table 8: The sequence of subexceptional varieties and the corresponding tripartite systems.

Remark 5.2.2. This sequence of systems can also be considered from the dual picture by looking for generalization of the Cayley hyperdeterminant (the dual equation of $X = \mathbb{P}^1 \times \mathbb{P}^1 \times \mathbb{P}^1$). In [71] it was also shown that all dual equations for the subexceptional series can be uniformly described. The tripartite entanglement of seven qubits [35], under constrains given by the Fano plane, also started with a generalization of Cayley's quartic hyperdeterminant in relation with black holes entropy formulas in the context of the black-hole/qubit correspondence [15].

Part II

THE GEOMETRY OF CONTEXTUALITY

In this second part of the thesis I discuss the finite geometry behind operator-based proofs of contextuality. I was introduced to the subject by Michel Planat [101, 99] and have worked on that topic over the past six years mostly with my co-authors Metod Saniga and Péter Lévay [59, 60, 80, 105, 16, 104]. Chapter 6 provides introductive material on operator-based proofs of contextuality (basic examples, how it can be tested, how it can be considered as a quantum resource) and I show why the Mermin square and pentagram can be considered as the "smallest" contextual configurations. In Chapter 7, I introduce the geometric description of the N-qubit Pauli group as a symplectic polar space of rank N over the two element field $\mathbb{F}_2$. This idea to model the commutation relations of the N-qubit Pauli group by a point-line structure goes back to the initial work of Metod Saniga and Michel Planat [106]. The contextual configurations belong to this space as subgeometries. In this chapter I show how we can parametrize geometrically the set of maximally isotropic subspaces (i.e. maximal sets of mutually commuting N-qubit operators). In Chapter 8, I work with the concept of Veldkamp geometry, also introduced by Metod Saniga and Michel Planat in the context of quantum infomation [108]. The Veldkamp space of a point-line incidence structure is the set of hyperplanes of the initial geometry. Therefore, it can be considered in some sense as a duality. To emphazise this, I describe the stratification of the projective space of dimension $2^N - 1$ over $\mathbb{F}_2$, $N = 2, 3, 4$, by the Veldkamp geometry of the Segre variety of dimension N. As explained in the text this stratification can be put in correspondence with this geometric parametrization of the maximal sets of mutually commuting N-qubit operators. Finally, in Chapter 9 I show how the notion of Veldkamp lines lead us to recognize weight diagrams of simple Lie algebras inside some specific arrangements of hyperplanes of the three-qubit Pauli group, establishing an intriguing correspondence between hyperplanes of the three-qubit Pauli group and representations of subgroups of $\mathrm{Spin}(14)$, the double cover of the Lie group $\mathrm{SO}(14)$.

6 OPERATOR-BASED PROOFS OF CONTEXTUALITY

This first chapter of the second part of this habilitation begins with general considerations on operator-based proofs of contextuality. I first recall two well-known configurations of operators: The Mermin-Peres square and the Mermin pentagram (Section 6.1). These configurations are examples of operator-based proofs of the Kochen-Specker (KS) Theorem (see Chapter 1). I also recall the work of Adán Cabello (Section 6.2) on testable state-independent proof of contextuality [25, 26], because it opens up a path to experimental tests and it also has an interesting connection with the geometry that will be developed in the next chapters. An example of quantum processing application, the quantum telepathy game of Aravind [2] is also presented in this section. Then I show (Section 6.3) that the Mermin-Peres square and the Mermin pentagram are the smallest, in terms of operators and contexts, configurations furnishing operator-based proofs of Kochen-Specker Theorem. This last result was obtained with Metod Saniga and published in [59].

6.1 PROOFS OF CONTEXTUALITY: SQUARES AND PENTAGRAMS

As explained in the introduction, operator-based proofs of the Kochen-Specker (KS) Theorem correspond to configurations of (mutli-Pauli) observables such that the operators on the same context (line) are mutually commuting and such that the product of the operators gives $\pm I$, with an odd number of negative contexts.

The Mermin-Peres square presented in the introduction is the first observable-based proof of the KS Theorem published in the literature. Using two-qubit observables one can show that only ten Mermin-Peres squares exist (Figure 13).

In [88], Mermin also proposed another proof involving three-qubit Pauli operators and known as the Mermin pentagram (Figure 14). The geometry of the three-qubit generalized Pauli group will be investigated in Chapters 7 and 8. In [101] we proved, by a computer argument, that there are 12096 different Mermin pentagrams living in the three-qubit Pauli group. Understanding the different types of realization of a contextual configuration will be the initial motivation to study geometrically the generalized N-qubit Pauli group.

Remark 6.1.1. Originally the first proof of the KS Theorem was not given in terms of configurations of multiqubit Pauli-operators, but by considering projection operators on some specific basis of the three-dimensional Hilbert space. Kochen and Specker found a set of 117 op-

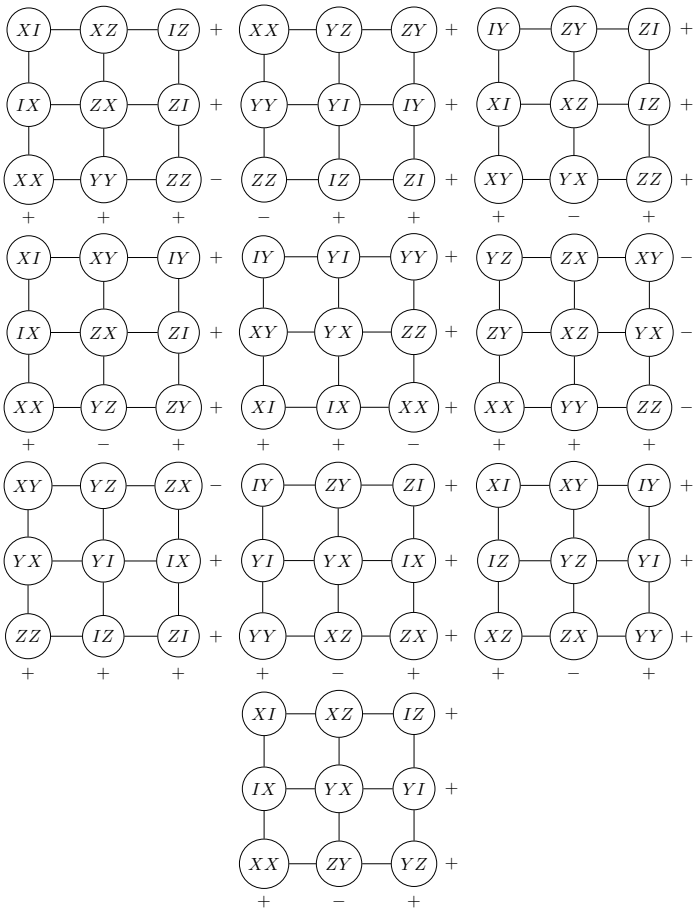

Figure 13: The full set of ten grids built with two-qubit operators. The + (resp. −) signs stand for the contexts whose product is +I (resp. −I). In Chapters 7 and 8 we will investigate the geometry in which these configurations lie.

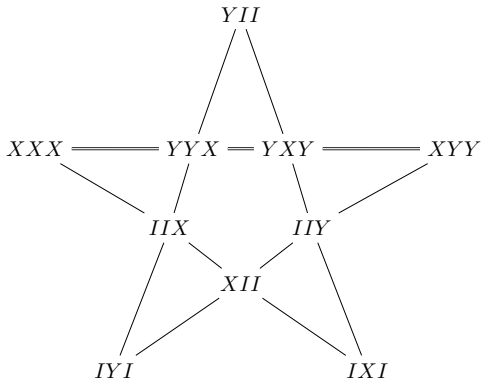

Figure 14: The Mermin pentagram: a configuration of 10 three-qubit operators proving KS Theorem. Operators on a line are mutually commuting and the doubled line corresponds to the context where the product gives $-I_8$.

erators and proved the impossibility to assign a deterministic value ± 1 to each of them by using a coloring argument on the corresponding basis vectors. Several simplifications of this original proof has been proposed in the literature. For instance, one can reduce to 18 the number of vectors needed to express the KS Theorem in terms of projectors [27].

6.2 TESTS OF CONTEXTUALITY AND QUANTUM GAMES

Adán Cabello [25, 26] used these operator-based proofs, the Mermin-Peres square and the Mermin pentagram, to design experimental tests for contextuality. Following Cabello to any operator-based proof of KS made of N contexts, one can assign an inequality of the following form

$$\chi = \sum_{i=0}^{S} \langle \mathcal{C}_i \rangle - \sum_{i=S+1}^{N} \langle \mathcal{C}'_i \rangle \leqslant b, \tag{77}$$

where $\langle \mathcal{C}_i \rangle$ (resp. $\langle \mathcal{C}'_i \rangle$) represents the expectation on a given positive (resp. negative) context, i.e. a set of mutually commuting observables such that their product is $+I_d$ (resp. $-I_d$). S represents the number of positive contexts and $N - S$ the number of negative ones. The bound b of this inequality depends on the assumption we want to test. Under the assumption of quantum mechanics the upper bound of inequality (77) is $b = N$, but if we consider a model based on a Non-Contextual Hidden Variables (NCHV) theory, then $b = 2s - N$, where s is the maximum number of quantum predictions that can be satisfied by the NCHV model. For instance, with the Mermin-Peres square on gets

$$b^{NCHV} = 4 \text{ and } b^{QM} = 6. \tag{78}$$

To take into account experimental imperfections, Cabello introduced a measure of robustness of the quantum violation of (77),

$$\varepsilon_N = \frac{b^{QM} - b^{NCHV}}{N}. \tag{79}$$

The quantity ε_N measures the tolerated error per correlation between the experimental value and the ideal quantum experiment [26].

Adán Cabello also proved in [26] that the most robust inequalities for testing contextuality with two-qubit Pauli operators are based on 15 operators and 15 contexts while for three-qubit operators it implies 63 operators and 315 contexts. We will see in Chapter 7 that these experimental settings correspond to the geometry of certain symplectic polar spaces.

Remark 6.2.1. One interesting advantage of inequalities of type (77) built from an operator-based proof of KS is that these inequalities are state independent.

In terms of quantum processing, the «magic» configurations have also been investigated under the scope of non-local games [2]. For each magic configuration one can define a game where cooperative players can win with certainty using a quantum strategy. Let us look at the magic square of Figure 2 and consider the following game involving two players Alice, Bob and a referee Charlie. As usual, Alice and Bob may define a strategy in advance, but cannot communicate once the game starts:

1. Charlie picks a number $r \in \{1, 2, 3\}$ for a row and $c \in \{1, 2, 3\}$ for a column and sends r to Alice and c to Bob.
2. Both Alice and Bob send back to the referee a triplet of ± 1 such that the number of -1 is odd for Alice and even for Bob.
3. Alice and Bob win the game if the number in position c of Alice triplet matches with the number in position r for Bob's triplet (and of course the triplets of Alice and Bob satisfy the parity condition of the previous step).

Such type of game is called a binary constrain game [33]. If Alice and Bob share a specific four-qubit entangled state (a product of two $|\mathrm{EPR}\rangle$-like states), they can win that game with certainty while it is easy to prove that there is no such classical strategy. In [3], Arkhipov gave a graph theoretic characterization of magic configurations in terms of planarity of the dual configuration.

6.3 SMALL KS OBSERVABLE-BASED PROOFS

The Mermin-Peres square and the Mermin pentagram are the smallest configurations, in terms of number of contexts and number of operators, providing observable-based proofs of contextuality [59]. Other proofs of the KS Theorem based on configurations of observables have been proposed by Waegel and Aravind [120, 121] or Planat and Saniga [100, 107].

To prove that a given configuration of observables is or is not a contextual one, we can first list the potential contextual configurations and provide a simple test by multiplying the operators on each context. Let us consider the configuration illustrated in Figure 15 in its most symmetric rendering known as the Pasch configuration. This configuration may represent a set of contexts with three points/operators per context and each node belongs to two contexts/lines. Such configuration is called a 2-context-geometry. Let us label its six points by observables $A_1, A_2, \ldots, A_6$ (with $A_i^2 = \mathrm{I}$).

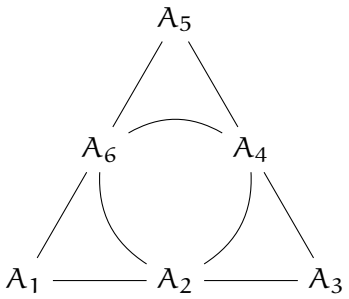

Figure 15: The Pasch configuration.

To find out whether this configuration is contextual, we can calculate the product of observables along each line/context, employing their associativity:

$$(A_1A_2A_3)(A_3A_4A_5)(A_5A_6A_1)(A_2A_4A_6) = A_1A_2A_4A_6A_1A_2A_4A_6. \tag{80}$$

Although the product of observables is, in general, not an observable, here the product of $A_1A_2A_4A_6$ is an observable. This is easy to see. As A_1, A_2 and A_3 are on the same context, $A_1A_2 = \pm A_3$ and, similarly, $A_4A_6 = \pm A_2$. But the same reasoning shows that $(\pm A_3)(\pm A_2) = \pm A_1$, i. e., $A_1A_2A_4A_6 = \pm A_1$. Therefore, we get

$$\begin{aligned}(A_1A_2A_3)(A_3A_4A_5)(A_5A_6A_1)(A_2A_4A_6) &= (A_1A_2A_4A_6)(A_1A_2A_4A_6)\\ &= (\pm A_1)^2\\ &= +\mathbf{Id},\end{aligned} \tag{81}$$

meaning that we cannot get an odd number of negative contexts; hence, the Pasch configuration is *not* contextual.

The same reasoning applied to the grid leads to the conclusion that the grid is pontentially contextual. Employing its labeling depicted in Figure 16, we have

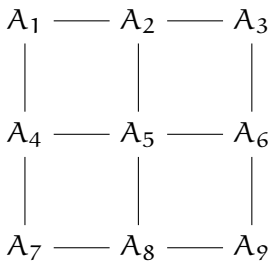

Figure 16: A grid.

$$(A_1A_2A_3)(A_3A_6A_9)(A_9A_8A_7)(A_7A_4A_1)(A_4A_5A_6)(A_2A_5A_8) = (A_1A_2A_6A_8)(A_1A_6A_2A_8), \tag{82}$$

which implies that if $A_2A_6 = -A_6A_2$ then the grid-configuration is contextual. Therefore, if the product of the observables on each context is $\pm\mathbf{Id}$ and if the observables that are not on the same context anti-commute, then we are sure to have a contextual grid. But these two properties are naturally satisfied by observables associated with grids contained in the N-qubit Pauli group, $N \geqslant 2$. In other words, a grid is always contextual when it is a subgeometry of a generalized Pauli group.

In a 2-contextual configuration the number l of lines/contexts and the number p of points/observables per line/context is related to the number of observables n_{obs} by the relation

$$n_{obs} = \frac{p \times l}{2}. \tag{83}$$

Thus by listing all 2-context configurations with $l \leqslant 6$ and $3 \leqslant p \leqslant 5$ and testing if these configurations are contextual, one showed in [59] that the Mermin-Peres square and the Mermin pentagrams are the smallest, in terms of number of observables and contexts, operator-based proofs of KS.

To conclude this section, we present a new operator-based proof made of 14 observables and 7 contexts realized with four-qubit Pauli operators. This configuration is a self-intersecting heptagon of Schläfli symbol $\{7/2\}$, depicted in Figure 17. Our heptagram belongs to a large

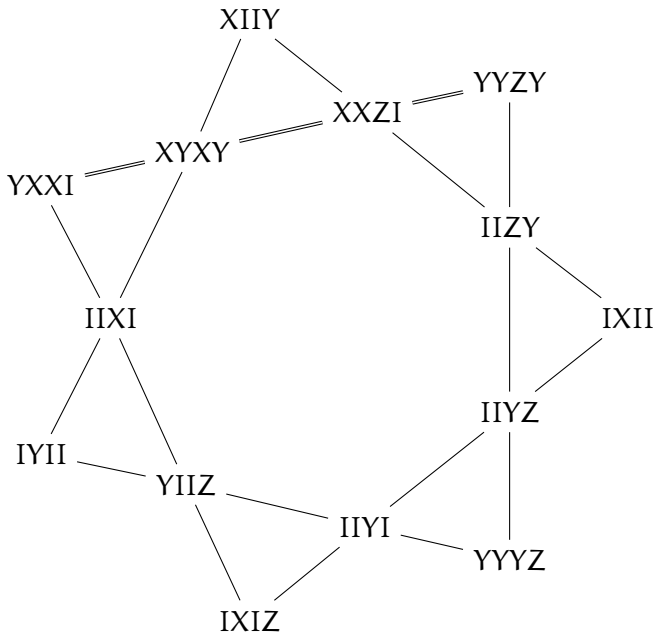

Figure 17: A «magic» heptagram of four-qubit observables.

family of regular star polygons. A $\{p/q\}$ regular star polygon, with p, q being positive integers, is obtained from a p-regular polygon by joining every qth vertex of the polygon. The pentagram is the first

regular star polygon of Schläfli symbol $\{5/2\}$. Regular star polygons are self-intersecting and, if also all points of self-intersections are included, they form a remarkable sequence of 2-context-geometries with pq points. The second regular star polygon of the sequence is a hexagram of Schläfi symbol $\{6/2\}$, but one can easly show using the same reasoning as for the Pasch configuration that the hexagon is not contextual. Therefore, our heptagram is the second contextual configuration of the sequence.

7

THE FINITE GEOMETRY OF THE GENERALIZED PAULI GROUP

In order to understand where the magic configurations live, I now start to describe geometrically the generalized N-qubit Pauli group $\mathcal{P}_N$, i.e. the group of Pauli operators acting on N-qubit systems. The main idea is the following: the non-trivial operators of an N-qubit Pauli group are, up to a scalar factor, in bijection with points in the projective space of dimension $2N-1$ over $\mathbb{F}_2$ and denoted by $PG(2N-1,2) = \mathbb{P}(\mathbb{F}_2^{2N})$. The commutation relations between the operators translate to the notion of colinearity with respect to a symplectic form at the level of the projective space. The space of isotropic subspaces of $PG(2N-1,2)$, known as the symplectic polar space of rank N over $\mathbb{F}_2$ and denoted by $\mathcal{W}(2N-1,2)$, is the geometry which accommodates the elements of the N-qubit Pauli group with its commutation relations. This idea of introducing $\mathcal{W}(2N-1,2)$ to describe geometrically the N-qubit Pauli group is due to Metod Saniga and Michel Planat [107, 49, 114] and has been employed in the past 10 years to address questions, with a finite geometric insight, about the commutation relations of Pauli observables in quantum information or about the structure of black-hole entropy formulas [15, 81, 82]. I first recall the principle of this construction (Section 7.1) and its connection with configurations well known in finite geometry (Section 7.2). Then I show (Section 7.3) how we can use this geometric language to bijectively associate maximal sets of mutually commuting operators of $\mathcal{P}_N$ with operators in $\mathcal{P}_{2^{N-1}}$, as we proved it with Metod Saniga and Péter Lévay in [60].

7.1 THE SYMPLECTIC POLAR SPACE OF RANK N AND THE N-QUBIT PAULI GROUP

Let us consider the subgroup $\mathcal{P}_N$ of $GL(2^N,\mathbb{C})$ generated by the tensor products of the Pauli matrices,

$$A_1 \otimes A_2 \otimes \cdots \otimes A_N \equiv A_1 A_2 \ldots A_N, \tag{84}$$

with $A_i \in \{\pm I, \pm iI, \pm X, \pm iX, \pm Y, \pm iY, \pm Z, \pm iZ\}$. The center of $\mathcal{P}_N$ is $\mathcal{C}(\mathcal{P}_N) = \{\pm I, \pm iI\}$ and $V_N = \mathcal{P}_N/\mathcal{C}(\mathcal{P}_N)$ is an abelian group.

To any class $\overline{\mathcal{O}} \in V_N$ there corresponds a unique element in $\mathbb{F}_2^{2N}$. More precisely, for any $\mathcal{O} \in \mathcal{P}_N$ we have $\mathcal{O} = sZ^{\mu_1}X^{\nu_1} \otimes \cdots \otimes Z^{\mu_N}X^{\nu_N}$ with $s \in \{\pm 1, \pm i\}$ and $(\mu_1, \nu_1, \ldots, \mu_N, \nu_N) \in \mathbb{F}_2^{2N}$. V_N is a vector space of dimension $2N$ over $\mathbb{F}_2$ and we can associate to any non-trivial

observable $\mathcal{O} \in \mathcal{P}_N \setminus I^N$ a point in the projective space $PG(2N-1,2) = \mathbb{P}(\mathbb{F}_2^{2N})$.

$$\pi : \begin{cases} \mathcal{P}_N \setminus I_N & \to \quad PG(2N-1,2) \\ \mathcal{O} = sZ^{\mu_1}X^{\nu_1} \otimes \cdots \otimes Z^{\mu_N}X^{\nu_N} & \mapsto \quad [\mu_1 : \nu_1 : \cdots : \mu_N : \nu_N]. \end{cases} \tag{85}$$

Because V_N is a vector space over $\mathbb{F}_2$, the lines of $PG(2N-1,2)$ are made of triplet of points (α, β, γ) such that $\gamma = \alpha + \beta$. The corresponding (class of) observables $\overline{\mathcal{O}_\alpha}$, $\overline{\mathcal{O}_\beta}$ and $\overline{\mathcal{O}_\gamma}$ satisfy $\overline{\mathcal{O}_\alpha}.\overline{\mathcal{O}_\beta} = \overline{\mathcal{O}_\gamma}$ (. denotes the product of operators). The representatives of a given class are defined up to $\pm 1, \pm i$.

Example 7.1.1. *For a single qubit one has $\pi(X) = [0:1]$, $\pi(Y) = [1:1]$ and $\pi(Z) = [1:0]$. The projective space $PG(1,2)$ is the projective line (X, Y, Z) (the projection π will be omitted).*

However the correspondence between non-trivial operators of $\mathcal{P}_N$ and points in $PG(2N-1,2)$ does not say anything about the commutation relations between the operators. To see geometrically these commutation relations, one needs to introduce an extra structure. Let $\mathcal{O}, \mathcal{O}' \in \mathcal{P}_N$ such that $\mathcal{O} = sZ^{\mu_1}X^{\nu_1} \otimes \cdots \otimes Z^{\mu_N}X^{\nu_N}$ and $\mathcal{O}' = s'Z^{\mu'_1}X^{\nu'_1} \otimes \cdots \otimes Z^{\mu'_N}X^{\nu'_N}$ with $s, s' \in \{\pm 1, \pm i\}$ and $\mu_i, \nu_i, \mu'_i, \nu'_i \in \mathbb{F}_2$. Then, we have

$$\mathcal{O}.\mathcal{O}' = (ss'(-1)^{\sum_{j=1}^N \mu'_j \nu_j}, \mu_1 + \nu'_1, \ldots, \mu_N + \nu'_N), \tag{86}$$

and the two Pauli operators $\mathcal{O}$ and $\mathcal{O}'$ of $\mathcal{P}_N$ commute if and only if

$$\sum_{j=1}^N (\mu_j \nu'_j + \mu'_j \nu_j) = 0. \tag{87}$$

Let us add to V_N the symplectic form

$$\langle \overline{\mathcal{O}}, \overline{\mathcal{O}'} \rangle = \sum_{j=1}^N (\mu_j \nu'_j + \mu'_j \nu_j), \tag{88}$$

and let us denote by $\mathcal{W}(2N-1,2)$, the symplectic polar space of rank N, i.e. the set of totally isotropic subspaces of $(PG(2N-1,2), \langle , \rangle)$. The symplectic polar space $\mathcal{W}(2N-1,2)$ encodes the commutation relations of $\mathcal{P}_N \setminus I_N$. The points of $\mathcal{W}(2N-1,2)$ correspond to (classes of) non trivial operators of $\mathcal{P}_N$ and the subspaces of $\mathcal{W}(2N-1,2)$ correspond to $\mathbb{P}(\mathcal{S}/\mathcal{C}(\mathcal{P}_N))$, where $\mathcal{S}$ is a set of mutually commuting elements of $\mathcal{P}_N$. The maximal totally isotropic subspaces of $PG(2N-1,2)$ are called generators of $\mathcal{W}(2N-1,2)$ and are of (projective) dimension $N-1$.

Let us also denote by $\mathcal{Q}^+(2N-1,2)$ the elements of $PG(2N-1,2)$ satisfying

$$Q_0(x) = x_1x_2 + x_3x_4 + \cdots + x_{2N-1}x_{2N} = 0. \tag{89}$$

Then it is clear that the elements of $\mathcal{P}_N$ which belong to $\mathcal{Q}^+(2N-1,2)$ correspond to elements which contain an even number of Y's and thus square to $+I_2 \otimes I_2 \otimes \cdots \otimes I_2$. These elements are called symmetric elements.

7.2 GENERALIZED POLYGONS

I now describe in detail $\mathcal{W}(3,2)$ and $\mathcal{W}(5,2)$, the symplectic polar spaces encoding the commutation relations of the 2- and 3-qubit Pauli groups and their relation with generalized polygons.

For the two-qubit Pauli group, Eq. (85) gives $\pi(XI) = [0:1:0:0]$, $\pi(IX) = [0:0:0:1]$, $\pi(XX) = [0:1:0:1]$, etc... The symplectic polar space $\mathcal{W}(3,2)$ consists of all 15 points of $PG(3,2)$ but only the 15 isotropic lines are kept. This gives a point-line representation of $\mathcal{W}(3,2)$ (Figure 18) known as the doily [49].

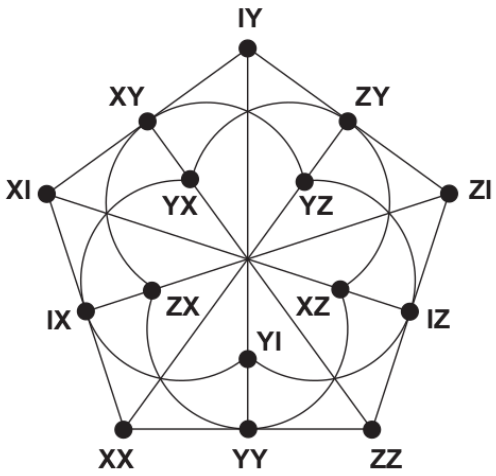

Figure 18: The labeling of the doily, i.e. $\mathcal{W}(3,2)$, by elements of the 2-qubit Pauli group.

The doily is an example of a generalized quadrangle.

Definition 7.2.1. *A point-line incidence structure is called a generalized quadrangle of type* (s,t) *and denoted by* $GQ(s,t)$ *iff it is an incidence structure such that every point is on* $t+1$ *lines and every line contains* $s+1$ *points such that if* $p \notin L, \exists! q \in L$ *such that* p *and* q *are colinear.*

In the following I will keep denoting by $\mathcal{W}(3,2)$ both the symplectic polar space and the associated point-line geometry $GQ(2,2)$, aka the doily.

Remark 7.2.1. The doily and all the generalized quadrangles are examples of generalized polygons in the sense that the generalized

quadrangles contain quadrangle but are triangle free. Similarly a generalized n-gon will contain n-gons but will be m-gons free for any $2 \leqslant m \leqslant n-1$ [102].

For the three-qubit Pauli group one has (Eq. (85)) $\pi(ZII) = [1:0:0:0:0:0], \pi(XII) = [0:1:0:0:0:0], \pi(YII) = [1:1:0:0:0:0], \ldots$. The projective space $PG(5,2)$ contains 63 elements and $\{XXY, XIZ, IXX\}$ is an example of projective line which is not isotropic while $\{XII, IXI, XXI\}$ is an example of an isotropic line. In the basis $ZII \leftrightarrow (1,0,0,0,0,0), XII \leftrightarrow (0,1,0,\ldots,0), \ldots, IIX \leftrightarrow (0,0,0,0,0,1)$, the symplectic form on $V_3 \simeq \mathbb{F}_2^3$ is given by

$$\langle \overline{p}, \overline{q} \rangle = {}^t p \begin{pmatrix} 0_3 & I_3 \\ I_3 & 0_3 \end{pmatrix} q.$$

The automorphism group of $\mathcal{W}(5,2)$ is $Sp(6,2)$ whose double covering is given by $W(E_7)$ the Weyl group of E_7. The symplectic polar space $\mathcal{W}(5,2)$ contains 63 points, 315 lines and 135 Fano planes. As mentioned in Chapter 6, one can build 12096 distinguished Mermin pentagrams from those 63 points [101, 81].

In the case of the three-qubit Pauli group there is no generalized polygon which accommodates the full geometry $\mathcal{W}(5,2)$. However there exists an embedding in $\mathcal{W}(5,2)$ of the split-Cayley Hexagon of order 2 which is a generalized hexagon with 63 points and 63 lines such that each line contains 3 points and each point belongs to 3 lines. The split-Cayley hexagon accommodates the 63 three-qubit operators of the three-qubit Pauli group such that the lines of the configuration are totally isotropic lines of $\mathcal{W}(5,2)$ (Figure 19).

Remark 7.2.2. According to Adán Cabello [26], the most robust state independent experiment to test quantum contextuality with two-qubit and three-qubit operators are obtained when we consider the full geometry of $\mathcal{W}(3,2)$ (i.e. 15 operators and 15 contexts) and $\mathcal{W}(5,2)$ (63 operators and 315 contexts).

7.3 GENERATORS OF $\mathcal{W}(2N-1,2)$ AND THE VARIETY $\mathcal{Z}_N$

In [81] Péter Lévay, Michel Planat and Metod Saniga found and analyzed in detail an explicit bijection between the set of 135 maximum sets of mutually commuting elements of the three-qubit Pauli group (that is, the set of generators of $\mathcal{W}(5,2)$) and the set of 135 symmetric operators of the four-qubit Pauli group (that is, the set of points lying on a particular $\mathcal{Q}^+(7,2)$ of $\mathcal{W}(7,2)$). Following the spirit of this work, we generalized with Metod Saniga and Péter Lévay in [60] this result and proved the existence of a similar bijection between the set of generators of any N-qubit Pauli group and a subvariety of the 2^N-qubit Pauli group.

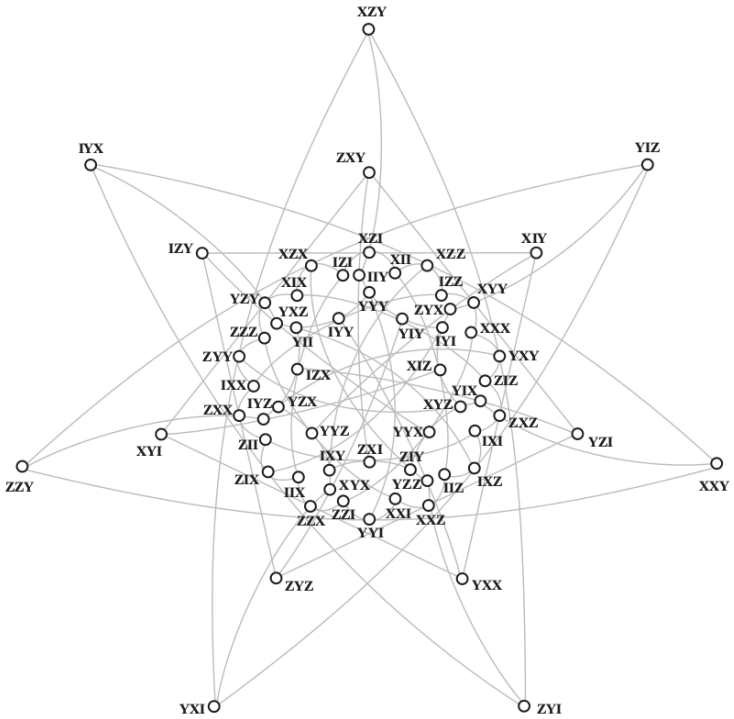

Figure 19: A 3-qubit Pauli group embedding of the split Cayley Hexagon [82].

Let us first define the variety of principal minors for symmetric matrices.

Definition 7.3.1. *Let $\mathbb{K}$ be a field and $I = [i_1, \ldots, i_N]$ a binary multi-index. Let us denote by $\mathcal{Z}_N \subset \mathbb{P}(\mathbb{K}^{2^N})$ the image of the following rational map [93]:*

$$\begin{array}{rccc} \varphi: & \mathbb{P}(S^2\mathbb{K}^N \oplus \mathbb{K}) & \dashrightarrow & \mathbb{P}((\mathbb{K}^2)^{\otimes N}) \\ & [A,t] & \mapsto & [t^{N-|I|}\Delta_I(A)X^I], \end{array}$$

where A is a symmetric matrix with coefficients in $\mathbb{K}$, $X^I = x_1^{i_1} \otimes \cdots \otimes x_N^{i_N}$ with $i_j = \begin{cases} 0 & \text{if } j \notin I \\ 1 & \text{if } j \in I \end{cases}$ is a tensorial basis of $(\mathbb{K}^2)^{\otimes N}$ and $\Delta_I(A)$ denotes the I principal minor, i.e. the determinant of the submatrix defined by the indices $i_j \neq 0$. The map φ being rational, $\mathcal{Z}_N = \varphi(\mathbb{P}(S^2\mathbb{K}^N \oplus \mathbb{K}))$ is an algebraic variety, called the variety of principal minors of symmetric matrices.

Remark 7.3.1. The variety $\mathcal{Z}_N$ has been studied over the complex numbers by algebraic geometers. The motivation for studying $\mathcal{Z}_N$ in the complex case comes from the Principal Minors Assignment Problem [59, 83]. This problem asks for necessary and sufficient conditions

for a collection of 2^N numbers to arise as the principal minors of an $N \times N$ matrix. In the case of symmetric matrices, a collection of 2^N numbers corresponds to principal minors of a symmetric matrix if and only if the corresponding point in $\mathbb{P}((\mathbb{C}^2)^{\otimes N})$ belongs to the variety $\mathcal{Z}_N$. This problem for symmetric matrices was solved by Luke Oeding [94, 93] who successfully described a set of degree 4 polynomials which cut out the variety $\mathcal{Z}_N$.

Let us consider $\mathbb{K} = \mathbb{F}_2$ and let us explain how one can map bijectively generators of the symplectic polar space of rank N to points of the variety of principal minors for symmetric matrices over the two-element field. The map is based on well-known classical constructions of algebraic geometry and turned out to be bijective over $\mathbb{F}_2$. The generators of $\mathcal{W}(2N-1,2)$ corresponds to N-dimensional isotropic spaces $PG(N-1,2)$ of $PG(2N-1,2)$. Once we fix a basis and a skew-symmetric symmetric form, one can map, using the Plücker embedding, those generators to points on the Lagrangian variety $LG(N,2N)$, i.e. the variety of isotropic N-planes of $PG(2N-1,2)$.

$$\begin{array}{ccc} \mathcal{W}(2N-1,2) & \to & LG(N,2N) = G(N,2N) \cap \mathbb{P}(L) \subset \mathbb{P}(\bigwedge^N \mathbb{F}_2^{2N}) \\ \{e_1,\ldots,e_N\} & \mapsto & [e_1 \wedge \cdots \wedge e_N], \end{array} \tag{90}$$

where $\mathbb{P}(L)$ is the linear space defined by the isotropic conditions.

The variety $LG(N,2N)$ can be parametrized by (all) minors of the set of symmetric matrices of size $N \times N$ [70] (like the usual Grassmannian variety which can be parametrized by minors of matrices). Therefore, $LG(N,2N)$ can be projected down to the variety $\mathcal{Z}_N$ by only keeping the coordinates corresponding to the principal minors. This defines a surjective map from $LG(N,2N)$ to $\mathcal{Z}_N$. Over $\mathbb{F}_2$, this projection is also an injective map. Indeed the off-diagonal entries of a symmetric matrix A can be determined by the principal minors because over $\mathbb{F}_2$ one has

$$\Delta_{[i,j]}(A) = a_{i,i}a_{j,j} - a_{i,j}^2 \Leftrightarrow a_{i,j} = \Delta_{[i]}(A)\Delta_{[j]}(A) - \Delta_{[i,j]}(A). \tag{91}$$

This construction shows that [60],

Theorem 6. *There exists a bijection between the generators of $\mathcal{W}(2N-1,2)$ and the points of $\mathcal{Z}_N \subset PG(2^N-1,2)$.*

In [60] one uses this construction to obtain the defining equations of $\mathcal{Z}_N = \Phi(\mathcal{W}(2N-1,2))$ for $N = 3$ and $N = 4$ by first computing the ideal of $LG(N,2N)$ and then computing the projection using techniques of elimination theory.

Example 7.3.1. *For $N = 2$, the generators of $\mathcal{W}(3,2)$ are bijectively mapped to the points of $PG(3,2)$.*

Example 7.3.2. *For $N = 3$, the ideal of the variety $LG(3,6)$ is defined by quadratic equations (the Plücker relations defining $G(3,6)$ and the isotropic*

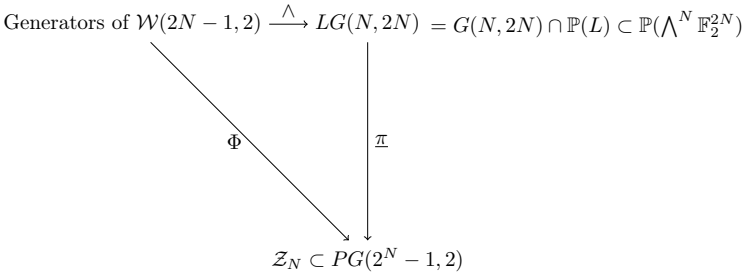

Figure 20: Mapping the set of generators of $\mathcal{W}(2N-1,2)$ to the variety of principal minors. We denote by $\wedge$ the Plücker embedding and $\underline{\pi}$ the projection of the Lagrangian variety. The mapping from the set of generators to the variety of principal minor is denoted by Φ and we have $\Phi = \underline{\pi} \circ \wedge$.

condition) which boils down to a single quadratic relation when we consider the projection to $\mathcal{Z}_3$. This quadratic equation is nothing but the equation of the hyperbolic quadric $\mathcal{Q}^+(7,2) \subset \mathrm{PG}(7,2)$, i.e. one recovers the result of [81].

The case $N = 4$ requires more work and calculations using Gröbner basis to compute the elimination ideal and the case $N = 5$ was out of reach for our computer resources [60]. Recently, in [116], it was proven that over $\mathbb{F}_2$, the variety $\mathcal{Z}_N$ is the spinor variety $\mathcal{S}_{N+1}$.

The mapping of Figure (20) allows us to assign symmetric operators of the 2^{N-1} Pauli group to maximal set of mutually commuting N-qubit Pauli operators. The knowledge of the $\mathrm{GL}(2)^{\times N}$ orbit stratification in $\mathrm{PG}(2^N-1,2)$ allows us to distinguish different classes of maximal set of mutually commuting operators in $\mathcal{W}(2N-1,2)$ as pull-back of the map Φ. The cases $N = 2,3,4$ are given in Appendix C.

8

THE GEOMETRY OF HYPERPLANES II: VELDKAMP SPACE OF A POINT-LINE GEOMETRY

One considers in this chapter the notion of Veldkamp space of a point-line geometry. Given an incidence geometry $\mathcal{G}$ endowed with geometric hyperplanes one can define the Veldkamp space of $\mathcal{G}$, i.e. the space where points are the hyperplanes of the geometry (see the definition in Section 8.1). This construction allows us to consider subspaces (hyperplanes) of $\mathcal{W}(2N-1,2)$ as points in a new geometry. In Chapter 9 this notion of Veldkamp geometry will provide a new connection between the generalized Pauli groups and weight diagrams of simple Lie algebras. In this chapter I first introduce the basic definitions in Section 8.1 and some illustrative examples in Section 8.2. In Section 8.3 I explain how the analysis of the geometric hyperplanes of the Segre variety $\mathcal{S}_N(2)$, i.e. the cartesian product of N projective lines over $\mathbb{F}_2$, was conducted in [104]. Thanks to the Lagrangian mapping described in Chapter 7, the classification of geometric hyperplanes of $\mathcal{S}_N(2)$ for $N=3$ and $N=4$ provides an alternative way of describing the stratification of the maximal sets of mutually commuting operators in $\mathcal{W}(5,2)$ and $\mathcal{W}(7,2)$. This chapter is based on [105, 104, 16].

8.1 THE VELDKAMP GEOMETRY

The points and lines of $\mathcal{W}(2N-1,2)$ define an incidence structure, i.e. a point-line geometry $\mathcal{G}=(\mathcal{P},\mathcal{L},\mathcal{I})$ where $\mathcal{P}$ are the points of $\mathcal{W}(2N-1,2)$, $\mathcal{L}$ are the lines and $\mathcal{I}\subset\mathcal{P}\times\mathcal{L}$ corresponds to the incidence relation. I now introduce some geometric notions for point-line incidence structures.

Definition 8.1.1. *Let $\mathcal{G}=(\mathcal{P},\mathcal{L},\mathcal{I})$ be a point-line incidence structure. A hyperplane $\mathcal{H}$ of $\mathcal{G}$ is a subset of $\mathcal{P}$ such that a line of the incidence structure is either contained in $\mathcal{H}$ or has a unique intersection with $\mathcal{H}$.*

Example 8.1.1. *Let us consider the grid 3×3 with 3 points per line, also known as $\mathrm{GQ}(2,1)$. This geometry has 15 hyperplanes splitting in two different types: the perp-sets (the union of two «perpendicular» lines) and the ovoids (hyperplanes that contain no lines).*

The notion of geometric hyperplanes leads to the notion of Veldkamp space as introduced in [108].

Definition 8.1.2. *Let $\mathcal{G}=(\mathcal{P},\mathcal{L},\mathcal{I})$ be a point-line geometry. The Veldkamp space of $\mathcal{G}$, denoted by $\mathcal{V}(\mathcal{G})$, if it exists, is a point-line geometry such that*

- *the points of $\mathcal{V}(\mathcal{G})$ are geometric hyperplanes of $\mathcal{G}$,*

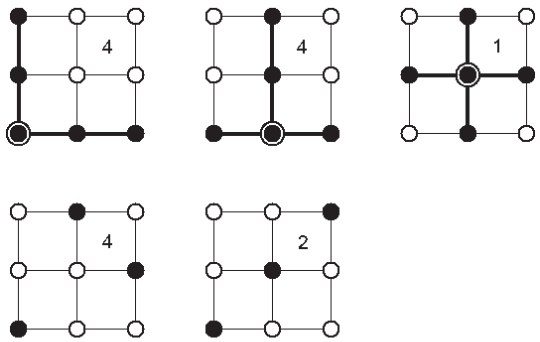

Figure 21: A pictorial representation of the 15 hyperplanes of the grid $GQ(2,1)$ (the figures indicate the number of representatives).

- *given two points* H_1 *and* H_2 *of* $\mathcal{V}(\mathcal{G})$*, the Veldkamp line defined by* H_1 *and* H_2 *is the set of hyperplanes* H *of* $\mathcal{G}$ *such that* $H_1 \cap H = H_2 \cap H = H_1 \cap H_2$ *or* $H = H_i, i = 1, 2$.

Figure 22 furnishes an example of a Veldkamp line in $\mathcal{V}(GQ(2,1))$. It is not difficult to show that the hyperplanes of $GQ(2,1)$ accommodate the 15 points and 35 lines of $PG(3,2)$, i.e. $\mathcal{V}(GQ(2,1)) = PG(3,2)$.

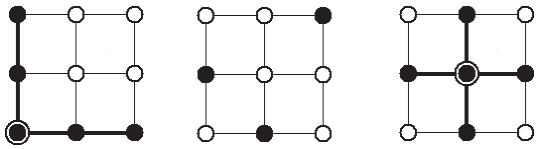

Figure 22: An example of Veldkamp line of $GQ(2,1)$, i.e. a line in $\mathcal{V}(GQ(2,1))$. The three hyperplanes share two by two the same intersection (and no other hyperplane of $GQ(2,1)$ does).

8.2 THE VELDKAMP SPACE OF $\mathcal{P}_2$ AND $\mathcal{P}_3$

Looking at the doily (Figure 18) one can identify the Mermin-Peres squares built with two-qubit Pauli operators as geometric hyperplanes of $\mathcal{W}(3,2)$.

In fact three different types of hyperplanes can be found in the doily as shown in Figure 23:

- The hyperplanes made of 9 points (red) correspond to grids $GQ(2,1)$ and it is easy to check that grids in the two-qubit Pauli group are always contextual configurations [59] (Chapter 6), i.e. all grids of $\mathcal{W}(3,2)$ are Mermin-Peres squares. Rotating by $\frac{2\pi}{5}$

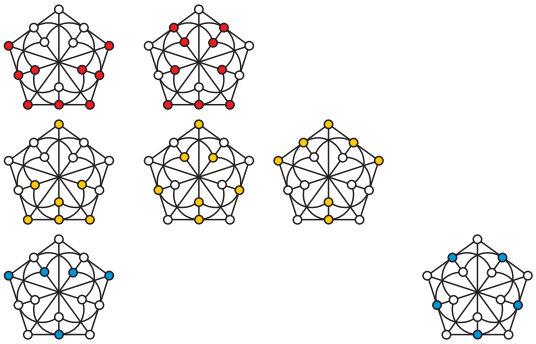

Figure 23: The different types of hyperplanes of the doily [108]. The hyperplanes in red correspond to grids inside the doily.

one gets 10 Mermin-Peres grids in the doily (See Figure 13 of Chapter 6).

- The second type of hyperplanes (yellow ones) are called perp-sets (all lines of the hyperplane meet in one point) and one sees from Figure 23 that there are 15 of them.
- Finally, the last type of hyperplanes of the doily (blue) are line-free and such type of hyperplanes are called ovoids. The doily contains 6 ovoids.

The geometry of $\mathcal{V}(GQ(2,2))$, the Veldkamp space of the doily, was described in full detail in [108]. Figure 24 illustrates the different types of Veldkamp lines that can be obtained from the hyperplanes of the doily. In particular, $\mathcal{V}(\mathcal{W}(3,2))$ comprises 31 points splitting in three orbits and 155 lines splitting in 5 different types. One can show that $\mathcal{V}(GQ(2,2)) \simeq PG(4,2)$.

The general structure of $\mathcal{V}(\mathcal{W}(2N-1,2))$ was studied in detail by Péter Vrana and Péter Lévay in [119] where the descriptions of the geometric hyperplanes of $\mathcal{W}(2N-1,2)$ are explicitly given. First, let us mention that for $\mathcal{G} = \mathcal{W}(2N-1,2)$ the Veldkamp line defined by two hyperplanes H_1 and H_2 is a 3-point line (H_1, H_2, H_3) where H_3 is given by the complement of the symmetric difference of the other two hyperplanes,

$$H_3 = H_1 \boxplus H_2 = \overline{H_1 \Delta H_2}. \tag{92}$$

To reproduce the description of $\mathcal{V}(\mathcal{W}(2N-1,2))$ of [119], let us recall the definition of the following quadratic form over V_N (already introduced in Chapter 7, Eq. (89)):

$$Q_0(x) = \sum_{i=1}^{2N-1} x_i x_{i+1} \text{ where } x = (x_1, x_2, \ldots, x_{2N-1}, x_{2N}). \tag{93}$$

Recall that an observable $\mathcal{O}$ is said to be symmetric if it contains an even number of Y's, or skew-symmetric if it contains an odd number

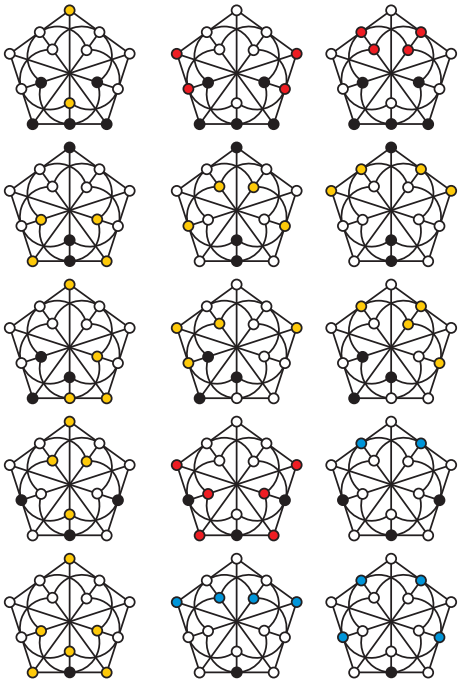

Figure 24: The 5 types of Veldkamp lines of the doily [108]. One can check that given any two hyperplanes on a line, the third one is the complement of the symmetric difference of the two, see Eq (92).

of Y's. In terms of the quadratic form Q_0, this leads to the conditions $Q_0(\overline{\mathcal{O}}) = 0$ or $Q_0(\overline{\mathcal{O}}) = 1$, respectively.

There are three types of geometric hyperplanes in $\mathcal{W}(2N-1,2)$:

$$\text{Type 1: } C_q = \{p \in \mathcal{W}(2N-1,2), \langle p, q\rangle = 0\}. \tag{94}$$

This set corresponds to the «perp-set» defined by q, i.e. in terms of operators, it is the set of elements commuting with $\overline{\mathcal{O}}_q$.

To define Type 2 and Type 3, let us introduce a family of quadratic forms on V_N parametrized by the elements of V_N: $Q_q(p) = Q_0(p) + \langle q, p\rangle$. Depending on the nature of $\overline{\mathcal{O}}_q$ (symmetric or skew-symmetric) the quadratic form will be called hyperbolic or elliptic.

Type 2: for $\overline{\mathcal{O}}_q$ symmetric,

$$H_q = \{p \in \mathcal{W}(2N-1,2), Q_q(p) = 0\} \simeq Q^+(2N-1,2), \tag{95}$$

and

Type 3: for $\overline{\mathcal{O}}_q$ skew-symmetric

$$H_q = \{p \in \mathcal{W}(2N-1,2), Q_q(p) = 0\} \simeq Q^-(2N-1,2), \tag{96}$$

where $Q^+(2N-1,2)$ denotes a hyperbolic quadric[1] of $\mathcal{W}(2N-1,2)$, and $Q^-(2N-1,2)$ denotes an elliptic quadric[2] of $\mathcal{W}(2N-1,2)$.

The set H_q represents the set of observables either symmetric and commuting with $\overline{\mathcal{O}}_q$ or skew-symmetric and anticommuting with $\overline{\mathcal{O}}_q$.

Moreover the following equalities hold

$$C_p \boxplus C_q = C_{p+q}, H_p \boxplus H_q = C_{p+q} \text{ and } C_p \boxplus H_q = H_{p+q}. \quad (97)$$

As proved in [119], this leads to five different types of Veldkamp lines in $\mathcal{W}(2N-1,2)$ depending on the nature (symmetric or not) of the points p and q (we also recover the 5 different types of Veldkamp lines illustrated in Figure 24).

8.3 STRATIFICATION OF PG($2^N-1,2$)

In Chapter 7, one showed that there exists a bijective mapping between generators of $\mathcal{W}(2N-1,2)$ and the image $\underline{\pi}(LG(N,2N)) \subset PG(2^N-1,2)$. In particular this mapping allows us to stratify the maximal sets of mutually commuting operators of $\mathcal{W}(2N-1,2)$ by G-orbits of $PG(2^N-1,2)$, where $G = SL(2,2) \times SL(2,2) \times \cdots \times SL(2,2) \rtimes \sigma_N$ (see Appendix C).

This stratification can be recovered by the Veldkamp space of the N-binary Segre variety. Indeed, let us consider $S_N(2) = PG(1,2) \times \cdots \times PG(1,2)$ the cartesian product of N projective lines. By general results on partial gamma spaces [34], one can show that $\mathcal{V}(S_N(2))$ is a projective space. More precisely, $\mathcal{V}(S_N(2)) = PG(2^N-1,2)$. By the Segre map[3], $S_N(2)$ can be embedded into $PG(2^N-1,2)$ and points $p \in PG(2^N-1,2)$ are in bijection with hyperplanes H of $S_N(2)$,

$$p \in PG(2^N-1,2) \longleftrightarrow H = p^\perp \cap Seg(S_N(2)) \in \mathcal{V}(S_N(2)). \quad (98)$$

It follows that G-orbits of $PG(2^N-1,2)$ are in bijection with $(S_3 \times \cdots \times S_3) \rtimes \sigma_N$-orbits of hyperplanes of $S_N(2)$. Therefore, a geometric classification of the hyperplanes of $S_N(2)$ will provide an alternative description of the G-orbits of $PG(2^N-1,2)$. For $N=3$ and $N=4$, the G-orbits of $PG(2^N-1,2)$ were obtained by computer calculations by Bremner and Stravou [19].

To compute and classify geometrically the hyperplanes in $S_N(2)$, we introduced in [104] the so-called blow-up construction. This procedure takes advantage of the fact that the knowledge of the Veldkamp lines of $S_{N-1}(2)$ allows one to construct all hyperplanes of $S_N(2)$. Indeed, a hyperplane of $S_N(2)$ defines a Veldkamp line of $\mathcal{V}(S_{N-1}(2))$ if one considers it «slice by slice». For instance, let us consider the

1 Up to a transformation of coordinates, this is a set of points $x \in PG(2N-1,2)$ satisfying the standard equation $Q_0(x) = 0$.

2 Up to a transformation of coordinates this is defined as a set of points $x \in PG(2N-1,2)$ such that $f(x_1,x_1) + x_2x_3 + \ldots x_{2N-1}x_{2N} = 0$.

3 See Chapter 2, Eq. (6).

grid $GQ(2,1)$, i.e. $S_2(2)$. Then there exists two types of hyperplanes denoted by H_1 and H_2 in Figure 21. The analysis of the corresponding Veldkamp lines of $\mathcal{V}(GQ(2,1))$ is reproduced in Table 9. These

	Core		Comp'n		
Tp	Ps	Ls	H_1	H_2	Crd
1	3	1	3	–	6
2	2	0	2	1	18
3	1	0	1	2	9
4	0	0	–	3	2

Table 9: The types of ordinary Veldkamp lines of $S_{(2)}$. The first column gives the type, the next two columns tell us about how many points and lines belong to all the three geometric hyperplanes a line of the given type consists of, then we learn about the line's composition and, finally, the last column lists cardinalities for each type.

collections of lines produce hyperplanes in $S_3(2)$ as shown in Figure 25. To generate all possible hyperplanes of $S_3(2)$ one also needs

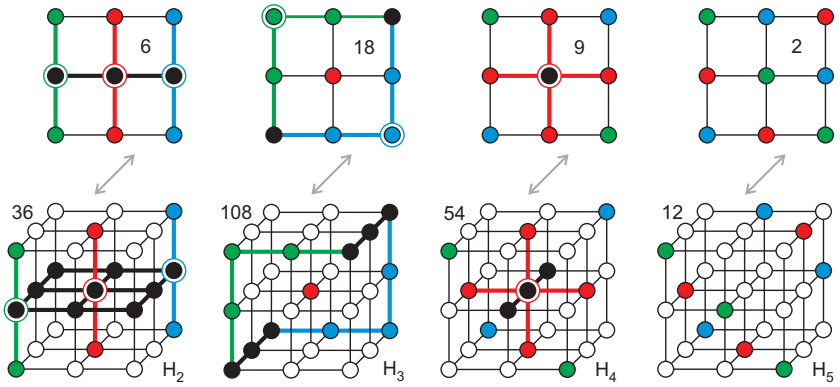

Figure 25: *Top:* – A descriptive illustration of the structure of the four distinct types (1 to 4, left to right) of ordinary Veldkamp lines of $S_{(2)}$ (Table 9); the three geometric hyperplanes comprising a Veldkamp line are distinguished by different colors, with the points and lines shared by all of them being colored black. *Bottom:* – The four distinct types of geometric hyperplanes of $S_{(3)}$, as well as the number of copies per each type, we get by blowing-up Veldkamp lines of $S_{(2)}$ of the type shown above the particular subfigure.

to generate what we named in [104] extraordinary Veldkamp line of $S_2(2)$ (the "usual" lines will be called ordinary). An extraordinary Veldkamp line of $S_2(2)$ will be a line composed by a full geometry $S_2(2)$ and two copies of the same hyperplane. Such triple (D, H, H) (with $D = S_2(2)$) is not a line of $\mathcal{V}(S_2(2))$ (because the full geometry is not considered as a hyperplane), but satisfies the relation $D \boxplus H = H$.

There are two type of extraordinary Veldkamp lines for $S_2(2)$: The lines of type I corresponding to the triple (D, H_1, H_1) and the lines of type II corresponding to the triple (D, H_2, H_2) (Figure 26). Adding the hyperplanes obtained from these extraordinary Veldkamp lines, one obtains all geometric hyperplanes of $S_3(2)$ (Table 10).

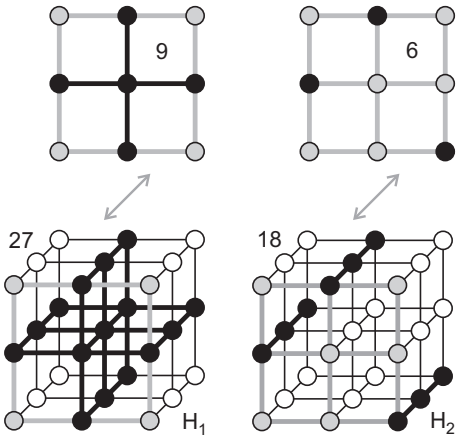

Figure 26: The same as in Figure 25, but for extraordinary Veldkamp lines of $S_{(2)}$ (*top*) and their $S_{(3)}$ blown-up cousins (*bottom*). The first type of lines will be denoted by type I and the second by type II.

			Points of Order				$S_{(2)}$'s of Type						
Tp	Ps	Ls	0	1	2	3	D	H_1	H_2	VL	Crd	BS	W
1	19	15	0	0	12	7	3	6	0	I	27	2	1
2	15	9	0	6	6	3	1	6	2	II, 1	54	3	2
3	13	6	1	6	6	0	0	6	3	2	108	4	2
4	11	3	4	6	0	1	0	3	6	3	54	5	3
5	9	0	9	0	0	0	0	0	9	4	12	6	3

Table 10: The 5 types of (ordinary) geometric hyperplanes of the Segre variety $S_{(3)}$. The first column gives the type ('Tp') of a hyperplane, which is followed by the number of points ('Ps') and lines ('Ls') it contains, and the number of points of given order. The next three columns tell us about how many of 9 $S_{(2)}$'s are fully located ('D') in the hyperplane and/or share with it a hyperplane of type H_1 or H_2. The VL-column lists the types of (ordinary and extraordinary) Veldkamp lines of $S_{(2)}$ we get by projecting a hyperplane of the given type into an $S_{(2)}$ along the lines of all three distinguished spreads. Finally, for each hyperplane type we give its cardinality ('Crd'), the corresponding large orbit of $2 \times 2 \times 2$ arrays over $\mathbb{F}_2$ ('BS') taken from Table 3 of Bremner and Stavrou [19], and its weight, or rank in the language of [19] ('W').

The hyperplanes of types 1, 2 and 4 correspond to points of the hyperbolic quadric $\mathcal{Q}^+(7,2) \subset \mathrm{PG}(7,2)$ and are in bijection with the 135 maximal set of mutually commuting operators of $\mathcal{W}(5,2)$. These three orbits should be compared with Table 17 of Appendix C, where maximal sets of mutually commuting operators are splitted into 3 classes.

In [104] one also obtained by the blow-up procedure the classification of the geometric hyperplanes of $S_4(2)$ without using any group action. The corresponding table is reproduced in Appendix D.

Remark 8.3.1. In [16] one conducted a similar study to analyze the Veldkamp space of the Segre varieties over the $\mathbb{F}_3$, the 3 element field. Over $\mathbb{F}_3$ the Veldkamp space $\mathcal{V}(S_N(3))$ is not a projective space anymore. Already for $N = 3$, some hyperplane of $S_3(3)$ are not projective, i.e. cannot be obtained as linear section of the Segre embedding of $S_3(3)$ in $\mathrm{PG}(7,3)$.

9

WHAT QUANTUM INFORMATION TELLS US ABOUT REPRESENTATION THEORY

In this last chapter of Part II I describe another connection between classical representation theory of simple Lie algebras and the geometry of quantum information. Instead of using representation theory to describe the geometry of entanglement, like in Chapter 5 of Part I, I use the geometry of a specific class of three-qubit Veldkamp lines to build weight diagrams of some Lie algebras.

This chapter is essentially based on part of the material of [80] where we investigated in detail, with Péter Lévay and Metod Saniga, different components of a specific class of Veldkamp lines of the three-qubit Pauli group. We studied the hyperplanes composing a representative of this class of lines in terms of representation theory, finite geometry and we established a connection between these objects and invariants of physical importance. Initially, our motivation was to extend the work of [83] where a representation theoretic interpretation of a set of Mermin pentagrams was given. Because the (class of the) Veldkamp lines we studied in [80] accommodates, as a subspace, the set of Mermin pentagrams considered in [83], we named this line the three-qubit magic Veldkamp line.

9.1 THE «MAGIC VELDKAMP LINE»

In [83] it was first proved that the 12096 Mermin pentagrams of the three-qubit Pauli group can be grouped into 1008 families, each familly containing 12 pentagrams. Those 1008 famillies can be mapped bijectively to the 1008 elements of a specific class of Veldkamp lines. Recall from Chapter 8 that in $\mathcal{V}(\mathcal{W}(2N-1,2))$ there are 5 classes of Veldkamp lines and let us consider, for $N=3$, the class of lines of type $\mathcal{H}-\mathcal{E}-\mathcal{P}$, i.e. hyperbolic-elliptic-perp. Because $Sp(6,2)$ acts transitivelly on this class of Veldkamp lines [119], one can use its canonical representative. Let us therefore consider in this class the Veldkamp line $(H_{III}, H_{YYY}, C_{YYY})$ as a representative. According to Chapter 8, one has the following description of the three hyperplanes composing the line H_{III}, H_{YYY} and C_{YYY} in terms of Pauli operators,

- C_{YYY} is the perp-set defined by the operator YYY, i.e. the points in C_{YYY} correspond to operators commuting with YYY.
- H_{III} is an hyperbolic quadric, i.e. defined by $Q_0(x) = 0$. In terms of operators it corresponds to the set of symmetric operators (i.e. containing an even number of Y).

- H_{YYY} is an elliptic quadric, i.e. defined by $Q_{YYY}(x) = 0$. In terms of operators it corresponds to the set of symmetric operators commuting with YYY or the skew-symmetric ones anti-commuting with YYY.

Figure 27 is a schematic representation of the 3 hyperplanes of a Veldkamp line of type $\mathcal{E} - \mathcal{H} - \mathcal{P}$. As it will be shown in the next section, the core set of this line is a doily.

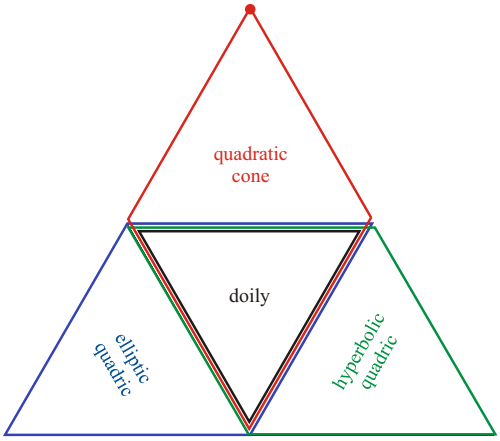

Figure 27: Schematic representation of the Veldkamp line $(H_{III}, H_{YYY}, C_{YYY})$. In [83] it was proved that a double-six configuration of pentagrams living in the hyperbolic quadric generates all 12096 magic pentagrams of $\mathcal{W}(5,2)$.

9.2 WEIGHT DIAGRAMS FROM THREE-QUBIT OPERATORS

I now show how we recovered in [80] some weight diagrams of simple Lie algebras in the commutation relations of the Pauli operators of the three hyperplanes of the magic Veldkamp line.

9.2.1 *The core set (15 irrep of A_5)*

The core set of the Veldkamp line is the set of elements commuting with YYY (they belong to C_{YYY}) and symmetric (they belong to H_{III}). An explicit list of these elements is given by:

$$\begin{array}{cccccccc} YYI, & YIY, & IYY, & ZZI, & ZIZ, & IZZ, & XXI, & XIX, \\ IXX, & ZXI, & ZIX, & IZX, & XZI, & XIZ, & IXZ. & \end{array} \tag{99}$$

This set of observables forms a doily in $\mathcal{W}(5,2)$ (see Figure 28).

Now let us show that this set of operators encapsulates the weight diagram of the second fundamental representation of A_5. To see this connection with simple Lie algebras, let us associate to the roots

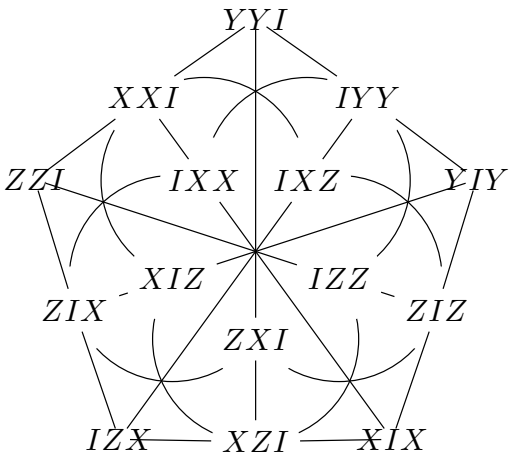

Figure 28: The core of the magic Veldkamp line which forms a doily.

$\alpha_1, \ldots, \alpha_5$ of A_5 five skew-symmetric observables as given in Figure 29. The action of the roots by translation on the weight vectors

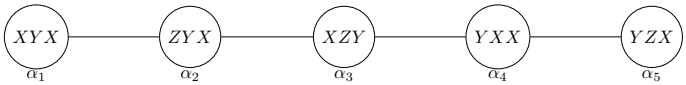

Figure 29: Realization of the Dynkin diagram of A_5 by 3-qubit Pauli operators.

[42] corresponds to multiplication in terms of operators. Taking ZIZ as the highest weight vector, one sees that Figure 30 reproduces the weight diagram of the 15-dimensional irreducible representation of A_5.

9.2.2 *The perp-set $\mathcal{P}$ ($\mathbf{31} = \mathbf{1} \oplus \mathbf{15} \oplus \mathbf{15}$ of A_5)*

Because the perp-set C_{YYY} is a quadratic cone with vertex YYY one obtains 15 operators of C_{YYY} outside the doily by multiplying the 15 operators of Eq. (99) by YYY. Then the 31 operators of C_{YYY} can be seen as the weight diagram of a 31-dimensional reducible representation of A_5, which can be decomposed as $\mathbf{31} = \mathbf{1} \oplus \mathbf{15} \oplus \mathbf{15}$.

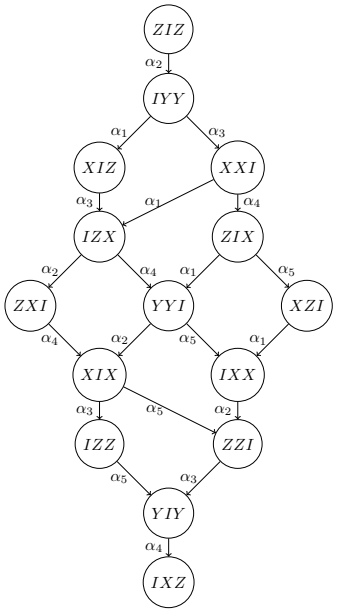

Figure 30: Weight diagram of the 15-dimensionnal representation of A_5 in terms of 3-qubit operators.

9.2.3 *The hyperbolic quadric $\mathcal{H}$ (35 irrep of A_6)*

If one considers the 20 elements of the hyperbolic quadric H_{III} which do not belong to the doily, i.e. the symmetric operators anticommuting with YYY, one gets the following elements:

$$\begin{array}{llllllllll} \mathrm{YYX}, & \mathrm{YXY}, & \mathrm{XYY}, & \mathrm{YYZ}, & \mathrm{YZY}, & \mathrm{ZYY}, & \mathrm{ZZX}, & \mathrm{ZXZ}, & \mathrm{XZZ}, \\ \mathrm{XXZ}, & \mathrm{XZX}, & \mathrm{ZXX}, & \mathrm{ZII}, & \mathrm{IZI}, & \mathrm{IIZ}, & \mathrm{XII}, & \mathrm{IXI}, & \mathrm{IIX}, \\ \mathrm{XXX}, & \mathrm{ZZZ}. & & & & & & & \end{array} \tag{100}$$

These elements form also the weight diagram of an irreducible representation of A_5 of dimension 20 (Figure 31).

Combining Figures 30 and 31 one obtains a representation theoretic interpretation of the hyperbolic quadric H_{III} as the weight diagram of a $\mathbf{35} = \mathbf{15} \oplus \mathbf{20}$ reducible module of A_5. Moreover, if we extend the diagram of the roots of A_5 (Figure 32) to an A_6 Dynkin diagram with $\alpha_6 = \mathrm{YXI}$, one obtains the weight diagram of the 35 irreducible representation of A_6.

9.2.4 *The elliptic quadric $\mathcal{E}$ (27 irrep of E_6)*

Let us now consider the elliptic quadric H_{YYY}, which is composed of operators that are either symmetric and commute with YYY, i.e. the 15 elements of the doily, plus skew symmetric elements anti-commuting with YYY. There are 12 of them,

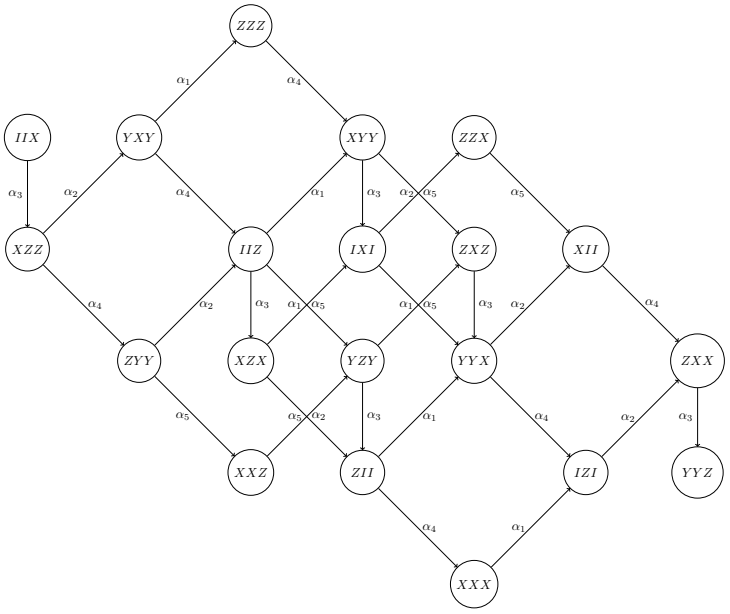

Figure 31: Weight diagram of the 20-dimensional representation of A_5 in terms of 3-qubit operators. This representation theoretic interpretation of the 20 symmetric elements anticommuting with YYY as an A_5 irreducible weight diagram first appeared in [83].

$$\begin{aligned} &\text{YIX}, \quad \text{YXI}, \quad \text{XYI}, \quad \text{IYX}, \quad \text{XIY}, \quad \text{IXY}, \\ &\text{ZIX}, \quad \text{IZI}, \quad \text{ZYI}, \quad \text{IYZ}, \quad \text{ZIY}, \quad \text{IZY}. \end{aligned} \tag{101}$$

We can identify the $15 + 12$ operators of the elliptic quadric with the weight vectors of the 27 E_6 fundamental representation. To do so, let us consider the Dynkin diagram of E_6 labelled by three-qubit operators according to Figure 32.

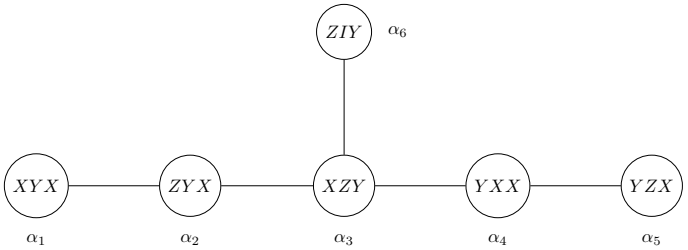

Figure 32: Realization of the Dynkin diagram of E_6 by 3-qubit Pauli operators.

Then the 27 operators of the elliptic quadric can be arranged as the weight diagram of the 27 irreducible representation of E_6 with IZY being the highest weight vector, as shown in Figure 33. This weight diagram contains the 15 of A_5 because the Doily lies inside the elliptic quadric, plus two copies of the weight diagram of the standard rep-

resentation of A_5. This corresponds to the branching $E_6 \supset SL_2 \times SL_6$: $\mathbf{27} = \mathbf{15} \oplus \mathbf{6} \oplus \mathbf{6}$ (see [112]).

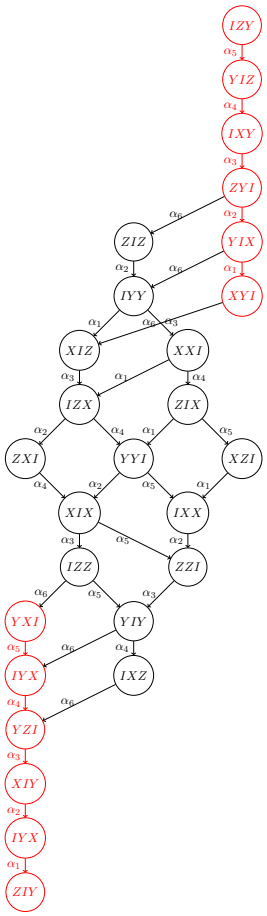

Figure 33: Weight diagram of the 27-dimensional irreducible representation of E_6 in terms of 3-qubit operators. The branching into A_5 irreducible representations $\mathbf{27} = \mathbf{15} \oplus \mathbf{6} \oplus \mathbf{6}$ is given by the two colorings of the diagram.

9.2.5 $\mathcal{HDE}$ (32 *irrep of* D_6)

Finally, let us consider the 32 operators coming from the 20 elements of the hyperbolic quadric which are not part of the doily and the 12 elements of the elliptic quadric which do not belong to the doily. This list of operators is the union of the sets given by Eqs. (100) and (101). These 32 operators accommodate the 32 irreducible representation of Spin(12), or the 32 irreducible representation of the Lie algebra $\mathfrak{so}(12)$. To show this, let us consider the labelling of the D_6 diagram by three-qubits operators given by Figure 34.

Then, like for the previous weight diagrams, one obtains the 32 irreducible representation of D_6 by properly choosing the highest

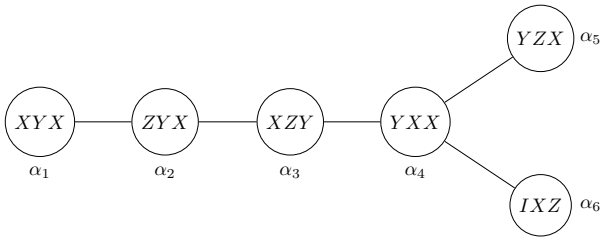

Figure 34: Realization of the Dynkin diagram of D_6 by 3-qubit operators.

weight which, for this choice of realization of D_6, should be YXI (see Figure 35).

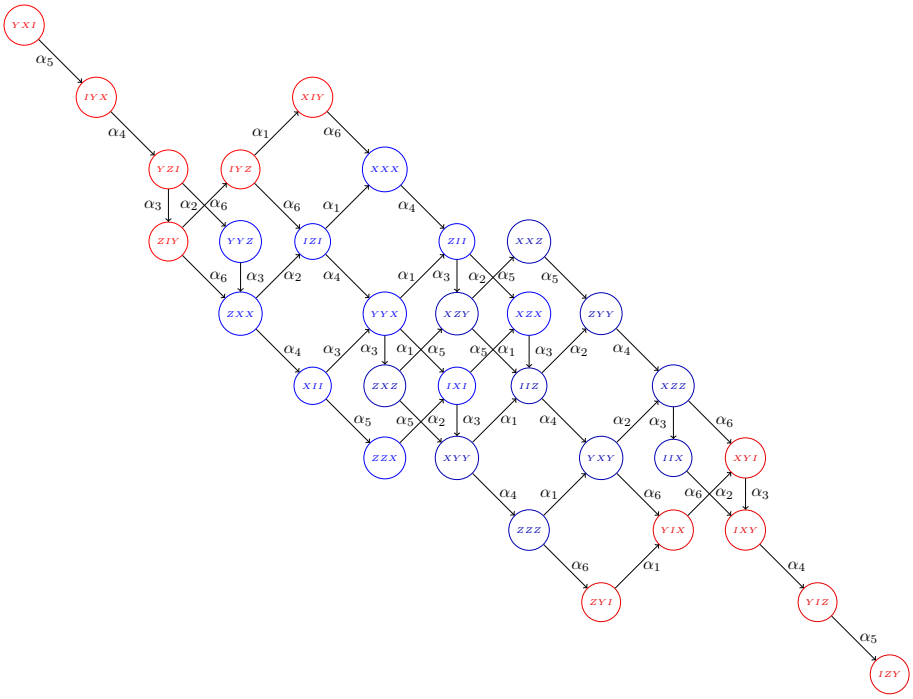

Figure 35: Weight diagram of the 32 irreducible representation of D_6 in terms of 3-qubit Pauli operators. The branching into A_5 irreducible representations $\mathbf{32} = \mathbf{12} \oplus \mathbf{6} \oplus \mathbf{6}$ is obtained by erasing the node α_6 of Figure 34 and the corresponding edges in the weight diagram.

9.3 Spin(14) decomposition and related invariants

Table 11 summarizes the previous calculations.

One can notice that some irreducible representations which were part of the sequence of irreducible representations controlling the geometry of tripartite entanglement (the subadjoint representations, see Chapter 5, Table 8), show up in our sequence of representations encoded in the magic Veldkamp line. It is the case for the 32 irreducible

Geometry	Representation	Branching
Doily, $\mathcal{H} \cap \mathcal{E}$	15 irrep of A_5	
Quadratic cone	$1 \oplus 15 \oplus 15$ rep of A_5	
Elliptic Quadric, $\mathcal{E}$	27 irrep of E_6	$\mathbf{27} = \mathbf{15} \oplus \mathbf{6} \oplus \mathbf{6}$ for $A_5 \subset E_6$
Hyperbolic Quadric, $\mathcal{H}$	35 irrep of A_6	$\mathbf{35} = \mathbf{15} \oplus \mathbf{20}$ for $A_5 \subset A_6$
$\mathcal{E}\Delta\mathcal{H}$	32 irrep of D_6	$\mathbf{32} = \mathbf{20} \oplus \mathbf{6} \oplus \mathbf{6}$ for $A_5 \subset D_6$

Table 11: From geometric hyperplanes to weight diagrams.

representation of D_6, or the 20 irreducible representation of A_5. One could be tempted to look for a manifestation of the 56 irreducible representation of E_7, which was the highest dimensional representation in the sequence of subadjoint representations. It turns out that it is not possible to recover the 56 fundamental representation of E_7 from the three-qubit magic Veldkamp line. It is, however, possible if we consider the four-qubit Veldkamp line. I propose a labelling by four-qubit operators in Appendix E.

In [80] the weight diagram analysis was conducted using the language of Clifford algebra. Consider the following seven three-qubit operators,

$$\Gamma_1 = ZYI, \Gamma_2 = YIX, \Gamma_3 = XYI, \Gamma_4 = IXY, \Gamma_5 = YIZ, \Gamma_6 = IZY, \Gamma_7 = YYY. \tag{102}$$

These operators satisfy $\{\Gamma_i, \Gamma_j\} = \Gamma_i\Gamma_j + \Gamma_j\Gamma_i = 2\delta_{ij}$ for $i, j = 1, \ldots, 7$ and $i\Gamma_1\Gamma_2\Gamma_3\Gamma_4\Gamma_5\Gamma_6\Gamma_7 = III$. They generate a Clifford algebra $\mathtt{Cliff}(7)$. The different parts of the magic Veldkamp line can be labelled by the Clifford operators as shown in Figure 36.

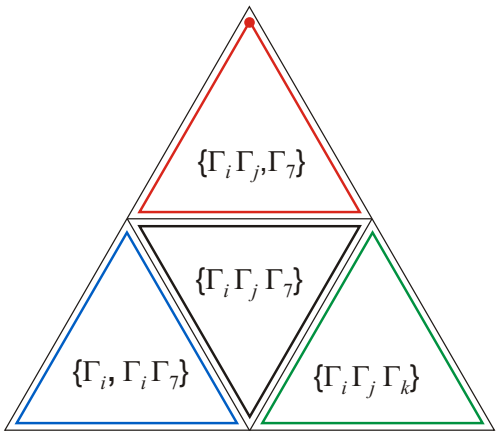

Figure 36: Decomposition of the magic Veldkamp line via the Clifford labeling. The basis vector Γ_7 corresponds to the red dot and is the vertex of the quadratic cone.

Using the Clifford algebra we showed that if we add the identity to the 63 operators of the Veldkamp line one can describe the (extended) full line as the 64-dimensional spinor representation of the group Spin(14) (D_7) of odd chirality. All the previous branchings explicitely described can be recast using the labeling by Clifford algebra and the subgroups of Spin(14). For instance, the decomposition into triangles of Figure 36 corresponds to the branching $A_5 \subset D_7$,

$$\mathbf{64} = \mathbf{6} \oplus \mathbf{6} \oplus \mathbf{15} \oplus \mathbf{20} \oplus \mathbf{15} \oplus \mathbf{1} \oplus \mathbf{1}. \tag{103}$$

Remark 9.3.1. To conclude this chapter I present through one example another contribution of [80], where we were able to associate to the different splittings of the magic Veldkamp line some classical invariants built on three-qubit operators. As an example, let us show how the core set of the magic Veldkamp line, i.e. the doily (Figure 28), encodes the Pfaffian of 6×6 skew-symmetric matrices, which is the invariant of the 15-irreducible representation of A_5. To see this, consider the observable $\Omega = \sum_{1 \leqslant i < j \leqslant 6} a_{ij} \mathcal{O}_{ij}$ where $\mathcal{O}_{ij}$ is a three-qubit observable located at (ij) (Figure 37). Then the polynomial $\mathrm{Tr}(\Omega^3)$ is proportional to the Pfaffian, $\mathrm{Pf}(A)$, where $A = (a_{ij})_{1 \leqslant i < j \leqslant 6}$ is a skew symmetric matrix.

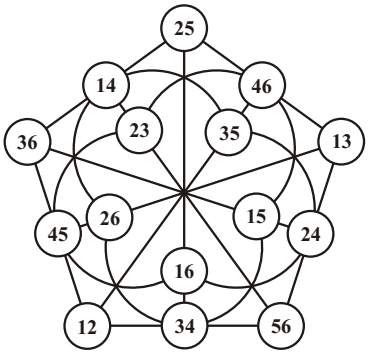

Figure 37: Labeling of the doily by duads.

Similarly, other invariants can be attached to and computed from the different parts of the Veldkamp line. Their physical meaning is discussed in [80].

Remark 9.3.2. In this Chapter I only detailed the point-line description of the core set of the magic Veldkamp line, which is a generalized quadrangle (the doily). It turns out that the finite geometric study of the different parts of the magic Veldkamp line has also been conducted in [80] and other structures, like extended quadrangles have been revealed in connection with the construction of invariants.

Part III

PERSPECTIVES

10

APPLICATIONS: QUANTUM ALGORITHMS, ENTANGLEMENT MEASURE AND ERROR-CORRECTING CODES

In this last chapter, I present some applications of the geometrical constructions of this thesis that I have been working on more recently. The idea is to look at concrete quantum processing with our geometrical perspective to provide new insights. The first type of applications I have been considering is the study of well-known quantum algorithms using the language of auxiliary varieties. To this purpose we can analyze with the language of Part I the evolution of the entangled states that are generated during some quantum algorithms. One can, for instance, use this idea of "atlas" of entanglement (Chapter 3) to learn which stratas are or are not reached by states generated by the algorithm (Section 10.1), or we can use specific invariants, like the dual variety (Chapter 4) to measure their entanglement (Section 10.2). Another type of interesting quantum processing is quantum error-correcting codes. In Section 10.3, I explain how our work with Péter Lévay on fermionic Fock space (Chapter 5) allows us to interpret a Majorana Fermionic code due to Hasting. Error-correction is also interesting as a language and in Section 10.4 I explain how the Lagrangian embedding that we used to parametrize generators of $\mathcal{W}(2N-1,2)$ by symmetric (2^N-1)-qubit operators (Chapter 7) can be seen as an error correction scheme. This leads to new ideas that could be useful in the future to connect the two geometrical constructions of Part I and II (Section 10.5).

10.1 ENTANGLEMENT IN QUANTUM ALGORITHMS

In Chapters 2 and 3 of Part I, I introduced tools from algebraic geometry and classical invariant theory to describe entanglement of pure multipartite systems. A first field of application of these techniques is the study of entanglement within quantum algorithms. For small quantum systems one knows how to identify the SLOCC classes of entanglement of a given state. With my students Hamza Jaffali and Ismaël Nounouh we analyzed in [52] the evolution of the entanglement in Grover's algorithm and with Hamza Jaffali we worked in detail the case of Shor's algorithm for 4-qubit systems [64].The interest in such studies is that it exhibits behaviour that numerical evaluations of entanglement do not show. For instance, we were able to show that for tripartite states ($2\times2\times2, 2\times2\times3$ and $2\times3\times3$) and 4-qubit ones, the state $|W\rangle$ never shows up in Grover's and Shor's algorithm. On the

other hand, the $|GHZ\rangle$ state appears in both algorithms. In fact, for Grover's algorithm one can easily see that when we apply the algorithm for searching one element in a (large) database of size $N = 2^n$, the states generated by the algorithm after the Oracle gate (that is the gate which marks with a minus sign the searched element) are SLOCC equivalent to $|GHZ_n\rangle$. Indeed, if $|x_0\rangle$ denotes the searched element, the Oracle and diffusion gate produce a state of type:

$$|\psi\rangle = \frac{\alpha}{\sqrt{N}}|x_0\rangle + \frac{\beta}{\sqrt{N}} \times \sum_{y\in\{0,1\}^n, y\neq x} |y\rangle = \frac{\alpha-\beta}{\sqrt{N}}|x_0\rangle + \beta\,|+^n\rangle\,. \quad (104)$$

The tensor $|\psi\rangle$ is a generic rank-two tensor and thus SLOCC equivalent to $|GHZ_n\rangle$. While running the algorithm, the amplitude $\frac{\alpha-\beta}{\sqrt{N}}$ increases and the amplitude $\frac{\beta}{\sqrt{N}}$ decreases at each iteration. This leads to the following pictorial interpretation of Grover's algorithm (Figure 38).

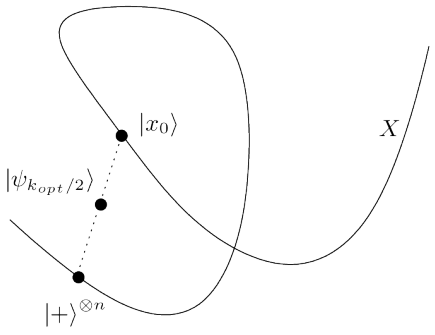

Figure 38: Evolution of the quantum state generated by Grover's algorithm viewed as points on a secant line of the variety of separable states [52]. The Geometric Measure of Entanglement (GME) is maximal [103] when the number of iterations is half of the optimal number of iterations to apply the algorithm. For large n it corresponds to the midpoint of the segment between the initial state $|+\rangle^{\otimes n}$ and the searched element $|x_0\rangle$.

This picture has to be compared with the classical geometric representation of Grover's algorithm that can be found in many textbooks [32] (Figure 39). Figure 38 tells us something about the evolution of the Geometric Measure of Entanglement [103] during the algorithm. Indeed, the GME is zero at the beginning of the algorithm ($|+\rangle^{\otimes n}$ is separable), increases when $|\psi_k\rangle$ is moving on the secant line and then decreases to get close to zero when $k = k_{opt}$. One shows geometrically [52] that the GME of $|\psi_k\rangle$ is maximal when $k \approx k_{opt/2}$,

i.e. when $|\psi_k\rangle$ is close to the midpoint. Similarly, for two orthogonal marked elements $|x_0\rangle, |x_1\rangle$, the maximum of the GME is achieved when the state is close to the centroid of $\{|+\rangle^{\otimes n}, |x_0\rangle, |x_1\rangle\}$, which corresponds to $k \approx 2/3 k_{opt}$. This picture provides a geometrical explanation of the GME curves computed numerically by [103] for one and two searched elements.

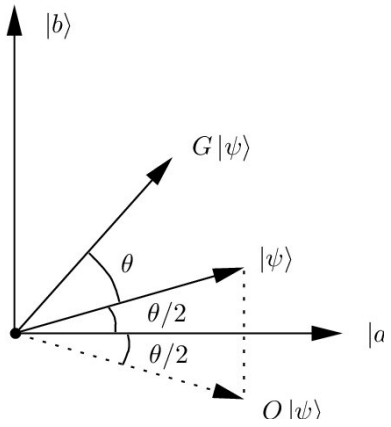

Figure 39: The usual geometrical representation of the evolution of the states during Grover's algorithm. The state $|\psi\rangle$ is transformed by the Grover gate G (composed of the Oracle and diffusion gates) to the state $G|\psi\rangle$. While this picture is useful to provide an estimation of the number of iterations needed to converge to the marked element, it does not give hints about the entanglement evolution of $|\psi_k\rangle$.

10.2 MEASURING ENTANGLEMENT

In Chapter 4, I introduced, following an idea of Miyake, the concept of dual variety to distinguish different SLOCC classes of entanglement by considering its singular locus. The polynomial equation defining the dual equation is SLOCC invariant but also invariant under local unitary operations and as such, its absolute value, can be used as a measure of entanglement. Gour and Wallach [45] used, for instance, the absolute value $|\mathrm{Det}_{2222}|$ of the $2 \times 2 \times 2 \times 2$ hyperdeterminant to determine numerically four-qubit maximally entangled states. Their result has been later proved analytically [29]. In particular, they proved that the 4-qubit states that maximize $|\mathrm{Det}_{2222}|$ are LU-equivalent to the quantum state

$$|L\rangle = \frac{1}{\sqrt{3}}(|u_0\rangle + \omega\,|u_1\rangle + \overline{\omega}\,|u_2\rangle), \tag{105}$$

where $|u_0\rangle = \frac{1}{2}(|0000\rangle + |0011\rangle + |1100\rangle + |1111\rangle$, $|u_1\rangle = \frac{1}{2}(|0000\rangle - |0011\rangle - |1100\rangle + |1111\rangle$, $|u_2\rangle = \frac{1}{2}(|0101\rangle + |0110\rangle + |1010\rangle + |1001\rangle$, and

$|u_3\rangle = \frac{1}{2}(|0101\rangle - |0110\rangle - |1001\rangle + |1010\rangle$. The 4-dimensional vector space $\langle |u_0\rangle, |u_1\rangle, |u_2\rangle, |u_3\rangle\rangle$ is a Cartan subspace of $\mathcal{H} = \mathbb{C}^2 \otimes \mathbb{C}^2 \otimes \mathbb{C}^2 \otimes \mathbb{C}^2$. This state is also known as the state that maximizes the average Tslasis α-entropy [45].

Similarly, one may try to maximize other hyperdeterminants. For instance, the hyperdeterminant for 3-qutrit systems is one of a few that can be computed by Schläfli's method [44]. Following Nurmiev [92], a Cartan subspace of $\mathcal{H}_{333} = \mathbb{C}^3 \otimes \mathbb{C}^3 \otimes \mathbb{C}^3$ can be chosen to be defined by $|u_0\rangle = \frac{1}{\sqrt{3}}(e_1 \otimes e_1 \otimes e_1 + e_2 \otimes e_2 \otimes e_2 + e_3 \otimes e_3 \otimes e_3)$, $|u_1\rangle = \frac{1}{\sqrt{3}}(e_1 \otimes e_2 \otimes e_3 + e_2 \otimes e_3 \otimes e_1 + e_3 \otimes e_1 \otimes e_2)$, $|u_2\rangle = \frac{1}{\sqrt{3}}(e_1 \otimes e_3 \otimes e_2 + e_2 \otimes e_1 \otimes e_3 + e_3 \otimes e_2 \otimes e_1)$. Then the evaluation of $|\psi\rangle = a|u_0\rangle + b|u_1\rangle + c|u_2\rangle$ on $|\mathrm{Det}_{333}|$ gives [18]:

$$\begin{aligned} |\mathrm{Det}_{333}| &= |4a^3b^3c^3(a+b+c)^3(a^2+b^2+c^2+2ab-ac-bc)^3 \\ &\times(a^2+b^2+c^2-ab+2ac-bc)^3 \times (a^2+b^2+c^2-ab-ac+2bc)^3 \\ &\times(a^2+b^2+c^2-ab-ac-bc)^3|. \end{aligned} \tag{106}$$

A numerical search for maximization of $|\mathrm{Det}_{333}|$ provides the following candidate for maximally entangled states with respect to the $3 \times 3 \times 3$ hyperdeterminant,

$$|L_{333}\rangle = \frac{1}{6}\sqrt{9+3\sqrt{3}}\,|u_0\rangle + \frac{1}{6}\sqrt{9+3\sqrt{3}}\,|u_1\rangle - \frac{1}{6}\sqrt{18-6\sqrt{3}}\,|u_2\rangle\,. \tag{107}$$

It would be interesting to get an analytical proof of this result, as well as some quantum information insight into this quantum state.

In this respect any new explicit examples of hyperdeterminants associated to a multipartite quantum system can be used to classify entanglement and also measure it according to this peculiar invariant.

Explicit (computable) examples of hyperdeterminants are not so easy to find. In [58] we obtained with Luke Oeding, by combining techniques coming from representation theory, geometry and numerical interpolation, explicit polynomial expressions for the dual varieties of the Grassmannians $G(3,9) \subset \mathbb{P}^{83}$ and $G(4,8) \subset \mathbb{P}^{69}$. Recall from Chapter 5 that the Grassmannian varieties $G(k,n) \subset \mathbb{P}(\bigwedge^k \mathbb{C}^n)$ correspond to the set of separable states of k-fermionic systems with n-single particles states. Therefore, the absolute values of those dual equations could be used as a measure of entanglement for these fermionic quantum systems.

If one considers the example of three fermions with nine single-particle states, a generic quantum state in $\mathcal{H} = \bigwedge^3 \mathbb{C}^9$ can be chosen to be [92]

$$|\psi\rangle = z_1 p_1 + z_2 p_2 + z_3 p_3 + z_4 p_4, \text{ with } \sum |z_i|^2 = \frac{1}{3}, \tag{108}$$

where

$$\begin{aligned} p_1 &= e_{123} + e_{456} + e_{789}, & p_2 &= e_{147} + e_{258} + e_{369}, \\ p_3 &= e_{159} + e_{267} + e_{348}, & p_4 &= e_{168} + e_{249} + e_{357}, \end{aligned} \tag{109}$$

with $e_{ijk} = e_i \wedge e_j \wedge e_k$. Then, the absolute value of the corresponding evaluation of $\Delta_{G(3,9)}$, the defining equation of the dual of $G(3,9)$, gives expression (110) with ω being a cubic root of unity,

$$\begin{aligned} |\Delta_{G(3,9)}(|\psi\rangle)| =& |z_4(z_1 - z_2 + z_3)(z_1 + \omega z_2 + z_3)(z_1 - z_2 - \omega z_3)(z_1 + \overline{\omega} z_2 + z_3)(z_1 - z_2 - \overline{\omega} z_3) \\ & (z_1 + \omega z_2 - \omega z_3)(z_1 + \omega z_2 - \overline{\omega} z_3)(z_1 + \overline{\omega} z_2 - \omega z_3)(z_1 + \overline{\omega} z_2 - \overline{\omega} z_3) \\ & z_3(z_1 + z_2 - z_4)(z_1 - \omega z_2 - z_4)(z_1 + z_2 + \omega z_4)(z_1 - \overline{\omega} z_2 - z_4)(z_1 + z_2 + \overline{\omega} z_4) \\ & (z_1 - \omega z_2 + \omega z_4)(z_1 - \overline{\omega} z_2 + \omega z_4)(z_1 - \omega z_2 + \overline{\omega} z_4)(z_1 - \overline{\omega} z_2 + \overline{\omega} z_4) \\ & z_2(z_1 - z_3 + z_4)(z_1 + \omega z_3 + z_4)(z_1 - z_3 - \omega z_4)(z_1 + \overline{\omega} z_3 + z_4)(z_1 - z_3 - \overline{\omega} z_4) \\ & (z_1 + \omega z_3 - \omega z_4)(z_1 + \omega z_3 - \overline{\omega} z_4)(z_1 + \overline{\omega} z_3 - \omega z_4)(z_1 + \overline{\omega} z_3 - \overline{\omega} z_4) \\ & z_1(z_2 + z_3 + z_4)(z_2 - \omega z_3 + z_4)(z_2 + z_3 - \omega z_4)(z_2 - \overline{\omega} z_3 + z_4)(z_2 + z_3 - \overline{\omega} z_4) \\ & (z_2 - \omega z_3 - \omega z_4)(z_2 - \overline{\omega} z_3 - \omega z_4)(z_2 - \omega z_3 - \overline{\omega} z_4)(z_2 - \overline{\omega} z_3 - \overline{\omega} z_4)|^3. \end{aligned} \tag{110}$$

Maximizing this quantity would provide us with some candidates for maximally entangled three fermionic states with 9 single particules states.

Remark 10.2.1. In [58] we also point out that all known (computable) expressions of hyperdeterminants that are meaningful to study entanglement (four-qubit, three-qutrit, three fermions with nine single-particle states, four fermions with eight single-particle states) can all be obtained as some specific projections of the E_8-discriminant. The E_8-discriminant is the equation of the dual of the E_8 adjoint variety, i.e. the projectivization of the unique closed orbit of the Lie group E_8 acting on its Lie algebra $\mathfrak{e}_8$.

10.3 HASTINGS ERROR-CORRECTING CODE AND THE E_8 GROUP

Another field of applications for quantum information of our geometric techniques is the topic of quantum error-correcting codes. Let us briefly recall the basic principle. In the stabilizer formalism of quantum error-correcting codes, the codewords are quantum states that span a linear subspace $\mathcal{C}$ of $\mathcal{H}_n = \mathbb{C}^2 \otimes \mathbb{C}^2 \cdots \otimes \mathbb{C}^2$ which are stabilized by a subgroup S of the n-qubit Pauli group $\mathcal{P}_n$. S is called the stabilizer group of the code. Such subgroup S is required to be abelian and it should also not contain $-I_{2^n}$. The centralizer of S, $C(S)$, is the group of Pauli operators that commute with S. The Pauli operators that belong to $C(S)\backslash S$ are called logical qubit operators and transform codewords into other codewords and therefore errors that belong to $C(S)\backslash S$ cannot be detected. The errors that can be detected correspond to operators of the n-qubit Pauli group that do not belong to $C(S)\backslash S$. More precisely, $\{E_i, i \in I\}$ is a collection of errors that can be corrected if, and only if, $E_i^\dagger E_k \notin C(S)\backslash S$ for all i, k (see [32]).

If S is generated by $n-k$ elements then one can encode k logical qubits in $\mathcal{C}$ ($\dim(\mathcal{C}) = 2^k$). The distance of a quantum code is the minimal weight[1] of the Pauli operators that belong to $C(S)\backslash S$. We call an $[n,k,d]$-code a quantum error-correcting code that encodes k-qubit in an n-qubit Hilbert space with distance d. Such code is capable of correcting any error affecting less than $d/2$ qubits of the transmitted codeword.

Example 10.3.1. *The first example of a nontrivial code in the stabilizer formalism is the five-qubit code. In this case* $S = \langle g_1, g_2, g_3, \text{and } g_4\rangle$ *with* $g_1 = XZZXI, g_2 = IXZZX, g_3 = XIXZZ, g_4 = ZXIXZ$. *Then one can encode* 1 *logical qubit and the minimal weight of the elements of* $C(S)\backslash S$ *is* 3. *So any error affecting one mode on the logical qubit can be detected and corrected. Such a code will be denoted as a* $[5,1,3]$*-code.*

A similar formalism can be developed for Majorana femionic codes. Instead of $\mathcal{H}_n$, consider as a Hilbert space the fermionic Fock space $\mathcal{F}_N = \bigoplus_{m=0}^{N} \bigwedge V$ where V is an $N = 2n$-dimensional vector space representing the vector space of a single particule state (see Chapter 5). Then, let us define the $2N$ Majorana operators by

$$c_{2I-1} = p_I + n_I, c_{2I} = i(p_I - n_I), I = 1, \ldots, N. \tag{111}$$

The group $Maj(2N) = \{\omega c_{\mathcal{A}}, \omega \in \{\pm 1, \pm i\}, c_{\mathcal{A}} = \Pi_{\mu\in\mathcal{A}} c_\mu\}$ will play the same role for $\mathcal{F}_N$ as the generalized Pauli group $\mathcal{P}_n$ for $\mathcal{H}_n$. The weight of a Majorana operator is the number of modes in its support, i.e. $\text{weight}(\mathcal{A}) = |\mathcal{A}|$.

A Majorana fermionic code is defined as a linear subspace of $\mathcal{F}_N$ that is stabilized by a subgroup $S \subset Maj(2N)$ such that

- S is abelian and does not contain $-I$,
- the weight of all elements in S is even (this condition guarantees that the chirality operator $\Gamma = (-i)^N \Pi_{I=1}^{N} c_{2I-1} c_{2I}$ commutes with the elements of S).

Like in the stabilizer formalism for qubits, if k is such that S is generated by $N-k$ generators, then $C(S)$ is generated by $N+k$ ones, i.e. one can choose a set of $2k$ operators in $C(S)\diagdown S$ as logical operators that act on the k logical fermionic qubits. The distance of a Majorana fermionic code is the minimal weight of the logical operators. A Majorana fermionic code $[4n,k,d]$ allows us to embed k logical qubits in $\mathcal{F}_N$ such that one can detect and correct any error affecting less than $d/2$ modes. Motivations to store quantum information in fermionic systems and therefore to develop a framework for Majorana fermionic codes are explained in [17]. The $[16,3,4]$ fermionic Majorana code of Hastings [48] is an example of a Majorana code that

1 The weight of a Pauli operator is the number of qubits on which the operator acts nontrivially.

cannot be built directly from a qubit code, i.e. it does not correspond to a qubit code embedded in the fermionic Fock space (because there is no $[4,3,4]$ qubit code). The stabilizer group of the Hastings code is $S_3 = \langle G_1, G_2, G_3, G_4, \Gamma\rangle$ with $G_j = \prod_{\mu=1}^{16} (c_\mu)^{\nu_j^\mu}$. The vectors ν_j are given by the rows of the following 4×16 matrix

$$\begin{pmatrix} 0 & 1 & 0 & 1 & 0 & 1 & 0 & 1 & 0 & 1 & 0 & 1 & 0 & 1 & 0 & 1 \\ 0 & 0 & 1 & 1 & 0 & 0 & 1 & 1 & 0 & 0 & 1 & 1 & 0 & 0 & 1 & 1 \\ 0 & 0 & 0 & 0 & 1 & 1 & 1 & 1 & 0 & 0 & 0 & 0 & 1 & 1 & 1 & 1 \\ 0 & 0 & 0 & 0 & 0 & 0 & 0 & 0 & 1 & 1 & 1 & 1 & 1 & 1 & 1 & 1 \end{pmatrix}. \tag{112}$$

In [78] one shows, using advantageously the fermionic embeddings of qubits via the double and single occupancy, that one can describe the $[16,3,4]$ Hastings code as two copies of a trivial $[4,2,2]$ qubit code of $\mathcal{H}_4$ embedded in $\mathcal{F}_8$: one within the double and the other within the single occupancy sector. Both codes can be "glued" together using an "intertwiner" operator $\Omega = c_1c_5c_9c_{13}$. Using the framework we introduced in [77] to embed in different ways $\mathcal{H}_n$ into $\mathcal{F}_N$, one showed that the code space V_{S_3} is given by

$$V_{S_3} = \langle |E_0\rangle, |E_1\rangle, |E_2\rangle, |E_3\rangle, \Omega|E_0\rangle, \Omega|E_1\rangle, \Omega|E_2\rangle, \Omega|E_3\rangle\rangle. \tag{113}$$

with $|E_0\rangle = (p_{1234} + p_{\overline{1234}})|vac\rangle$, $|E_1\rangle = (p_{1\overline{234}} + p_{\overline{1}2\overline{34}})|vac\rangle$, $|E_2\rangle = (p_{1\overline{2}3\overline{4}} + p_{\overline{1}2\overline{3}4})|vac\rangle$, and $|E_3\rangle = (p_{12\overline{34}} + p_{\overline{12}34})|vac\rangle$. The subspace $\langle |E_0\rangle, |E_1\rangle, |E_2\rangle, |E_3\rangle\rangle$ is an embedding of the qubit code $[4,2,2]$ into the single occupancy subspace of $\mathcal{F}_8$ [78].

Finally, in [78] one also exhibits a connection between the Lie algebra $\mathfrak{e}_8$ and the $[16,3,4]$ Hastings code. Consider the following branching of $\mathfrak{e}_8$,

$$\mathfrak{e}_8 = \mathfrak{so}(16) \oplus \mathfrak{m}_{128}. \tag{114}$$

The restriction of the E_8 adjoint action on $\mathfrak{m}_{128}$ corresponds to the Spin(16) action on $\mathfrak{m}_{128} = \mathcal{F}_8^+$. Then, one can show, using the commutation relations, that V_{S_3} is a Cartan subspace of $\mathfrak{m}_{128}$. Like in the previous section (Remark 10.2.1), this shows that if the representations of the exceptional Lie group E_7 showed up several times in this thesis (Chapter 5, Chapter 9, Appendix E), the study of the E_8 representations for the geometry of entanglement and contextuality could also be worth investigating in future work.

10.4 THE LAGRANGIAN MAP AND ERROR-CORRECTION

The development of the theory of subspace codes [68, 69] over finite fields allows us to reconsider our study of the Lagrangian embedding for multiqubit operators (Chapter 7) in the language of error-correcting codes. A subspace code is a collection of subspaces of

$PG(d,q)$ such that the distance between two subspaces is large enough to allow correction. The metric introduced in subspace codes theory is given by

$$d(A,B) = dim(A) + dim(B) - dim(A \cap B), A, B \subset V_q^{d+1}. \quad (115)$$

In the theory of subspace codes the messages are not vectors (points in the projective space) but (projective) linear spaces. If all the messages, i.e. subspaces, of a given code have the same projective dimension $k-1$, then the code is a collection of points in $G(k,d+1)$, the Grassmannian variety that can be embedded via the Plücker map in $PG(\binom{d+1}{k}-1,2)$. Such a code will be called a Grassmannian code. An issue in subspace codes theory is to produce efficient algorithms to recover a given subspace when the transmission has been corrupted by errors, i.e. the transmitted subspace is a linear space that is contained in, or contains the original one. In [113] a geometrical algorithm based on the Plücker embedding and Schubert calculus was given.

To illustrate this geometric principle, consider the particular case of the Klein correspondence (i.e. $k=2$ and $d=3$) between lines of $PG(3,2)$ and points of the hyperbolic quadric $Q^+(5,2) = G(2,4) \subset PG(5,2)$,

$$\begin{array}{ccc} PG(3,2) & \to & PG(5,2) \\ ([v],[w]) & \mapsto & [v \wedge w]. \end{array} \quad (116)$$

Under the Klein correspondence, 35 lines (messages) of $PG(3,2)$ are

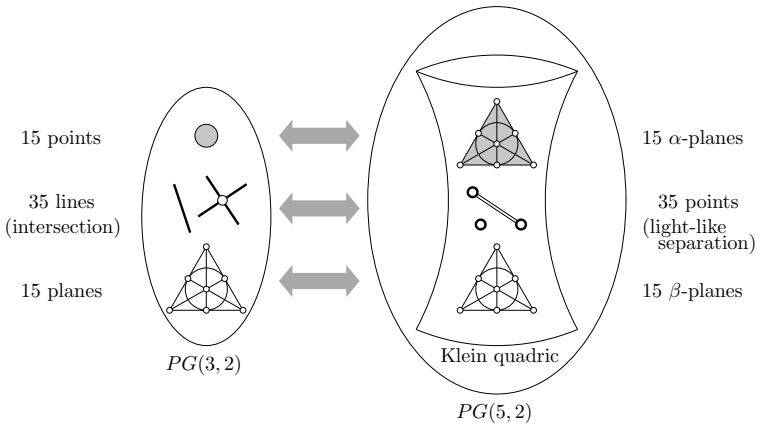

Figure 40: The Klein correspondence given by the Plücker embedding $G(2,4) \subset PG(5,2)$. In subspace codes theory the messages are lines forming a spread in $PG(3,2)$, the codewords are the points of the Klein quadric associated to these lines. The Klein correspondence over $GF(2)$ can also be seen as a finite analogue of the twistor correspondence of Penrose [97].

mapped to the 35 points (codewords) of the Klein quadric, the 15 points of $PG(3,2)$ are mapped to the 15 α-planes in the Klein quadric and the 15 planes of $PG(3,2)$ are mapped to the β-planes of the Klein

quadric (Figure 40). A code, i.e. a set of messages, will be defined by a *spread* of lines of $\mathrm{PG}(3,2)$. A spread is a collection of subsets that partition the ambient space and, therefore, such that every pair of subsets is at the maximal distance according to Eq. (115). The codewords, i.e. the images of the messages by the Plücker embedding, will correspond to points on the Klein quadric that are well separated in order to allow error corrections. For instance, if the message is a line of $\mathrm{PG}(3,2)$, a corrupted message would be a point of the original message (i.e. a point of the line) or a plane containing the message (a plane containing the line). By the Klein correspondence, errors of both types will be sent to planes. When the code is given by a spread, the codewords are such that all planes (errors) in $\mathcal{Q}^+(5,2)$ contain a unique codeword of the original code. This allows us to determine from the corrupted message the original one (by the inverse of the Klein correspondence).

The Klein correspondence over the complex number between lines of $\mathbb{P}(\mathbb{C}^3)$ and points on the Klein quadric hypersurface $\mathcal{M}_{\mathbb{C}} \subset \mathbb{P}(\mathbb{C}^5)$ was introduced in the physics literature by Roger Penrose [97] to express properties of the complexified and compactified Minkowski space time $\mathcal{M}_{\mathbb{C}}$ in terms of properties of twistors in $\mathbb{P}(\mathbb{C}^3)$. In our picture we have a $\mathbb{F}_2$-(reverse)-analogue where the geometry of $\mathrm{Q}^+(5,2)$ is built from the geometry of $\mathrm{PG}(3,2)$ by an error correction scheme.

When we restrict ourself to $\mathcal{W}(3,2)$, i.e. we only consider isotropic lines for a given symplectic form, then the image of $\mathcal{W}(3,2)$ by the Klein correspondence is the Lagrangian variety $\mathrm{LG}(2,4) \subset \mathrm{Q}^+(5,2) \subset \mathrm{PG}(5,2)$ (Chapter 7) which is, in this case, isomorphic to the doily $\mathrm{LG}(2,4) \simeq \mathcal{W}(3,2)$. In the language of subspace codes, the Lagrangian variety is the image of all isotropic codes (isotropic spreads) of $\mathrm{PG}(3,2)$ and the images of the messages of one particular code correspond to codewords forming an ovoid in $\mathrm{LG}(2,4)$ (See Figure 41).

Remark 10.4.1. Given the fact that the Lagrangian variety $\mathrm{LG}(2,4)$ is a linear section of $\mathcal{Q}^+(5,2)$, it is possible to extend the analogy with twistor theory where the real Minkowski space-time is identified in the Klein correspondence with the real slice of $\mathcal{M}_{\mathbb{C}}$. Those analogies leaded us to consider the mapping from $\mathcal{W}(3,2)$ to $\mathrm{LG}(2,4)$ as a correcting code construction of a toy $\mathbb{F}_2$- model of space-time [79].

10.5 ENTANGLEMENT AND CONTEXTUALITY

The new ingredient that comes with our finite geometry/error correction picture is the possibility to parametrize our finite geometry by multiqubit Pauli operators using the constructions of Part II.

When we label the points of $\mathcal{W}(2n-1,2)$ by observables there is a freedom in choosing the representative because the observables $\pm\mathcal{O}$ and $\pm i\mathcal{O}$ of $\mathcal{P}_n$ map to the same point in $\mathcal{W}(2n-1,2)$. Given a spread $\mathcal{S}$ of 2^n+1 $(n-1)$-planes in $\mathcal{W}(2n-1,2)$, it is always possi-

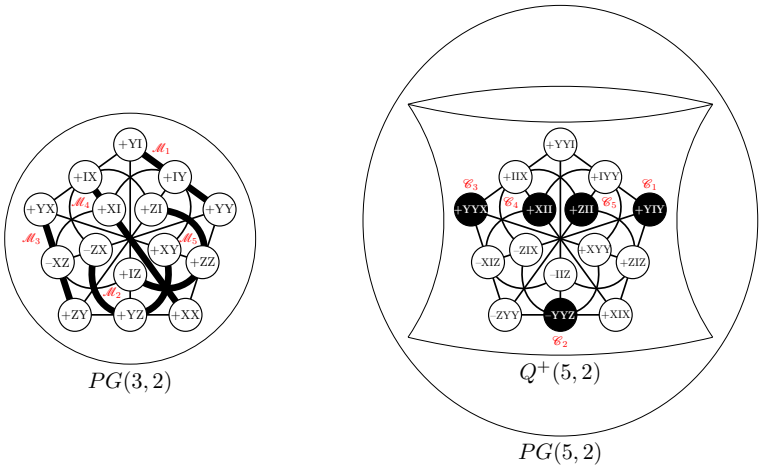

Figure 41: An isotropic code under the Klein correspondence. A spread of the doily corresponds to 5 possible messages that are sent to 5 points (codewords) on an ovoid of the Lagrangian variety $LG(2,4)$. If a corrupted message is sent, i.e. only one point of the isotropic line/message is sent, then under the Klein correspondence the corrupted codeword is a line of $LG(2,4)$ passing through the initial codeword. The fact that the 5 codewords make an ovoid allows us to recover the correct codeword.

ble to choose the representatives of the operators of each generators $PG(n-1,2)$ of the spread such that the lines of all the $PG(n-1,2)$ of $\mathcal{S}$ are all positive. In fact, for one generator $PG(n-1,2)$, there exists 2^n different ways of choosing the representatives by n-qubit Pauli operators such that all lines of the generator are positive. Such labeling allows us to define a group $S = \langle \mathcal{O}_1, \ldots, \mathcal{O}_n \rangle$ where the operators correspond to n linearly independent points of the generator $PG(n-1,2)$. Because of the choice of signs for the representatives $\mathcal{O}_i$ and because we are considering generators of $\mathcal{W}(2n-1,2)$, the group S is a stabilizer group of $\mathcal{P}_n$. Therefore, the choice of a labeling of a generator of $\mathcal{W}(2n-1,2)$, which respects the sign constraint, defines a unique stabilized state $|\psi\rangle_S$. But one knows that there exist for each generator 2^n compatible labelings. The corresponding 2^n stabilizer states will form a basis of $\mathcal{H}_n$. Because a spread contains 2^n+1 generators, one can generate from our sign constraint 2^n+1 bases. It turns out that these 2^n+1 bases are mutually unbiased[2]. Therefore, from a spread of isotropic generators of $\mathcal{W}(2n-1,2)$, the sign condition naturally leads to the construction of 2^n+1 pairwise MUBs [79]. It is well known [123] that the maximal number of MUBs in $\mathcal{H}_n$ is 2^n+1.

As we discussed in Chapter 6 the existence of operator-based proofs of the Kochen Specker Theorem is linked to the existence of "negative

2 Two bases (e_i), (f_k) of a Hilbert space of dimension d are said to be mutually unbiased iff $|\langle e_j, f_k\rangle| = 1/\sqrt{d}$. MUBs are important for quantum tomography and entanglement detection [11, 37].

lines" in the finite geometric incidence structure underlying the commutation properties of our set of observables. Because $\mathcal{W}(2n-1,2)$ contains contextual configurations, one deduces that a labelling defined for a given isotropic code (spread of generators), such that all lines of all generators are positive, cannot be compatible with all possible codes. Therefore, the impossibility to label in a unique way all codes in our geometric picture should be related to contextuality.

As a first step toward looking for a direct relation between entanglement and contextuality one may be tempted to use the formalism of stabilizer codes, induced by our subspace codes picture of $\mathcal{W}(2n-1,2)$. The first naive question to address is to look at the entanglement classes of the states forming the 2^n+1 MUBs associated to a spread. In the case $n=2$ and $n=3$ we completed these calculations in [79]. In the $n=2$ case a spread of $\mathcal{W}(3,2)$ is composed of 5 lines, to these 5 lines one can associate 5 MUBs. Among the 5 MUBs, three are defined by separable two qubit states and two are given in terms of EPR like states. In the $n=3$ case, a spread is made of 9 planes. The corresponding 9 MUBs in $\mathcal{H}_3$ are made of 2 bases defined by separable states, 3 bases corresponding to bi-separable states and 4 bases made of states SLOCC equivalent to $|GHZ\rangle$. Interestingly, like in Grover's and Shor's algorithm, the $|W\rangle$-state does not show up in this construction (Section 10.1).

The language of error-correcting codes could be an efficient way of connecting the two geometric approaches of Part I and II because, as we just showed, it naturally involves the main objects of studies of Part I and II, namely quantum states of $\mathcal{H}_n$ on the one side and maximal isotropic subspaces of $\mathcal{W}(2n-1,2)$ on the other side. In the future, we hope that finding a correspondence between these two geometric perspectives, the projective geometry over the complex numbers and the one over the two-element field, will provide a better understanding of the relation between entanglement and contextuality.

Part IV

APPENDIX

A

COVARIANTS FOR THE 4-QUBIT CLASSIFICATION

For the sake completeness, I reproduce in this appendix the expressions of the covariants used in Chapters 3 and 4 to distinguish the orbits of the nullcone (Eq. (49)) and to identify the normal form of a given four-qubit state (Algorithm 4.3.1). A generating system of this $2 \times 2 \times 2 \times 2$-covariant algebra was already provided by Emmanuel Briand, Jean-Gabriel Luque and Jean-Yves Thibon in [20], but the one proposed in [55] for our investigation of the four-qubit case is slightly different.

The only covariant of degree 1 is the ground form

$$f = \sum_{i,j,k,l \in \{0,1\}} a_{ijkl} x_i y_j z_k t_l.$$

Degree 2

Symbol	Transvectant
B_{0000}	$\frac{1}{2}(f,f)^{1111}$
B_{2200}	$\frac{1}{2}(f,f)^{0011}$
B_{2020}	$\frac{1}{2}(f,f)^{0101}$
B_{2002}	$\frac{1}{2}(f,f)^{0110}$
B_{0220}	$\frac{1}{2}(f,f)^{1001}$
B_{0202}	$\frac{1}{2}(f,f)^{1010}$
B_{0022}	$\frac{1}{2}(f,f)^{1100}$

Degree 3

Symbol	Transvectant
C^1_{1111}	$(f,B_{2200})^{1100} + (f,B_{0022})^{0011}$
C^2_{1111}	$(f,B_{0220})^{0110} + (f,B_{2002})^{1001}$
C_{3111}	$\frac{1}{3}\left((f,B_{2200})^{0100} + (f,B_{2020})^{0010} + (f,B_{2002})^{0001}\right)$
C_{1311}	$\frac{1}{3}\left((f,B_{2200})^{1000} + (f,B_{0220})^{0010} + (f,B_{0202})^{0001}\right)$
C_{1131}	$\frac{1}{3}\left((f,B_{2020})^{1000} + (f,B_{0220})^{0100} + (f,B_{0022})^{0001}\right)$
C_{1113}	$\frac{1}{3}\left((f,B_{2002})^{1000} + (f,B_{0202})^{0100} + (f,B_{0022})^{0010}\right)$

Degree 4

Symbol	Transvectant
D^1_{0000}	$(f,C^1_{1111})^{1111}$
D^2_{0000}	$(f,C^2_{1,1,1,1})^{1111}$
D_{2200}	$(f,C^1_{1111})^{0011}$
D_{2020}	$(f,C^1_{1111})^{0101}$
D_{2002}	$(f,C^1_{1111})^{0110}$
D_{0220}	$(f,C^1_{1111})^{1001}$
D_{0202}	$(f,C^1_{1111})^{1010}$
D_{0022}	$(f,C_{1111})^{1100}$

Symbol	Transvectant
D_{4000}	$(f,C_{3111})^{0111}$
D_{0400}	$(f,C_{1311})^{1011}$
D_{0040}	$(f,C_{1131})^{1101}$
D_{0004}	$(f,C_{1113})^{1110}$
D^1_{2220}	$(f,C^1_{1111})^{0001}$
D^2_{2220}	$(f,C^2_{1111})^{0001}$
D^1_{2202}	$(f,C^1_{1111})^{0010}$
D^2_{2202}	$(f,C^2_{1111})^{0010}$
D^1_{2022}	$(f,C^1_{1111})^{0100}$
D^2_{2022}	$(f,C^2_{1111})^{0100}$
D^1_{0222}	$(f,C^1_{1111})^{1000}$
D^2_{0222}	$(f,C^2_{1111})^{1000}$

Degree 5

Symbol	Transvectant
E_{1111}	$(f, D_{2200})^{1100}$
E^1_{3111}	$(f, D_{2200})^{0100} + (f, D_{2020})^{0010} + (f, D_{2002})^{0001}$
E^2_{3111}	$(f, D^1_{2220})^{0110} - (f, D^1_{2022})^{0011} + (f, D^1_{2202})^{0101}$
E^3_{3111}	$(f, D^2_{2220})^{0110} - (f, D^2_{2022})^{0011} + (f, D^2_{2202})^{0101}$
E^1_{1311}	$(f, D_{2200})^{1000} + (f, D_{0220})^{0010} + (f, D_{0202})^{0001}$
E^2_{1311}	$(f, D^1_{2220})^{1010} - (f, D^1_{2202})^{1001} + (f, D^1_{0222})^{0011}$
E^3_{1311}	$f, D^2_{2220})^{1010} - (f, D^2_{2202})^{1001} + (f, D^2_{0222})^{0011}$
E^1_{1131}	$(f, D_{2020})^{1000} + (f, D_{0220})^{0100} + (f, D_{0022})^{0001}$
E^2_{1131}	$(f, D^1_{2220})^{1100} - (f, D^1_{2022})^{1001} + (f, D^1_{0222})^{0101}$
E^3_{1131}	$(f, D^2_{2220})^{1100} - (f, D^2_{2022})^{1001} + (f, D^2_{0222})^{0101}$
E^1_{1113}	$(f, D_{2002})^{1000} + (f, D_{0202})^{0100} + (f, D_{0022})^{0010}$
E^2_{1113}	$(f, D^1_{2202})^{1100} - (f, D^1_{2022})^{1010} + (f, D^1_{0222})^{0110}$
E^3_{1113}	$(f, D^2_{2202})^{1100} - (f, D^2_{2022})^{1010} + (f, D^2_{0222})^{0110}$

Degree 6

Symbol	Transvectant
F_{0000}	$(f, E_{1111})^{1111}$
F_{2200}	$(f, E^1_{1111})^{0011}$
F_{2020}	$(f, E_{1111})^{0101}$
F_{2002}	$(f, E^1_{1111})^{0110}$
F_{0220}	$(f, E^1_{1111})^{1001}$
F_{0202}	$(f, E^3_{1111})^{1010}$
F_{0022}	$(f, E^1_{1111})^{1100}$
F^1_{2220}	$(f, E^1_{1311})^{0101} - (f, E^1_{3111})^{1001}) + (f, E^1_{1131})^{0011}$
F^2_{2220}	$(f, E^1_{1311})^{0101} + (f, E^1_{3111})^{1001}) - (f, E^1_{1131})^{0011}$
F^1_{2202}	$(f, E^1_{1311})^{0110} - (f, E^1_{3111})^{1010}) + (f, E^1_{1113})^{0011}$
F^2_{2202}	$(f, E^1_{1311})^{0110} + (f, E^1_{3111})^{1010}) - (f, E^1_{1113})^{0011}$
F^1_{2022}	$(f, E^1_{3111})^{1100} - (f, E^1_{1131})^{0110}) + (f, E^1_{1113})^{0101}$
F^2_{2022}	$(f, E^1_{3111})^{1100} + (f, E^1_{1131})^{0110}) - (f, E^1_{1113})^{0101}$
F^1_{0222}	$(f, E^1_{1311})^{1100} - (f, E^1_{1131})^{1010}) + (f, E^1_{1113})^{1001}$
F^2_{0222}	$(f, E^1_{1311})^{1100} + (f, E^1_{1131})^{1010}) - (f, E^1_{1113})^{1001}$

Symbol	Transvectant
F_{4200}	$(f, E^1_{3111})^{0011}$
F_{4020}	$(f, E^1_{3111})^{0101}$
F_{4002}	$(f, E^1_{3111})^{0110}$
F_{0420}	$(f, E^1_{1311})^{1001}$
F_{0402}	$(f, E^1_{1311})^{1010}$
F_{0042}	$(f, E^1_{1131})^{1100}$
F_{2400}	$(f, E^1_{1311})^{0011}$
F_{2040}	$(f, E^1_{1131})^{0101}$
F_{2004}	$(f, E^1_{1113})^{0110}$
F_{0240}	$(f, E^1_{1131})^{1001}$
F_{0204}	$(f, E^1_{1113})^{1010}$
F_{0024}	$(f, E^1_{1113})^{1100}$

Degree 7

Symbol	Transvectant
G^1_{3111}	$(f, F_{4200})^{1100}$
G^2_{3111}	$(f, F_{4020})^{1010}$
G^3_{3111}	$(f, F_{4002})^{1001}$
G^1_{1311}	$(f, F_{2400})^{110}$
G^2_{1311}	$(f, F_{0420})^{0110}$
G^3_{1311}	$(f, F_{0402})^{0101}$
G^1_{1131}	$(f, F_{2040})^{1010}$
G^2_{1131}	$(f, F_{0240})^{0110}$
G^3_{1131}	$(f, F_{0024})^{0011}$
G^1_{1113}	$(f, F_{2004})^{1001}$
G^2_{1113}	$(f, F_{0204})^{0101}$
G^3_{1113}	$(f, F_{0024})^{0011}$

Symbol	Transvectant
G_{5111}	$(f, F_{4002})^{0001} + (f, F_{4020})^{0010} + (f, F_{4200})^{0100}$
G_{1511}	$(f, F_{0402})^{0001} + (f, F_{0420})^{0010} + (f, F_{2400})^{1000}$
G_{1151}	$(f, F_{0042})^{0001} + (f, F_{0240})^{0100} + (f, F_{2040})^{1000}$
G_{1115}	$(f, F_{0204})^{0100} + (f, F_{0024})^{0010} + (f, F_{2004})^{1000}$
G_{3311}	$(f, F_{2400})^{0100}$
G_{3131}	$(f, F_{2040})^{0010}$
G_{3113}	$(f, F_{2004})^{0001}$
G_{1331}	$(f, F_{0240})^{0010}$
G_{1313}	$(f, F_{0204})^{0001}$
G_{1133}	$(f, F_{0024})^{0001}$

Degree 8

Symbol	Transvectant
H_{4000}	$(f, G_{3111})^{0111}$
H_{0400}	$(f, G_{1311})^{1011}$
H_{0040}	$(f, G_{1131})^{1101}$
H_{0004}	$(f, G_{1113})^{1110}$
H^1_{2220}	$(f, G^1_{1311})^{0101} + (f, G^1_{3111})^{1001} + (f, G^1_{1131})^{0011}$
H^2_{2220}	$(f, G^2_{1311})^{0101} + (f, G^2_{3111})^{1001} + (f, G^2_{1131})^{0011}$
H^1_{2202}	$(f, G^1_{1311})^{0110} + (f, G^1_{3111})^{1010} + (f, G^1_{1113})^{0011}$
H^2_{2202}	$(f, G^2_{1311})^{0110} + (f, G^2_{3111})^{1010} + (f, G^2_{1113})^{0011}$
H^1_{2022}	$(f, G^1_{3111})^{1100} + (f, G^1_{1131})^{0110} + (f, G^1_{1113})^{0101}$
H^2_{2022}	$(f, G^2_{3111})^{1100} + (f, G^2_{1131})^{0110} + (f, G^2_{1113})^{0101}$
H^1_{0222}	$(f, G^1_{1311})^{1100} + (f, G^1_{1131})^{1010} + (f, G^1_{1113})^{1001}$
H^2_{0222}	$(f, G^2_{1311})^{1100} + (f, G^2_{1131})^{1010} + (f, G^2_{1113})^{1001}$

Symbol	Transvectant
H_{4200}	$(f, G_{5111})^{1011}$
H_{4020}	$(f, G_{5111})^{1101}$
H_{4002}	$(f, G_{5111})^{1110}$
H_{0420}	$(f, G_{1511})^{1101}$
H_{0402}	$(f, G_{1511})^{1110}$
H_{0042}	$(f, G_{1151})^{1110}$
H_{2400}	$(f, G^1_{1511})^{0111}$
H_{2040}	$(f, G_{1151})^{0111}$
H_{2004}	$(f, G^1_{1115})^{0111}$
H_{0240}	$(f, G_{1151})^{1011}$
H_{0204}	$(f, G_{1115})^{1011}$
H_{0024}	$(f, G^1_{1115})^{1101}$

Degree 9

Symbol	Transvectant
I_{3111}	$(f, H_{4020})^{1010} + (f, H_{4200})^{1100} + (f, H_{4002})^{1001}$
I_{1311}	$(f, H_{0420})^{0110} + (f, H_{2400})^{1100} + (f, H_{0402})^{0101}$
I_{1131}	$(f, H_{0240})^{0110} + (f, H_{2040})^{1010} + (f, H_{0042})^{0011}$
I_{1113}	$(f, H_{0204})^{0101} + (f, H_{2004})^{1001} + (f, H_{0024})^{0011}$
I^1_{5111}	$(f, H_{4020})^{0010} + (f, H_{4200})^{0100} + (f, H_{4002})^{0001}$
I^2_{5111}	$(f, H_{4020})^{0010} - (f, H_{4200})^{0100} + (f, H_{4002})^{0001}$
I^1_{1511}	$(f, H_{0420})^{0010} + (f, H_{2400})^{1000} + (f, H_{4002})^{0001}$
I^2_{1511}	$(f, H_{0420})^{0010} - (f, H_{2400})^{1000} + (f, H_{4002})^{0001}$
I^1_{1151}	$(f, H_{0240})^{0100} + (f, H_{2040})^{1000} + (f, H_{0042})^{0001}$
I^2_{1151}	$(f, H_{0240})^{0100} - (f, H_{2040})^{1000} + (f, H_{0042})^{0001}$
I^1_{1115}	$(f, H_{0204})^{0100} + (f, H_{2004})^{1000} + (f, H_{0024})^{0010}$
I^2_{1115}	$(f, H_{0204})^{0100} - (f, H_{2004})^{1000} + (f, H_{0024})^{0010}$

Symbol	Transvectant
I^1_{3311}	$(f, H^1_{2220})^{0010} + (f, H^1_{2202})^{0001}$
I^2_{3311}	$(f, H^2_{2220})^{0010} + (f, H^2_{2202})^{0001}$
I^1_{3131}	$(f, H^1_{2220})^{0100} + (f, H^1_{2022})^{0001}$
I^2_{3131}	$(f, H^2_{2220})^{0100} + (f, H^2_{2022})^{0001}$
I^1_{3113}	$(f, H^1_{2202})^{0100} + (f, H^1_{2022})^{0010}$
I^2_{3113}	$(f, H^2_{2202})^{0100} + (f, H^2_{2022})^{0010}$
I^1_{1331}	$(f, H^1_{2220})^{1000} + (f, H^1_{0222})^{0001}$
I^2_{1331}	$((f, H^2_{2202})^{0100} + (f, H^2_{2022})^{0010}$
I^1_{1313}	$(f, H^1_{0222})^{0010} + (f, H^1_{2202})^{1000}$
I^2_{1313}	$(f, H^2_{0222})^{0010} + (f, H^2_{2202})^{1000}$
I^1_{1133}	$(f, H^1_{0222})^{010} + (f, H^1_{2022})^{1000}$
I^2_{1133}	$(f, H^2_{0222})^{010} + (f, H^2_{2022})^{1000}$

Degree 10

Symbol	Transvectant
J_{4200}	$(f, I_{5111})^{1011}$
J_{4020}	$(f, I_{5111})^{1101}$
J_{4002}	$(f, I_{5111})^{1110}$
J_{0420}	$(f, I_{1511})^{1101}$
J_{0402}	$(f, I_{1511})^{1110}$
J_{0042}	$(f, I_{1151})^{1110}$
J_{2400}	$(f, I_{1511})^{0111}$
J_{2040}	$(f, I_{1151})^{0111}$
J_{2004}	$(f, I_{1115})^{0111}$
J_{0240}	$(f, I_{1151})^{1011}$
J_{0204}	$(f, I_{1115})^{1011}$
J_{0024}	$(f, I_{1115})^{1101}$

Degree 11

Symbol	Transvectant
K_{3311}	$= (f, J_{4200})^{1000} - (f, J_{2400})^{0100}$
K_{3131}	$= (f, J_{4020})^{1000} - (f, J_{2040})^{0010}$
K_{3113}	$= (f, J_{4002})^{1000} - (f, J_{2004})^{0001}$
K_{1331}	$= (f, J_{0420})^{0100} - (f, J_{0240})^{0010}$
K_{1313}	$= (f, J_{0402})^{0100} - (f, J_{0204})^{0001}$
K_{1133}	$= (f, J_{0042})^{0010} - (f, J_{0024})^{0001}$
K_{5111}	$= (f, J_{4200})^{0100} - (f, J_{4020})^{0010} + (f, J_{4002})^{0001}$
K_{1511}	$= (f, J_{2400})^{1000} - (f, J_{0420})^{0010} + (f, J_{0402})^{0001}$
K_{1151}	$= (f, J_{2040})^{1000} - (f, J_{0240})^{0100} + (f, J_{0042})^{0001}$
K_{1115}	$= (f, J_{2004})^{1000} - (f, J_{0204})^{0110} + (f, J_{0024})^{0010}$

Degree 12

Symbol	Transvectant
L_{6000}	$= (f, K_{5111})^{0111}$
L_{0600}	$= (f, K_{1511})^{1011}$
L_{0060}	$= (f, K_{1151})^{1101}$
L_{0006}	$= (f, K_{1115})^{1110}$

B

SINGULARITIES AND ENTANGLED STATES

Theorems 4 and 5 were proved in [57] and [51] by computing for each normal form of the four-qubit and three-qutrit classification the corresponding hypersurface singularities. As explained in Chapter 4, we first computed the polynomial corresponding to the hyperplane section defined by a quantum state $|\psi\rangle$ and then we looked for the isolated singularities of these hypersurfaces. The isolated singularities were caracterized by computing their co-rank and their Milnor number.

Here we list for each normal form of the two classifications the corresponding isolated singularity types.

B.1 ISOLATED SINGULAR POINTS OF VERSTRAETE'S FORMS

The 9 normal forms of Verstraete *et al.* classification split into two sets: the nilpotent forms and the families of states that depend on parameters.

B.1.1 *Nilpotent states*

The 3 families that correspond to nilpotent orbits in the four-qubit classification and their corresponding singularities are given in Table 12.

Verstraete's notation	**Hyperplane**	**Singular type**
$L_{0_{7\oplus\bar{1}}}$	$\langle 0000\| + \langle 1011\| + \langle 1101\| + \langle 1110\|$	D_4
$L_{0_{5\oplus\bar{3}}}$	$\langle 0000\| + \langle 0101\| + \langle 1000\| + \langle 1110\|$	non-isolated
$L_{0_{3\oplus\bar{1}}0_{3\oplus\bar{1}}}$	$\langle 0000\| + \langle 0111\|$	non-isolated

Table 12: The normal forms' names [117], the hyperplanes and the singular type of the corresponding sections.

B.1.2 *Parameters states*

The 6 families that depend on parameters and their corresponding singularities are given in Table 13.

Verstraete's notation	Hyperplane	Params	Singular type
G_{abcd}	$\frac{a+d}{2}(\langle 0000\| \langle 1111\|) + \frac{a-d}{2}(\langle 0011\| + \langle 1100\|)$ $+\frac{b+c}{2}(\langle 0101\| + \langle 1010\|) + \frac{b-c}{2}(\langle 0110\| + \langle 1001\|)$	a, b, c, d generic Table V of [57]	smooth A_1
L_{abc_2}	$\frac{a+b}{2}(\langle 0000\| + \langle 1111\|) + \frac{a-b}{2}(\langle 0011\| + \langle 1100\|)$ $c(\langle 1010\| + \langle 0101\|) + \langle 0110\|$	a, b, c generic $a = \pm b$ $c = 0$	A_1 A_1 A_1
$L_{a_2b_2}$	$a(\|0000\rangle + \|1111\rangle) + b(\|0101\rangle + \|1010\rangle)$ $+\|0110\rangle + \|0011\rangle$	a, b generic	$2A_1$
L_{ab_3}	$a(\langle 0000\| + \langle 1111\|) + \frac{a+b}{2}(\langle 0101\| + \langle 1010\|)$ $+\frac{a-b}{2}(\langle 0110\| + \langle 1001\|)$ $+\frac{i}{\sqrt{2}}(\langle 0001\| + \langle 0010\| - \langle 0111\| - \langle 1011\|)$	a, b generic	A_2
L_{a_4}	$a(\langle 0000\| + \langle 0101\| + \langle 1010\| + \langle 1111\|)$ $+i\langle 0001\| + \langle 0110\| - i\langle 1011\|$	a generic $a = 0$	A_3
$L_{a_2 0_{3\oplus 1}}$	$a(\langle 0000\| + \langle 1111\|) + \langle 0011\| + \langle 0101\| + \langle 0110\|$	a generic	A_1

Table 13: The normal forms' names [117], the hyperplanes and the singular type of the corresponding sections which depend on parameters.

B.2 ISOLATED SINGULAR TYPE OF NURMIEV'S FORMS

Nurmiev's classfication of $3 \times 3 \times 3$ complex matrices is given in [92]. As in the four-qubit classification, there are nilpotent states and families that are parameter-dependent.

B.2.1 *Nilpotent states*

The 24 nilpotent states (the 0 state is omitted) and their corresponding singularities are given in 14.

B.2.2 *Parameter states*

For defining more easily each family of Nurmiev's normal forms and the corresponding hyperplanes, let us denote $X_1 = \langle 000| + \langle 111| + \langle 222|$, $X_2 = \langle 012| + \langle 120| + \langle 201|$ and $X_3 = \langle 021| + \langle 102| + \langle 210|$. Each family is a linear combination of these linear forms, plus a nilpotent part, and the complex coefficients associated to X_1, X_2 and X_3 must satisfy a set of conditions, listed as follows:

- First family: $abc \neq 0$, $(a^3 + b^3 + c^3)^3 - (3abc)^3 \neq 0$.
- Second family: $b(a^3 + b^3) \neq 0$, $c = 0$.
- Third family: $a \neq 0$, $b = c = 0$.
- Fourth family: $c = -b \neq 0$, $a = 0$.

The singularities of the corresponding hyperplane sections are given in Table 15.

Orbit	Hyperplane	Singular type
N_1	$\langle 012\vert + \langle 021\vert + \langle 102\vert + \langle 111\vert + \langle 120\vert + \langle 200\vert$	A_3
N_2	$\langle 012\vert + \langle 021\vert + \langle 102\vert + \langle 110\vert + \langle 111\vert + \langle 200\vert$	D_4
N_3	$\langle 002\vert + \langle 011\vert + \langle 020\vert + \langle 101\vert + \langle 112\vert + \langle 200\vert$	Non-Isolated
N_4	$\langle 002\vert + \langle 011\vert + \langle 101\vert + \langle 110\vert + \langle 220\vert$	Non-isolated
N_5	$\langle 002\vert + \langle 020\vert + \langle 021\vert + \langle 110\vert + \langle 201\vert$	Non-isolated
N_6	$\langle 002\vert + \langle 011\vert + \langle 101\vert + \langle 120\vert + \langle 210\vert$	Non-isolated
N_7	$\langle 002\vert + \langle 011\vert + \langle 020\vert + \langle 101\vert + \langle 210\vert$	Non-isolated
N_8	$\langle 002\vert + \langle 020\vert + \langle 111\vert + \langle 200\vert$	Non-isolated
N_9	$\langle 000\vert + \langle 011\vert + \langle 111\vert + \langle 122\vert$	Non-isolated
N_{10}	$\langle 002\vert + \langle 011\vert + \langle 020\vert + \langle 101\vert + \langle 110\vert + \langle 200\vert$	Non-isolated
N_{11}	$\langle 002\vert + \langle 020\vert + \langle 101\vert + \langle 210\vert$	Non-isolated
N_{12}	$\langle 002\vert + \langle 020\vert + \langle 100\vert + \langle 111\vert$	Non-isolated
N_{13}	$\langle 002\vert + \langle 011\vert + \langle 020\vert + \langle 101\vert + \langle 110\vert$	Non-isolated
N_{14}	$\langle 002\vert + \langle 010\vert + \langle 021\vert + \langle 100\vert + \langle 201\vert$	Non-isolated
N_{15}	$\langle 011\vert + \langle 022\vert + \langle 100\vert$	Non- isolated
N_{16}	$\langle 002\vert + \langle 011\vert + \langle 020\vert + \langle 100\vert$	Non-isolated
N_{17}	$\langle 001\vert + \langle 010\vert + \langle 102\vert + \langle 120\vert$	Non-isolated
N_{18}	$\langle 000\vert + \langle 011\vert + \langle 101\vert + \langle 112\vert$	Non- isolated
N_{19}	$\langle 002\vert + \langle 010\vert + \langle 101\vert$	Non- isolated
N_{20}	$\langle 000\vert + \langle 111\vert$	Non-isolated
N_{21}	$\langle 001\vert + \langle 010\vert + \langle 100\vert$	Non-isolated
N_{22}	$\langle 000\vert + \langle 011\vert + \langle 022\vert$	Non-isolated
N_{23}	$\langle 000\vert + \langle 011\vert$	Non-isolated
N_{24}	$\langle 000\vert$	Non-isolated

Table 14: The normal forms' names [92], the hyperplanes and the singular type of the corresponding sections.

Orbits	Hyperplane	Params	Singular type
$F_{1,1}$	$a.X_1 + b.X_2 + c.X_3$	a,b,c generic	Smooth
$F_{2,1}$	$a.X_1 + b.X_2 + \langle 021| + \langle 102|$	a,b generic $a = 0$	A_1 $3A_1$
$F_{2,2}$	$a.X_1 + b.X_2 + \langle 021|$	a,b generic $a = 0$	$2A_1$ $3A_1$
$F_{2,3}$	$a.X_1 + b.X_2 + \langle 201|$	a,b generic $a = 0$	$3A_1$ $3A_1$
$F_{3,1}$	$a.X_1 + \langle 012| + \langle 021| + \langle 102| + \langle 120|$	a generic	$2A_1$
$F_{3,2}$	$a.X_1 + \langle 012| + \langle 021| + \langle 102|$	a generic	$3A_1$
$F_{3,3}$	$a.X_1 + \langle 012| + \langle 021| + \langle 120|$	a generic	$3A_1$
$F_{3,4}$	$a.X_1 + \langle 012| + \langle 021|$	a generic	$4A_1$
$F_{3,5}$	$a.X_1 + \langle 012| + \langle 120|$	a generic	$4A_1$
$F_{3,6}$	$a.X_1 + \langle 021| + \langle 102|$	a generic	$4A_1$
$F_{3,7}$	$a.X_1 + \langle 012|$	a generic	$5A_1$
$F_{3,8}$	$a.X_1 + \langle 021|$	a generic	$5A_1$
$F_{3,9}$	$a.X_1$	a generic	$6A_1$
$F_{4,1}$	$b(X_2 - X_3) + \langle 002| + \langle 020| + \langle 111| + \langle 200|$	b generic	A_2
$F_{4,2}$	$b(X_2 - X_3) + \langle 002| + \langle 011| + \langle 020| + \langle 101|$ $+ \langle 110| + \langle 200|$	b generic	A_3
$F_{4,3}$	$b(X_2 - X_3) + \langle 000| + \langle 111|$	b generic	D_4
$F_{4,4}$	$b(X_2 - X_3) + \langle 001| + \langle 010| + \langle 100| + \langle 200|$	b generic	Non- isolated
$F_{4,5}$	$b(X_2 - X_3) + \langle 000|$	b generic	Non-isolated
$F_{4,6}$	$b(X_2 - X_3)$	b generic	Non-isolated

Table 15: The normal forms' names [92], the hyperplanes and the singular type of the corresponding sections which depend on parameters.

C

THE LAGRANGIAN BIJECTION

In Chapter 7, I explained how we used the projection of the Lagrangian variety (Lagrangian mapping, see Figure 20) to associate bijectively generators of $\mathcal{W}(2N-1,2)$ with a subset of symmetric operators in $\mathcal{W}(2^N-1,2)$. In [60], we worked out explicitely this bijection for the case $N=2,3$ and $N=4$. We obtained the set-theoretical ideal of the variety corresponding to the projection of $\mathrm{LG}(N,2N)$. Using the natural action of $\mathrm{SL}(2,2)\times\cdots\times\mathrm{SL}(2,2)$ on $\mathrm{PG}(2^N-1,2)$, one considers the orbit stratification[1] of $\mathrm{PG}(2^N-1,2)$ [19] to distinguish different classes of generators in $\mathcal{W}(2N-1,2)$. In this appendix we reproduce the tables (for $N=2,3,4$) published in [60], which associate to each of the orbits of $\mathrm{PG}(2^N-1,2)$, that are partitionning the projection of $\mathrm{LG}(N,2N)$, the corresponding (class of) generators in $\mathcal{W}(2N-1,2)$.

C.1 TWO DISTINGUISHED CLASSES OF MUTUALLY COMMUTING TWO-QUBIT OPERATORS

It is well known (see, e. g., [49]) that the projective space $\mathrm{PG}(3,2)$ is the union of two G orbits,

$$\mathrm{PG}(3,2)=\mathcal{O}_1\cup\mathcal{O}_2,$$

with $\sharp\mathcal{O}_1=9$ and $\sharp\mathcal{O}_2=6$. The orbit $\mathcal{O}_1$, comprising the points lying on a hyperbolic quadric $\mathcal{Q}^+(3,2)$, and the orbit $\mathcal{O}_2$, consisting of six off-quadric points.

Orbit	Size	Representative	Observable	Set of mutually commuting two-qubit observables
$\mathcal{O}_1$	9	$[0:0:1:0]$	XI	$\mathrm{PG}(1,2)_a$
$\mathcal{O}_2$	6	$[1:0:1:0]$	YI	$\mathrm{PG}(1,2)_b$

Table 16: Classes of mutually commuting 2-qubits operators; here, $\mathrm{PG}(1,2)_a=\langle XI, IX\rangle$ and $\mathrm{PG}(1,2)_b=\langle ZX, XZ\rangle$.

The partition of $\mathrm{PG}(3,2)$ into two orbits $\mathcal{O}_1$ and $\mathcal{O}_2$ tells us that we can similarly partition $\mathrm{LG}(2,4)$ into two classes of lines; a class of cardinality 9, which is the G-orbit of $\mathrm{PG}(1,2)_a$, and a class of cardinality 6, which is the G-orbit of $\mathrm{PG}(1,2)_b$.

1 A constructive way of producing the orbit stratification pf $\mathrm{PG}(2^N-1,2)$ for $N=2,3$ and 4, via the concept of Veldkamp geometry is proposed in Chapter 8 and Appendix D.

C.2 THREE DISTINGUISHED CLASSES OF MUTUALLY COMMUTING THREE-QUBIT OPERATORS

The projective space $\mathrm{PG}(7,2)$ is the union of five G-orbits (see [19, 49]),

$$\mathrm{PG}(7,2) = \mathcal{O}_1 \cup \mathcal{O}_2 \cup \mathcal{O}_3 \cup \mathcal{O}_4 \cup \mathcal{O}_5,$$

with $\sharp\mathcal{O}_1 = 27$, $\sharp\mathcal{O}_2 = 54$, $\sharp\mathcal{O}_3 = 108$, $\sharp\mathcal{O}_4 = 54$ and $\sharp\mathcal{O}_5 = 12$. It is also well known (see, e. g., [49]) that $\mathcal{Q}^+(7,2) = \mathcal{O}_1 \cup \mathcal{O}_2 \cup \mathcal{O}_4$. Hence, the projection of the Lagrangian variety, $\mathrm{LG}(3,6)$, is partitioned into three different G-orbits whose properties are summarized in Table 2; here, we used the representatives of the orbits $\mathcal{O}_i$ from [19].

Orbit	Size	Representative	Symmetric four-qubit observable	Set of mutually commuting three-qubit observables
$\mathcal{O}_1$	27	[0:0:0:0:1:0:0:0]	XIII	$\mathrm{PG}(2,2)_a$
$\mathcal{O}_2$	54	[0:0:0:1:0:0:1:0]	IIXZ	$\mathrm{PG}(2,2)_b$
$\mathcal{O}_4$	54	[0:0:0:1:0:1:1:0]	IXXZ	$\mathrm{PG}(2,2)_c$

Table 17: Classes of mutually commuting 3-qubits operators; here, $\mathrm{PG}(2,2)_a = \langle \mathrm{XII}, \mathrm{IXI}, \mathrm{IIX}\rangle$, $\mathrm{PG}(2,2)_b = \langle \mathrm{ZZI}, \mathrm{XXI}, \mathrm{IIX}\rangle$, and $\mathrm{PG}(2,2)_c = \langle \mathrm{XIX}, \mathrm{IXX}, \mathrm{ZZZ}\rangle$.

C.3 SIX DISTINGUISHED CLASSES OF MUTUALLY COMMUTING FOUR-QUBIT OPERATORS

The stratification of $\mathrm{PG}(15,2)$ in terms of 29 G-orbits was also established in [19] and [104]. The projection of $\mathrm{LG}(4,8)$ is the union of 6 orbits that were identified in [60] thanks to the defining ideal of $\mathrm{LG}(4,8)$. The results of our calculations are portrayed in Table 18.

Orbit	Size	Representative	Symmetric 8-qubit obs'le	Set of mut. comm. 4-qubit obs'les
$\mathcal{O}_2$	81	[0:0:0:0:0:0:0:0:1:0:0:0:0:0:0:0]	XIIIIIII	$\mathrm{PG}(3,2)_a$
$\mathcal{O}_3$	324	[0:0:0:0:0:0:0:0:0:1:1:0:0:0:0:0]	IXXIIIII	$\mathrm{PG}(3,2)_b$
$\mathcal{O}_6$	648	[0:0:0:0:0:0:0:0:0:1:1:0:1:0:0:0]	IXXIXIII	$\mathrm{PG}(3,2)_c$
$\mathcal{O}_{14}$	162	[0:0:0:0:0:0:0:1:0:1:1:0:1:0:0:0]	IXXIXIIZ	$\mathrm{PG}(3,2)_d$
$\mathcal{O}_{17}$	108	[0:0:0:0:0:1:1:0:0:0:0:0:0:1:1:0]	IIIIIYYI	$\mathrm{PG}(3,2)_e$
$\mathcal{O}_{18}$	972	[0:0:0:0:0:1:1:0:1:0:0:0:0:1:1:0]	XIIIIYYI	$\mathrm{PG}(3,2)_f$

Table 18: Classes of mutually commuting 4-qubits operators; here, $\mathrm{PG}(3,2)_a = \langle \mathrm{XIII}, \mathrm{IXII}, \mathrm{IIXI}, \mathrm{IIIX}\rangle$, $\mathrm{PG}(3,2)_b = \langle \mathrm{XIII}, \mathrm{IXII}, \mathrm{IIZZ}, \mathrm{IIYY}\rangle$, $\mathrm{PG}(3,2)_c = \langle \mathrm{XIII}, \mathrm{IZZZ}, \mathrm{IYYZ}, \mathrm{IYZY}\rangle$, $\mathrm{PG}(3,2)_d = \langle \mathrm{ZYYY}, \mathrm{YZYY}, \mathrm{YYZY}, \mathrm{YYYZ}\rangle$, $\mathrm{PG}(3,2)_e = \langle \mathrm{XXII}, \mathrm{ZZII}, \mathrm{IIZZ}, \mathrm{IIYY}\rangle$ and $\mathrm{PG}(3,2)_f = \langle \mathrm{XIZZ}, \mathrm{IXZZ}, \mathrm{ZZXI}, \mathrm{ZZIX}\rangle$.

D

GEOMETRIC HYPERPLANES OF $S_4(2)$

From the knowledge of the Veldkamp geometry of $S_3(2)$, one can built by the blow-up procedure the Veldkamp geometry of $S_4(2)$ (Chapter 8). Because of the Segre embedding, the different types of geometric hyperplanes of $\mathcal{V}(S_4(2))$ are in bijection with the orbits of $PG(15,2)$ under the group action $G = SL(2,2) \times SL(2,2) \times SL(2,2) \times SL(2,2) \rtimes \sigma_4$.

Table 19, from [104], provides a description of the 29 types of hyperplanes of $S_4(2)$. These types of hyperplanes are caracterized by the number of points, lines and composition (like in Table 10 of Chapter 8). To generate such a table, one needs to know the Veldkamp lines of $\mathcal{V}(S_3(2))$. The Veldkamp geometry of $S_3(2)$ was elaborated by Richard Green and Metod Saniga in [39]. The same labeling of the Veldkamp lines as used in [39, Table 2] is employed in Table 19 to indicate from which Veldkamp line of $S_3(2)$ a hyperplane of $S_4(2)$ originates. As in Table 10, Latin numbers denote extraordinary Veldkamp lines of $S_3(2)$ (the number corresponds to the hyperplane type to build the line).

Tables 20 and 21 identify among the hyperplanes of $\mathcal{V}(S_4(2))$ those ones that belong to the hyperbolic quadric $\mathcal{Q}^+(7,2)$ (Table 20) and those corresponding to the image of the projection of $LG(4,8)$ (Table 21). In particular, one can see that the 6 orbits of Table 21 correspond to the 6 orbits of maximal sets of mutually commuting four-qubit operators given by Table 18.

			# of Points of Order					# of $S_{(3)}$'s of Type									
Tp	Ps	Ls	0	1	2	3	4	D	H_1	H_2	H_3	H_4	H_5	VL	Crd	BS	W
1	65	76	0	0	0	32	33	4	8	0	0	0	0	I	81	2	1
2	57	60	0	0	12	24	21	2	6	4	0	0	0	II, 1	324	3	2
3	53	52	0	2	12	26	13	1	6	3	2	0	0	III, 2	1296	4	2
4	51	48	1	0	12	32	6	0	8	0	4	0	0	3	648	5	2
5	49	44	0	8	12	16	13	1	3	6	0	2	0	IV, 4	648	6	3
6	47	40	0	4	18	20	5	0	4	4	4	0	0	5	3888	11	3
7	45	36	0	18	0	18	9	1	0	9	0	0	2	V, 6	144	7	3
8	45	36	0	0	36	0	9	0	0	12	0	0	0	10	108	17	4
9	45	36	2	4	18	16	5	0	4	2	4	2	0	7, 8	3888	8	3
10	45	36	0	6	18	18	3	0	3	3	6	0	0	9, 11	2592	9	3
11	43	32	1	8	18	12	4	0	2	4	4	2	0	12, 13	7776	12	3
12	41	28	8	0	24	0	9	0	4	0	0	8	0	14	162	14	4
13	41	28	0	12	18	8	3	0	0	6	4	2	0	15, 18	1944	19	4
14	41	28	0	14	12	14	1	0	1	3	6	2	0	17, 21	2592	15	4
15	41	28	2	8	18	12	1	0	1	3	7	0	1	16, 20	2592	10	3
16	41	28	0	8	24	8	1	0	0	4	8	0	0	19	1944	20	4
17	39	24	4	12	12	8	3	0	1	3	3	4	1	22, 25	5184	16	4
18	39	24	3	12	12	12	0	0	0	4	6	0	2	23, 26	1296	22	4
19	39	24	1	12	18	8	0	0	0	2	8	2	0	24, 27	7776	23	4
20	39	24	3	0	36	0	0	0	0	0	12	0	0	28	216	13	3
21	37	20	4	16	12	0	5	0	0	4	0	8	0	29	972	18	4
22	37	20	4	14	12	6	1	0	0	2	5	4	1	30–32	7776	21	4
23	37	20	3	12	18	4	0	0	0	0	8	4	0	33	3888	24	4
24	35	16	4	20	6	4	1	0	0	0	4	8	0	35	1296	28	5
25	35	16	7	12	12	4	0	0	0	0	6	4	2	34, 36	3888	25	4
26	33	12	12	12	6	0	3	0	0	2	0	6	4	37, 38	648	26	5
27	33	12	11	12	6	4	0	0	0	0	4	4	4	39	1296	29	5
28	31	8	13	16	0	0	2	0	0	0	0	8	4	40	648	27	5
29	27	0	27	0	0	0	0	0	0	0	0	0	12	41	24	30	6

Table 19: The 29 types of geometric hyperplanes of $S_{(4)}$; also shown is the partition of hyperplane types into 15 classes according to the number of points/lines. As in corresponding Table 10, one first gives the type ('Tp') of a hyperplane, then the number of points ('Ps') and lines ('Ls') it contains, and the number of points of given order. The next six columns tell us about how many of 12 $S_{(3)}$'s are fully located ('D') in the hyperplane and/or share with it a hyperplane of type H_i (see Table 10 of Chapter 8). The VL-column lists the types of ordinary and/or extraordinary Veldkamp lines of $S_{(3)}$ we get by projecting a hyperplane of the given type into $S_{(3)}$'s along the lines of all four distinguished spreads. Finally, for each hyperplane type we give its cardinality ('Crd'), the corresponding large orbit of $2 \times 2 \times 2 \times 2$ arrays over $\mathbb{F}_2$ ('BS') taken from Table 5 of [19], and its weight/rank ('W').

			# of Points of Order					# of $S_{(3)}$'s of Type									
Tp	Ps	Ls	0	1	2	3	4	D	H_1	H_2	H_3	H_4	H_5	VL	Crd	BS	W
1	65	76	0	0	0	32	33	4	8	0	0	0	0	I	81	2	1
2	57	60	0	0	12	24	21	2	6	4	0	0	0	II, 1	324	3	2
3	53	52	0	2	12	26	13	1	6	3	2	0	0	III, 2	1296	4	2
5	49	44	0	8	12	16	13	1	3	6	0	2	0	IV, 4	648	6	3
7	45	36	0	18	0	18	9	1	0	9	0	0	2	V, 6	144	7	3
8	45	36	0	0	36	0	9	0	0	12	0	0	0	10	108	17	4
9	45	36	2	4	18	16	5	0	4	2	4	2	0	7, 8	3888	8	3
10	45	36	0	6	18	18	3	0	3	3	6	0	0	9, 11	2592	9	3
12	41	28	8	0	24	0	9	0	4	0	0	8	0	14	162	14	4
13	41	28	0	12	18	8	3	0	0	6	4	2	0	15, 18	1944	19	4
14	41	28	0	14	12	14	1	0	1	3	6	2	0	17, 21	2592	15	4
15	41	28	2	8	18	12	1	0	1	3	7	0	1	16, 20	2592	10	3
16	41	28	0	8	24	8	1	0	0	4	8	0	0	19	1944	20	4
21	37	20	4	16	12	0	5	0	0	4	0	8	0	29	972	18	4
22	37	20	4	14	12	6	1	0	0	2	5	4	1	30–32	7776	21	4
23	37	20	3	12	18	4	0	0	0	0	8	4	0	33	3888	24	4
26	33	12	12	12	6	0	3	0	0	2	0	6	4	37, 38	648	26	5
27	33	12	11	12	6	4	0	0	0	0	4	4	4	39	1296	29	5

Table 20: Types of geometric hyperplanes of $S_{(4)}$ lying on the unique hyperbolic quadric $Q^+(15,2) \subset PG(15,2)$ that contains the $S_{(4)}$ (the first orbit).

			# of Points of Order					# of $S_{(3)}$'s of Type									
Tp	Ps	Ls	0	1	2	3	4	D	H_1	H_2	H_3	H_4	H_5	VL	Crd	BS	W
1	65	76	0	0	0	32	33	4	8	0	0	0	0	I	81	2	1
2	57	60	0	0	12	24	21	2	6	4	0	0	0	II, 1	324	3	2
5	49	44	0	8	12	16	13	1	3	6	0	2	0	IV, 4	648	6	3
8	45	36	0	0	36	0	9	0	0	12	0	0	0	10	108	17	4
12	41	28	8	0	24	0	9	0	4	0	0	8	0	14	162	14	4
21	37	20	4	16	12	0	5	0	0	4	0	8	0	29	972	18	4

Table 21: Six types of hyperplanes lying on $Q^+(15,2)$ that in their totality correspond to the image of the set of 2295 maximal subspaces of the symplectic polar space $W(7,2)$. Interestingly, one orbit consists of homogeneous hyperplanes, viz. of those whose all $S_{(3)}$'s are of type H_2.

E

THE 56 IRREDUCIBLE REPRESENTATION OF E_7 FROM FOUR-QUBIT OPERATORS

In Chapter 9 I showed that the fundamental 27-dimensional irreducible representation of E_6 was encoded in the hyperplane corresponding to the elliptic quadric of the magic Veldkamp line. To find the weight diagram of the 56-dimensional irreducible representation of the Lie group E_7, one needs to consider a magic Veldkamp line of type $\mathcal{E}-\mathcal{H}-\mathcal{P}$ in $\mathcal{W}(7,2)$, i.e. we need to use four-qubit Pauli operators. To this respect one can choose as the canonical line of this type, the line $(H_{IIIY}, H_{IIII}, C_{IIIY})$. The elliptic quadric H_{IIIY} contains 119 operators that are either symmetric and commuting with IIIY or skew-symmetric and anti-commuting with IIIY , the hyperbolic quadric H_{IIII} consists of 135 symmetric operators and the perp-set C_{IIIY} is made of 127 observables commuting with IIIY. The core set of this Veldkamp line is made of 63 operators and it is a copy of the symplectic polar space encoding three-qubit operators, $\mathcal{W}(5,2)$. A pictorial representation of this four-qubit magic Veldkamp line is given in Figure 42.

The cardinalities indicate that the set of operators in H_{IIIY} that are skew symmetric could be a good candidate to encode the weight diagram of the 56-dimensional fundamental irreducible representation of E_7. Let us consider the labeling of the roots of E_7 by four-qubit operators as given in Figure 43.

Then choosing YYYZ to be the highest weight, one gets the following weight diagram, Figure 44, which is the weight diagram of the 56 fundamental representation of E_7 and it accommodates the 56 operators of $H_{IIIY} \setminus (H_{IIIY} \cap H_{III})$.

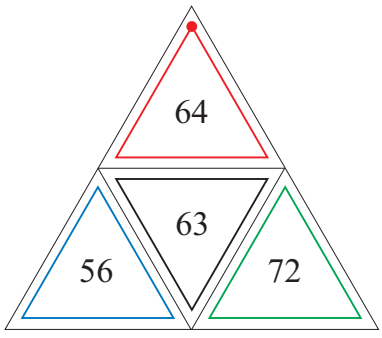

Figure 42: A schematic representation of the four-qubit magic Veldkamp line. The red dot represents the four-qubit operator IIIY.

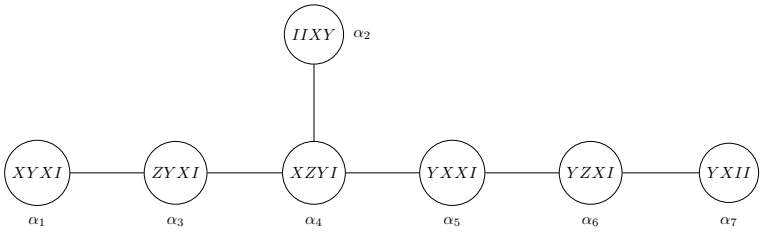

Figure 43: Root system of E_7 labeled by four-qubit operators.

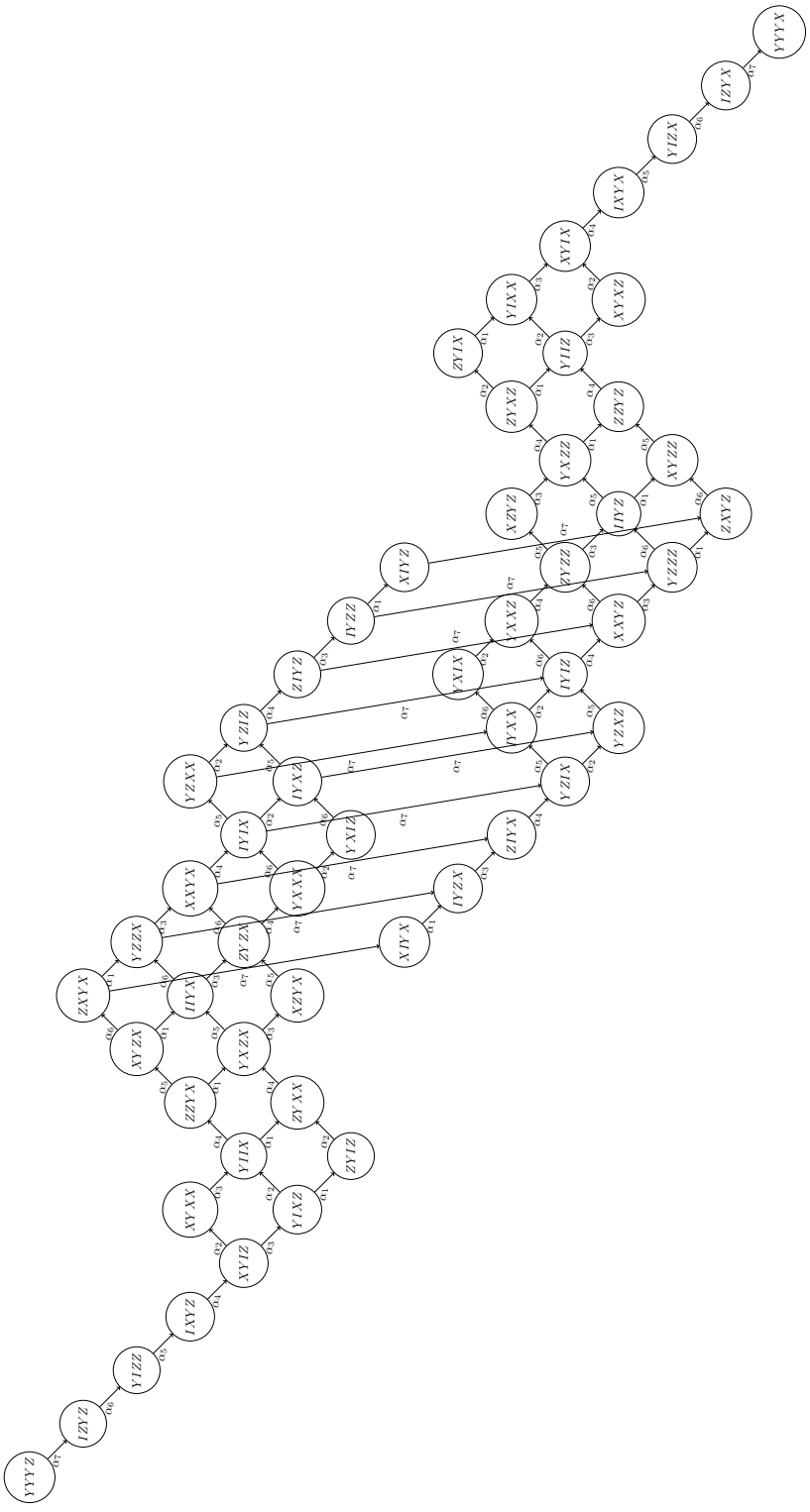

Figure 44: The 56 fundamental irreducible representation of E_7 as a subset of the four-qubit magic Veldkamp line.

BIBLIOGRAPHY

[1] Amselem, E., Rådmark, M., Bourennane, M., & Cabello, A. (2009). State-independent quantum contextuality with single photons. Physical review letters, 103(16), 160405.

[2] Aravind, P. K. (2004). Quantum mysteries revisited again. American Journal of Physics, 72(10), 1303-1307.

[3] Arkhipov, A. (2012). Extending and characterizing quantum magic games. arXiv preprint arXiv:1209.3819.

[4] Arnold, V. I. (1974). Critical points of smooth functions. In Proceedings of ICM-74 (Vol. 1, pp. 19-40).

[5] Arnold, V. I. (1981). Singularity theory (Vol. 53). Cambridge University Press.

[6] Aspect, A., Dalibard, J., & Roger, G. (1982). Experimental test of Bell's inequalities using time-varying analyzers. Physical review letters, 49(25), 1804.

[7] Aulbach, M. (2012). Classification of entanglement in symmetric states. International Journal of Quantum Information, 10(07), 1230004.

[8] Aulbach, M., Markham, D., & Murao, M. (2010). Geometric entanglement of symmetric states and the majorana representation. In Conference on Quantum Computation, Communication, and Cryptography (pp. 141-158). Springer, Berlin, Heidelberg.

[9] Bartosik, H., Klepp, J., Schmitzer, C., Sponar, S., Cabello, A., Rauch, H., & Hasegawa, Y. (2009). Experimental test of quantum contextuality in neutron interferometry. Physical review letters, 103(4), 040403.

[10] Bell, J. S. (1966). On the problem of hidden variables in quantum mechanics. Reviews of Modern Physics, 38(3), 447.

[11] Bengtsson, I., & Życzkowski, K. (2017). Geometry of quantum states: an introduction to quantum entanglement. Cambridge university press.

[12] Bennett, C. H., Popescu, S., Rohrlich, D., Smolin, J. A., & Thapliyal, A. V. (2000). Exact and asymptotic measures of multipartite pure-state entanglement. Physical Review A, 63(1), 012307.

[13] Borsten, L., Dahanayake, D., Duff, M. J., Marrani, A., & Rubens, W. (2010). Four-qubit entanglement classification from string theory. Physical review letters, 105(10), 100507.

[14] Borsten, L., Dahanayake, D., Duff, M. J., Rubens, W., & Ebrahim, H. (2009). Freudenthal triple classification of three-qubit entanglement. Physical Review A, 80(3), 032326.

[15] Borsten, L., Duff, M. J., & Lévay, P. (2012). The black-hole/qubit correspondence: an up-to-date review. Classical and Quantum Gravity, 29(22), 224008.

[16] Boulmier, J., Holweck, F., Pinard, M., & Saniga, M. (2019). Veldkamp Spaces of Low-Dimensional Ternary Segre Varieties. Results in Mathematics, 74(1), 54.

[17] Bravyi, S., Terhal, B. M., & Leemhuis, B. (2010). Majorana fermion codes. New Journal of Physics, 12(8), 083039.

[18] Bremner, M., Hu, J., & Oeding, L. (2014). The $3 \times 3 \times 3$ Hyperdeterminant as a Polynomial in the Fundamental Invariants for $SL_3(\mathbb{C}) \times SL_3(\mathbb{C}) \times SL_3(\mathbb{C})$. Mathematics in Computer Science, 8(2), 147-156.

[19] Bremner, M. R., & Stavrou, S. G. (2013). Canonical forms of $2 \times 2 \times 2$ and $2 \times 2 \times 2 \times 2$ arrays over $\mathbb{F}_2$ and $\mathbb{F}_3$. Linear and Multilinear Algebra, 61(7), 986-997.

[20] Briand, E., Luque, J.-G., & Thibon, J.-Y. (2003). A complete set of covariants of the four qubit system. Journal of Physics A: Mathematical and General, 36(38), 9915.

[21] Briand, E., Luque, J.-G., Thibon, J.-Y., & Verstraete, F. (2004). The moduli space of three-qutrit states. Journal of Mathematical Physics, 45(12), 4855-4867.

[22] Brody, D. C., Gustavsson, A. C., & Hughston, L. P. (2007). Entanglement of three-qubit geometry. In Journal of Physics: Conference Series (Vol. 67, No. 1, p. 012044). IOP Publishing.

[23] Brylinski, J. L. (2002). Algebraic measures of entanglement. In Mathematics of quantum computation (pp. 19-40). Chapman and Hall/CRC.

[24] Buczyński, J., & Landsberg, J. M. (2014). On the third secant variety. Journal of Algebraic Combinatorics, 40(2), 475-502.

[25] Cabello, A. (2008). Experimentally testable state-independent quantum contextuality. Physical review letters, 101(21), 210401.

[26] Cabello, A. (2010). Proposed test of macroscopic quantum contextuality. Physical Review A, 82(3), 032110.

[27] Cabello, A., Estebaranz, J., & García-Alcaine, G. (1996). Bell-Kochen-Specker theorem: A proof with 18 vectors. Physics Letters A, 212(4), 183-187.

[28] Chen, L., Đoković, D. Ž., Grassl, M., & Zeng, B. (2013). Four-qubit pure states as fermionic states. Physical Review A, 88(5), 052309.

[29] Chen, L., & Đoković, D. Ž. (2013). Proof of the Gour-Wallach conjecture. Physical Review A, 88(4), 042307.

[30] Chterental, O., & Đoković, D. Ž. (2006). Normal forms and tensor ranks of pure states of four qubits. arXiv preprint quant-ph/0612184.

[31] Chryssomalakos, C., Guzmán-González, E., & Serrano-Ensástiga, E. (2018). Geometry of spin coherent states. Journal of Physics A: Mathematical and Theoretical, 51(16), 165202.

[32] Nielsen, M. A., & Chuang, I. (2002). Quantum computation and quantum information. Cambridge: Cambridge University Press.

[33] Cleve, R., & Mittal, R. (2014). Characterization of binary constraint system games. In International Colloquium on Automata, Languages, and Programming (pp. 320-331). Springer, Berlin, Heidelberg.

[34] Cohen, A. M. (1995). Point-line spaces related to buildings. In Handbook of incidence geometry (pp. 647-737).

[35] Duff, M. J., & Ferrara, S. (2007). E_7 and the tripartite entanglement of seven qubits. Physical Review D, 76(2), 025018.

[36] Dür, W., Vidal, G., and Cirac, J. I. (2000). Three qubits can be entangled in two inequivalent ways. Physical Review A, 62(6), 062314.

[37] Durt, T., Englert, B. G., Bengtsson, I., & Życzkowski, K. (2010). On mutually unbiased bases. International journal of quantum information, 8(04), 535-640.

[38] Gour G. & Wallach N. (2014) On symmetric SL-invariant polynomials in four-qubit. In Symmetry: Representation Theory and Its Applications, 259-267. Springer New York.

[39] Green, R. M., & Saniga, M. (2013). The Veldkamp space of the smallest slim dense near hexagon. International Journal of Geometric Methods in Modern Physics, 10(02), 1250082.

[40] Einstein, A., Podolsky, B., & Rosen, N. (1935). Can quantum-mechanical description of physical reality be considered complete?. Physical review, 47(10), 777.

[41] Fulton, W. and Hansen, J. (1979). A connectedness theorem for projective varieties, with applications to intersections and singularities of mappings. Annals of Mathematics, 110(1), pp.159-166.

[42] Fulton, W., Harris, J. (1991). Representation Theory (Vol. 129). Springer Science & Business Media.

[43] Gelfand, I. M., Kapranov, M. M., & Zelevinsky, A. V. (1992). Hyperdeterminants. Advances in Mathematics, 96(2), 226-263.

[44] Gelfand, I. M., Kapranov, M., and Zelevinsky, A. (2008). Discriminants, resultants, and multidimensional determinants. Springer Science & Business Media.

[45] Gour, G., & Wallach, N. R. (2010). All maximally entangled four-qubit states. Journal of Mathematical Physics, 51(11), 112201.

[46] Greenberger, D. M., Horne, M. A., & Zeilinger, A. (1989). Going beyond Bell's theorem. In Bell's theorem, quantum theory and conceptions of the universe (pp. 69-72). Springer, Dordrecht.

[47] Harris, J. (2013). Algebraic geometry: A first course (Vol. 133). Springer Science & Business Media.

[48] Hastings, M. B. (2017). Small Majorana fermion codes. Quantum Information & Computation, 17(13-14), 1191-1205.

[49] Havlicek, H., Odehnal, B., & Saniga, M. (2009). Factor-group-generated polar spaces and (multi-) qudits. Symmetry, Integrability and Geometry. Methods and Applications, 5.

[50] Holweck, F. (2019) Geometric constructions over $\mathbb{C}$ and $\mathbb{F}_2$ for Quantum Information. In Quantum Physics and Geometry, Lecture Notes of the Unione Matematica Italiana Springer.

[51] Holweck, F., & Jaffali, H. (2016). Three-qutrit entanglement and simple singularities. Journal of Physics A: Mathematical and Theoretical, 49(46), 465301.

[52] Holweck, F., Jaffali, H., & Nounouh, I. (2016). Grover's algorithm and the secant varieties. Quantum Information Processing, 15(11), 4391-4413.

[53] Holweck, F., & Lévay, P. (2016). Classification of multipartite systems featuring only $|W\rangle$ and $|GHZ\rangle$ genuine entangled states. Journal of Physics A: Mathematical and Theoretical, 49(8).

[54] Holweck, F., Luque, J.-G., & Thibon, J.-Y. (2012). Geometric descriptions of entangled states by auxiliary varieties. Journal of Mathematical Physics, 53(10), 102203.

[55] Holweck, F., Luque, J.-G., & Thibon, J.-Y. (2014). Entanglement of four qubit systems: A geometric atlas with polynomial compass I (the finite world). Journal of Mathematical Physics, 55(1), 012202.

[56] Holweck, F., Luque, J.-G., & Thibon, J.-Y. (2017). Entanglement of four-qubit systems: A geometric atlas with polynomial compass II (the tame world). Journal of Mathematical Physics, 58(2), 022201.

[57] Holweck, F., Luque, J.-G., & Planat, M. (2014). Singularity of type D_4 arising from four-qubit systems. Journal of Physics A: Mathematical and Theoretical, 47(13), 135301.

[58] Holweck, F., & Oeding, L. (2018). Hyperdeterminants from the E_8 Discriminant. arXiv preprint arXiv:1810.05857.

[59] Holweck, F., & Saniga, M. (2017). Contextuality with a small number of observables. International Journal of Quantum Information, 15(04), 1750026.

[60] Holweck, F., Saniga, M., & Lévay, P. (2014). A Notable Relation between N-Qubit and 2^{N-1}-Qubit Pauli Groups via Binar $LGr(N, 2N)$. SIGMA. Symmetry, Integrability and Geometry: Methods and Applications, 10, 041.

[61] Heydari, H. (2008). Geometrical structure of entangled states and the secant variety. Quantum Information Processing, 7(1), 43-50.

[62] Howard, M., Wallman, J., Veitch, V., & Emerson, J. (2014). Contextuality supplies the "magic" for quantum computation. Nature, 510(7505), 351-355.

[63] Ivey, T. A., & Landsberg, J. M. (2003). Cartan for beginners: differential geometry via moving frames and exterior differential systems (Vol. 61). Providence, RI: American Mathematical Society.

[64] Jaffali, H., & Holweck, F. (2019). Quantum entanglement involved in Grover's and Shor's algorithms: the four-qubit case. Quantum Information Processing, 18(5), 133.

[65] Kac, V. G., Popov, V. L., Vinberg, E.B. (1976). Sur les groupes lineaires algebriques dont l'algèbre des invariants est libres. CR Acad. Sci. Paris, 283, 875-878.

[66] Kirchmair, G., Zähringer, F., Gerritsma, R., Kleinmann, M., Gühne, O., Cabello, A., Blatt, R. & Roos, C. F. (2009). State-independent experimental test of quantum contextuality. Nature, 460(7254), 494-497.

[67] Kochen, S., & Specker, E. P. (1967). The problem of hidden variables in quantum mechanics. In The logico-algebraic approach to quantum mechanics (pp. 293-328). Springer Netherlands.

[68] Khaleghi, A., Silva, D., & Kschischang, F. R. (2009). Subspace codes. In IMA International Conference on Cryptography and Coding (pp. 1-21). Springer, Berlin, Heidelberg.

[69] Koetter, R., & Kschischang, F. R. (2008). Coding for errors and erasures in random network coding. IEEE Transactions on Information theory, 54(8), 3579-3591.

[70] Landsberg, J. M. (2012) *Tensors: geometry and applications*. American Mathematical Society.

[71] Landsberg, J. M., & Manivel, L. (2001). The projective geometry of Freudenthal's magic square. Journal of Algebra, 239(2), 477-512.

[72] Landsberg, J. M., & Manivel, L. (2004). On the ideals of secant varieties of Segre varieties. Foundations of Computational Mathematics, 4(4), 397-422.

[73] Landsberg, J. M., & Ottaviani, G. (2013). Equations for secant varieties of Veronese and other varieties. Annali di Matematica Pura ed Applicata, 192(4), 569-606.

[74] Le Paige C. (1881). Sur la théorie des formes binaires à plusieurs séries de variables. Bull. Acad. Roy. Sci. Belgique **2** (3), 40-53.

[75] Lévay, P. (2007). Strings, black holes, the tripartite entanglement of seven qubits, and the Fano plane. Physical Review D, 75(2), 024024.

[76] Lévay, P. (2010). STU black holes as four-qubit systems. Physical Review D, 82(2), 026003.

[77] Lévay, P., & Holweck, F. (2015). Embedding qubits into fermionic Fock space: Peculiarities of the four-qubit case. Physical Review D, 91(12), 125029.

[78] Lévay, P., & Holweck, F. (2018). A fermionic code related to the exceptional group E_8. Journal of Physics A: Mathematical and Theoretical.

[79] Lévay, P., & Holweck, F. (2019). A finte geometric toy model of space time as an error correction code. Accepted in Physical Review D.

[80] Lévay, P., Holweck, F., & Saniga, M. (2017). Magic three-qubit Veldkamp line: A finite geometric underpinning for form theories of gravity and black hole entropy. Phys. Rev. D 96, 026018

[81] Lévay, P., Planat, M., & Saniga, M. (2013). Grassmannian connection between three-and four-qubit observables, Mermin's contextuality and black holes. Journal of High Energy Physics, 2013(9), 37.

[82] Lévay, P., Saniga, M., Vrana, P., & Pracna, P. (2009). Black hole entropy and finite geometry. Physical Review D, 79(8), 084036.

[83] Lévay, P., & Szabó, Z. (2017). Mermin pentagrams arising from Veldkamp lines for three qubits. Journal of Physics A: Mathematical and Theoretical, 50(9), 095201.

[84] Lévay, P., & Vrana, P. (2008). Three fermions with six single-particle states can be entangled in two inequivalent ways. Physical Review A, 78(2), 022329.

[85] Luque, J.-G. (2008). Invariants des hypermatrices (Habilitation dissertation, Université de Marne la Vallée).

[86] Luque, J.-G., & Thibon, J.-Y. (2003). Polynomial invariants of four qubits. Physical Review A, 67(4), 042303.

[87] Luque, J. G., & Thibon, J. Y. (2005). Algebraic invariants of five qubits. Journal of Physics A: Mathematical and General, 39(2), 371.

[88] Mermin, N. D. (1993). Hidden variables and the two theorems of John Bell. Reviews of Modern Physics, 65(3), 803.

[89] Miyake, A. (2003). Classification of multipartite entangled states by multidimensional determinants. Physical Review A, 67(1), 012108.

[90] Miyake, A., & Verstraete, F. (2004). Multipartite entanglement in 2x2xn quantum systems. Physical Review A, 69(1), 012101.

[91] Miyake, A., & Wadati, M. (2002). Multipartite entanglement and hyperdeterminants. Quantum information & computation, 2(7), 540-555.

[92] Nurmiev, A. G. (2000). Orbits and invariants of third-order matrices. Mat. Sb., 191(5), 101-108.

[93] Oeding, L. (2011). Set-theoretic defining equations of the variety of principal minors of symmetric matrices. Algebra & Number Theory, 5(1), 75-109.

[94] Oeding, L. (2011). Set-theoretic defining equations of the tangential variety of the Segre variety. Journal of Pure and Applied Algebra, 215(6), 1516-1527.

[95] P. Olver. (1999). Classical Invariant Theory. Cambridge University Press, Cambridge UK.

[96] Parfenov, P. G. (1998). Tensor products with finitely many orbits. Russian Mathematical Surveys, 53(3), 635-636.

[97] Penrose, R. (1967) Twistor Algebra. Journal of Mathematical Physics 8, 345.

[98] Peres, A. (1991). Two simple proofs of the Kochen-Specker theorem. Journal of Physics A: Mathematical and General, 24(4), L175.

[99] Planat, M., Giorgetti, A., Holweck, F., & Saniga, M. (2015). Quantum contextual finite geometries from dessins d'enfants. International Journal of Geometric Methods in Modern Physics, 12(07), 1550067.

[100] Planat, M., & Saniga, M. (2012). Five-qubit contextuality, noise-like distribution of distances between maximal bases and finite geometry. Physics Letters A, 376(46), 3485-3490.

[101] Planat, M., Saniga, M., & Holweck, F. (2013). Distinguished three-qubit «magicity» via automorphisms of the split Cayley hexagon. Quantum information processing, 12(7), 2535-2549.

[102] Polster, B. (2012). A geometrical picture book. Springer Science & Business Media.

[103] Rossi, M., Bruß, D., & Macchiavello, C. (2013). Scale invariance of entanglement dynamics in Grover's quantum search algorithm. Physical Review A, 87(2), 022331.

[104] Saniga, M., Havlicek, H., Holweck, F., Planat, M., & Pracna, P. (2015). Veldkamp-space aspects of a sequence of nested binary Segre varieties. Annales de l'Institut Henri Poincaré D, 2(3), 309-333.

[105] Saniga, M., Holweck, F., & Pracna, P. (2017). Veldkamp spaces: From (Dynkin) diagrams to (Pauli) groups. International Journal of Geometric Methods in Modern Physics, 14(05), 1750080.

[106] Saniga, M., & Planat, M. (2007). Multiple Qubits as Symplectic Polar Spaces of Order Two. Advanced Studies in Theoretical Physics, 1, 1-4.

[107] Saniga, M., & Planat, M. (2012). Finite geometry behind the Harvey-Chryssanthacopoulos four-qubit magic rectangle. Quantum Information & Computation, 12(11-12), 1011-1016.

[108] Saniga, M., Planat, M., Pracna, P., & Havlicek, H. (2007). The Veldkamp space of two-qubits. SIGMA. Symmetry, Integrability and Geometry: Methods and Applications, 3, 075.

[109] Sanz, M., Braak, D., Solano, E., & Egusquiza, I. L. (2017). Entanglement classification with algebraic geometry. Journal of Physics A: Mathematical and Theoretical, 50(19), 195303.

[110] Sárosi, G., & Lévay, P. (2014). Entanglement in fermionic Fock space. Journal of Physics A: Mathematical and Theoretical, 47(11), 115304.

[111] Sawicki, A., & Tsanov, V. V. (2013). A link between quantum entanglement, secant varieties and sphericity. Journal of Physics A: Mathematical and Theoretical, 46(26), 265301.

[112] Slansky, R. (1981). Group theory for unified model building. Physics reports, 79(1), 1-128.

[113] Stokes, K. (2016). Geometric decoding of subspace codes with explicit Schubert calculus applied to spread codes. arXiv preprint arXiv:1610.02022.

[114] Thas, K. (2009). The geometry of generalized Pauli operators of N-qudit Hilbert space, and an application to MUBs. EPL (Europhysics Letters), 86(6), 60005.

[115] Terracini, A. (1911). Sulle v_k per cui la varietà degli $s_h(h+1)$ seganti ha dimensione minore dell'ordinario. Rendiconti del Circolo Matematico di Palermo (1884-1940), 31(1), 392-396.

[116] van Geemen, B., & Marrani, A. (2019). Lagrangian Grassmannians and spinor varieties in characteristic two. arXiv preprint arXiv:1903.01228.

[117] Verstraete, F., Dehaene, J., De Moor, B., & Verschelde, H. (2002). Four qubits can be entangled in nine different ways. Physical Review A, 65(5), 052112.

[118] Vrana, P., & Lévay, P. (2009). Special entangled quantum systems and the Freudenthal construction. Journal of Physics A: Mathematical and Theoretical, 42(28), 285303.

[119] Vrana, P., & Lévay, P. (2010). The Veldkamp space of multiple qubits. Journal of Physics A: Mathematical and Theoretical, 43(12), 125303.

[120] Waegell, M., & Aravind, P. K. (2012). Proofs of the Kochen-Specker theorem based on a system of three qubits. Journal of Physics A: Mathematical and Theoretical, 45(40), 405301.

[121] Waegell, M., & Aravind, P. K. (2013). Proofs of the Kochen-Specker theorem based on the N-qubit Pauli group. Physical Review A, 88(1), 012102.

[122] Weyman, J., & Zelevinsky, A. (1996). Singularities of hyperdeterminants. In Annales de l'Institut Fourier (Vol. 46, No. 3, pp. 591-644).

[123] Wootters, W. K., & Fields, B. D. (1989). Optimal state-determination by mutually unbiased measurements. Annals of Physics, 191(2), 363-381.

[124] Zak, F. L. (1993). Tangents and secants of algebraic varieties, Translations of Mathematical Monographs, vol. 127. American Mathematical Society, Providence, RI.

ABSTRACT

Entanglement and contextuality are two quantum phenomena considered as essential in quantum information theory in particular to achieve quantum speed-up in quantum algorithms or to provide quantum communication protocols that have no classical counterparts. In this dissertation, presented for the Habilitation (HDR), I present my work in applied algebraic geometry to describe, classify and understand these two resources by geometrical concepts. The problem of classifying entanglement of pure quantum states is investigated in the first part of the thesis using ideas of complex projective geometry such as auxiliary varieties, projective duality, singularities of hypersurfaces and classical invariant theory. In the second part I consider operator-based proofs of the Kochen-Specker Theorem. The discussion starts by a finite geometry description of the commutation relations of the generalized Pauli group. The concepts of symplectic polar spaces, Veldkamp spaces are also introduced to look at generalized Pauli operators with a geometric perspective. Interestingly in these two distinct geometric descriptions of entanglement and contextuality, the same semi-simple Lie groups are acting behind the scene.